Texto que sistematiza o trabalho científico do candidato para a obtenção do título de Livre Docência.

Prof. Osvaldo Novais de Oliveira Junior

Departamento de Física e Ciência dos Materiais

Instituto de Física e Química de São Carlos

UNIVERSIDADE DE SÃO PAULO

Agosto, 1992

ÍNDICE

I. Introdução

São duas as principais razões pelas quais decidi apresentar um texto que descreve minhas atividades de pesquisa, ao invés da tradicional tese de livre-docência. Primeiro, por estar atuando em diferentes linhas de pesquisa, uma tese que cobrisse todo o meu trabalho científico não teria unidade; por outro lado, uma tese com unidade cobriria apenas uma parte deste trabalho. Em segundo lugar, uma vez que este texto conterá muito menos detalhes (que podem ser obtidos nos artigos em anexo) do que uma tese conteria, há espaço para que se faça uma análise crítica das contribuições advindas do meu trabalho científico.

Embora atuando em várias linhas, tenho uma área principal de atuação. É a área de filmes Langmuir-Blodgett (LB), na qual obtive o doutoramento na Universidade de Bangor, País de Gales, em Junho de 1990. A tecnologia de filmes LB foi implantada recentemente no Departamento de Física e Ciência dos Materiais, e após um período de instalação, testes dos equipamentos e treinamento de pessoal, já começamos a obter os primeiros resultados. Na Seção II apresento uma breve descrição da técnica, de sua importância, e das contribuições para a área proporcionadas pelo nosso grupo de pesquisa em São Carlos. Os trabalhos referentes às outras linhas de pesquisa, ou seja, polímeros ferroelétricos, aspectos fundamentais da Física e Linguística Computacional, são descritos sucintamente na Seção III. Este texto termina com comentários finais na Seção IV, e uma lista das minhas contribuições após o doutoramento. Os artigos referentes a estas contribuições são colocados no Apêndice.

II. Linha principal - Filmes Langmuir-Blodgett (LB)

Filmes Langmuir-Blodgett (LB) são obtidos a partir da transferência de camadas monomoleculares orgânicas da superfície da água para um substrato sólido. Os filmes LB caracterizam-se pela alta precisão no controle da espessura, uniformidade da superfície e elevado grau de ordem estrutural. O nome Langmuir-Blodgett foi consagrado em homenagem aos pesquisadores americanos

Irving Langmuir, que em 1917 demonstrou que se pode transferir o filme da água para um substrato, e Katharine Blodgett, que criou a técnica de deposição de várias camadas num mesmo substrato.

O primeiro passo na fabricação de filmes LB consiste na obtenção de filmes monomoleculares sobre a superfície da água, chamados filmes de Langmuir. A formação de camadas monomoleculares insolúveis sobre a água é possível porque certos compostos possuem moléculas anfipáticas, ou seja, moléculas que possuem uma extremidade atraída pela água (hidrofílica) e outra repelida pela água (hidrofóbica). Para a fabricação de filmes LB, tais compostos são dissolvidos em um solvente orgânico volátil (clorofórmio, por exemplo) e a solução, colocada sobre a água com uma micropipeta, espalha-se espontaneamente. O solvente evapora-se em seguida, e as moléculas do composto, confinadas por barreiras móveis que restringem a área onde se encontram, são comprimidas de forma que seus eixos fiquem perpendiculares à superfície da água. Mantendo-se constante a pressão de superfície do filme, este pode ser transferido para um substrato sólido apropriado, que é imerso na água e retirado de modo adequado através da camada monomolecular. Imersões e retiradas subsequentes do mesmo substrato permitem a produção de estruturas com várias camadas e diferentes ordenamentos; eventualmente, podem-se obter estruturas com centenas de camadas.

Para a produção de filmes de Langmuir e subsequente transferência aos substratos, emprega-se um sistema experimental conhecido como cuba de Langmuir, que consiste basicamente de um reservatório para a água e barreiras móveis que confinam e comprimem o filme, além de equipamentos para a caracterização dos filmes de Langmuir e deposição de filmes LB. Ácidos graxos, assim como outros compostos alifáticos, são considerados tradicionais no estudo de filmes de Langmuir e produção de filmes LB. Nos últimos tempos, entretanto, uma grande variedade de materiais tem sido empregada para este fim. Polímeros, por exemplo, têm sido estudados devido às excelentes características mecânicas que apresentam, e compostos biológicos têm atraído atenção pela sua importância para a pesquisa das propriedades de membranas

celulares e desenvolvimento de novos produtos farmacêuticos.

Embora tenha sido criada há mais de 50 anos, apenas nos últimos tempos a técnica LB passou a ser explorada intensivamente do ponto de vista de aplicações. Nos anos 60, pesquisadores alemães mostraram que a técnica poderia ser usada para crescer estruturas supermoleculares de maneira precisa, empregando ácidos graxos e moléculas similares para pesquisas em ótica e transferência de energia. No entanto, somente a partir da década de 70 os resultados experimentais sobre propriedades elétricas de filmes LB passaram a ser reprodutíveis e confiáveis. A partir de então, várias possíveis aplicações têm sido sugeridas, principalmente porque a técnica LB permite otimização das propriedades de materiais orgânicos, através da modificação da estrutura da molécula ou da arquitetura do filme.

O interesse a longo prazo nos filmes LB reside na utilização de moléculas orgânicas como blocos formadores de dispositivos eletrônicos, no que se convencionou chamar Eletrônica Molecular. Como os filmes são ultrafinos e possuem um alto grau de ordenamento estrutural, eles têm sido propostos para uma grande variedade de aplicações. Algumas destas aplicações são: camadas isolantes em estruturas MIS (metal-isolante-semicondutor), "resists" para microlitografia, lubrificação de filmes magnéticos para discos rígidos, sensores químicos e biológicos, dispositivos piro- e piezoelétricos, recobrimento de fibras óticas, e dispositivos de ótica não linear. A única aplicação comercial de um dispositivo utilizando filmes LB de que se tem notícia, entretanto, é um dispositivo para calibração de dosímetros. Ocorre que existem vários problemas tecnológicos que precisam ser resolvidos antes que dispositivos possam ser fabricados em escala industrial. Entre eles encontram-se os problemas de estabilidade térmica, e o alto custo, no momento, da produção dos filmes. Uma revisão das pesquisas mais recentes no campo pode ser encontrada no artigo da Brazilian Journal of Physics [1], que escrevi a convite da revista.

2.1 Atuação do grupo de São Carlos

O trabalho nesta área de pesquisa consistiu inicialmente da

instalação de duas cubas de Langmuir e demais equipamentos essenciais para a fabricação e caracterização de filmes LB em uma sala limpa. Para isso recursos foram obtidos do CNPq (num projeto de Eletrônica Molecular liderado pelo Prof. Sérgio Mascarenhas), da FAPESP (projeto individual), e da Prefeitura do Campus de São Carlos e Departamento de Física e Ciência dos Materiais para a instalação da sala limpa. Esta sala tem pressão interna positiva e o ar do seu interior é filtrado. Contamos com duas cubas de Langmuir KSV LB5000, que permitem a deposição de filmes LB alternados, e a caracterização dos filmes de Langmuir através de medidas de pressão e de potencial de superfície. O sistema de purificação de água é um sistema Millipore, que inclui vários filtros para remover íons e impurezas orgânicas. Devo mencionar aqui, que o trabalho dos técnicos Ademir Soares, José Roberto Bertho e Níbio José Mangerona, foi fundamental para a instalação, e continua sendo para a manutenção da sala limpa e dos equipamentos.

Uma equipe de cerca de dez pessoas trabalha atualmente em projetos da área, sendo que duas teses de mestrado e uma de doutorado versando sobre filmes LB deverão ser defendidas até o final de 1992. Nossas áreas de atuação abrangem estudos fundamentais das propriedades elétricas de filmes obtidos a partir de compostos simples (disponíveis comercialmente), e também a fabricação de filmes de polímeros conjugados sintetizados por membros do grupo. Estes polímeros são mais complexos, mas extremamente promissores do ponto de vista de aplicações tecnológicas.

Tempo considerável foi dispendido na instalação, teste dos equipamentos e treinamento de pessoal para trabalhar com a técnica LB, mas alguns resultados já foram obtidos. A seguir apresento um breve resumo destes resultados.

2.1.1 Novo modelo para interpretar curvas de pressão de superfície

Participação: Prof. Guilherme Fontes Leal Ferreira

Os modelos usualmente empregados para explicar curvas de pressão de superfície versus área por molécula de filmes de

Langmuir são baseados em equações de estado fenomenológicas (derivadas da equação de gases), ou em análises termodinâmicas e de mecânica estatística, que levam em conta as possíveis configurações moleculares. Inicialmente demonstramos que a tensão superficial pode ser obtida de um modelo puramente mecânico [2], ou seja, como o deficit de atração na direção paralela à do líquido. Sugerimos, posteriormente, que várias informações a respeito da pressão de superfície de um filme de Langmuir podem ser obtidas de uma análise das forças de interação entre as fases da interface água/filme/ar [3]. Embora não tenhamos resultados quantitativos conclusivos, acreditamos que esta abordagem pode ser extremamente útil para fornecer parâmetros adequados em modelos mais sofisticados, como simulações por Monte Carlo e dinâmica molecular.

2.1.2 Homogeneidade e condutância

Participação: Mestrando Ailton Cavalli e Bacharelanda Patrícia Medeiros

A reprodutibilidade dos resultados experimentais tem sido um dos mais importantes aspectos da pesquisa em filmes de Langmuir e Langmuir-Blodgett, uma vez que, por terem dimensões moleculares, estes filmes são altamente sensíveis a impurezas. De fato, a irreprodutibilidade de resultados experimentais fez com que este campo de pesquisa fosse quase que completamente abandonado nos anos 40 e 50. Os problemas que causam tal irreprodutibilidade têm sido em grande parte resolvidos nos últimos anos, a partir da utilização de compostos cada vez mais puros, de sistemas sofisticados de purificação de água, e de ambientes adequados (salas limpas) para a realização das experiências. Entretanto, ainda é comum encontrarem-se discrepâncias nos resultados de diferentes autores, de maneira que a reprodutibilidade continua a ser um assunto de extrema importância.

Recentemente surgiu uma controvérsia a respeito da homogeneidade dos filmes de Langmuir. A existência de domínios de dimensões micrométricas foi confirmada por diversos autores para filmes de ácidos graxos e fosfolipídios, utilizando várias

técnicas experimentais como microscopia ótica sob o ângulo de Brewster [4,5], e microscopia de fluorescência [6]. Os domínios aparecem mesmo para filmes expandidos, com grandes áreas por molécula do filme. Além disso, na última conferência sobre filmes LB em Paris (1991), pesquisadores alemães disseram ter observado que o potencial de superfície de um filme poderia depender de fatores como a posição da prova de potencial. Aventou-se a possibilidade, então, de que o filme seria heterogêneo, também do ponto de vista macroscópico.

Em São Carlos, conseguimos desfazer tal controvérsia através de medidas de potencial de superfície. Observamos que o potencial de superfície de filmes de Langmuir expandidos não varia quando é alterada a posição da prova de potencial, e que portanto, qualquer heterogeneidade em medidas de potencial deve ser fruto de artefatos experimentais, possivelmente causados por impurezas.

Ainda com relação a controvérsias da literatura, pesquisadores americanos [7] questionaram a existência de condutância lateral observada pelo Grupo de Bangor [8]. Após uma série de medidas com ácidos graxos e fosfolipídios, estamos em condição de confirmar que o aumento da condutância devido à presença do filme de Langmuir sobre a superfície da água é um efeito real [9].

2.1.3 Simulação de curvas de potencial por computador

Participação: Bacharelandos Antonio Riul Jr. e Luiz Eduardo Amancio, Prof. Guilherme Fontes Leal Ferreira

Este trabalho foi iniciado ainda durante o meu doutoramento, sendo que um capítulo da tese é dedicado ao assunto [10], e representa a primeira tentativa na literatura de explicar curvas de potencial de superfície de filmes de Langmuir quantitativamente. Após minha volta ao Brasil, fiz pequenas modificações no modelo originalmente proposto e publicamos os resultados recentemente para filmes de ácido esteárico [11]. O modelo é baseado na abordagem de Demchak-Fort (DF) [12], na qual um filme de Langmuir sobre a superfície da água é considerado como sendo um capacitor de 3 camadas, com momentos de dipolo e constantes dielétricas distintos. É pressuposto que cada camada

contribui independentemente para o momento de dipolo total, ou seja, a substituição dos dipolos ou da constante dielétrica de uma camada só muda a contribuição daquela camada, não devendo afetar as outras.

Em São Carlos verificamos, através da aplicação do modelo para o potencial de filmes mistos [13], que esta hipótese não é universalmente válida. Estes filmes mistos consistem de misturas de ácido palmítico e ácido tri-fluoropalmítico em várias proporções, depositados sobre uma superfície de água pura. A presença dos átomos de flúor traz uma contribuição negativa relativamente grande para o potencial de superfície, de maneira que o aumento da concentração de ácido tri-fluoropalmítico causa um decréscimo no potencial do filme. Entretanto, este decréscimo não é linear com a variação da concentração como deveria ocorrer de acordo com o modelo DF. Nossa explicação para este desvio de comportamento (vide [14]) é que a constante dielétrica efetiva do filme sofre alterações devido à mudança na polarizabilidade do meio com a introdução dos átomos de flúor no final das caudas, e principalmente porque os filmes mistos não apresentam um grau de estruturação na interface água/filme tão alto como os filmes puros. Este resultado é intrigante pois aparentemente não há razões para que o filme misto seja menos estruturado; a solução deste problema pode ter importantes consequências para os estudos de filmes mistos apresentados na literatura.

2.1.4 Filmes LB de polímeros conjugados

Participação: Doutorandos Luiz Henrique C. Mattoso, Marysilvia Ferreira e Agnieszka Pawlicka, Mestranda Débora Gonçalves, Bacharelandos Antonio Riul Jr. e Cláudia Bonardi, Prof. Roberto Mendonça Faria, e Luiz Otávio de Souza Bulhões.

Uma das áreas mais atraentes para o emprego da técnica Langmuir-Blodgett (LB) é, sem dúvida, a da fabricação de filmes condutores a partir de polímeros de estrutura conjugada. Os filmes LB, após depositados, são dopados de maneira a tornarem-se condutores. O principal interesse nesse tipo de filme está na produção de dispositivos eletrônicos em que o filme de polímero

desempenhe um papel ativo, algo que já foi demonstrado com a construção de FETs (a nível de laboratório) [15]. Dentre os polímeros mais utilizados para este fim estão os derivados da polianilina, politiofeno e polipirrol. A nossa equipe de trabalho está envolvida em pesquisas com polímeros dessas três classes, sendo que já dominamos as técnicas de síntese para os politiofenos e polianilinas, e uma aluna de doutoramento está aprendendo a síntese de polipirróis no Massachusetts Institute of Technology (M.I.T.), Estados Unidos.

Os primeiros resultados com os filmes de Langmuir e LB de poli(o-metoxianilina) serão publicados em breve [16]. A contribuição mais importante do trabalho é de se ter obtido um polímero solúvel em solventes orgânicos, uma vez que esta é a maior dificuldade para a fabricação de filmes LB de polímeros conjugados. Além disso, este é um polímero altamente estável em condições ambientais normais. Pesquisas com estes filmes, agora na tentativa de estudar suas propriedades óticas e elétricas, estão em andamento, assim como as pesquisas com filmes LB de politiofenos. A linha de pesquisa com polímeros conjugados é hoje a que conta com maior número de pesquisadores no grupo de São Carlos.

2.1.5 Filmes de Langmuir de ligninas

Participação: Bacharelando Carlos José Leopoldo Constantino, Doutoranda Débora Balogh, Prof. Antonio Aprígio da Silva Curvello.

A disponibilidade da técnica LB propiciou a realização de um projeto, ainda em andamento, de caracterização de ligninas em conjunto com o Departamento de Físico-Química do IFQSC. Este interesse pela lignina advém de sua grande importância tecnológica, sendo que a técnica LB pode fornecer informações importantes a nível molecular. Por serem anfipáticas, as moléculas de lignina permitem a formação de camadas insolúveis sobre a superfície da água. Esperamos com estes estudos obter informações a respeito do arranjo estrutural das moléculas de lignina sobre a superfície da água. Medidas preliminares já realizadas nos permitiram constatar que há uma perda de filme

quando este é submetido a várias compressões sucessivas. Como as ligninas dificilmente se dissolvem em água, a perda do filme pode estar associada a um empacotamento em camadas bi ou tri-moleculares, mas esta hipótese está sujeita a confirmação.

2.2 Avaliação da Situação Atual da Área de Filmes LB

Em pouco menos de dois anos, conseguimos instalar os equipamentos para produção de filmes de boa qualidade e estabelecemos uma equipe de trabalho bastante dinâmica. Várias frentes de pesquisa foram abertas, uma característica salutar por ser esta uma área altamente interdisciplinar, em que o sucesso de um projeto específico pode depender de resultados obtidos em outros afins. Particularmente importante foi o recrutamento de químicos que estão se especializando em síntese de substâncias orgânicas para a produção de filmes LB. Como em quase todos os ramos da ciência de novos materiais, a síntese química na área de filmes LB é fundamental. Outra característica importante é que o nosso Grupo tem atacado problemas tanto de propriedades fundamentais dos filmes, utilizando compostos simples como ácidos graxos e fosfolipídios, como de possíveis aplicações com o trabalho com polímeros conjugados.

Nos meios científicos parece haver consenso que a avaliação do trabalho de um pesquisador (ou grupo de pesquisa) deve ser centrada na sua produção científica. Portanto, para avaliar os resultados que já obtivemos, poderíamos examinar nossa produção científica neste período de duração das pesquisas em filmes LB em São Carlos. Esta produção, em termos de artigos e comunicações, é ainda bastante modesta para uma equipe relativamente grande (os participantes da equipe foram mencionados nos projetos específicos). Deve-se levar em conta, entretanto, que só agora estamos colhendo os primeiros frutos do trabalho inicial, já que um grande esforço foi dedicado à instalação de equipamentos e da sala limpa, além do treinamento de estudantes. E estes primeiros resultados são altamente promissores, prenúncio de uma produção satisfatória quando o trabalho da equipe estiver em "regime estacionário". Ressalte-se, também, que formamos o grupo, no Brasil, com maior experiência

e contribuição nesta importante área.

III. Outras linhas de pesquisa.

Quando da minha chegada de volta ao Brasil em Julho de 1990, após concluir o doutoramento, tive que esperar algum tempo antes de iniciar o trabalho experimental com filmes LB, embora o processo de aquisição dos equipamentos para a área de filmes LB já tivesse sido iniciado. Procurei, então, engajar-me em projetos de pesquisa de colegas, principalmente na área de polímeros submetidos à descarga corona, um tópico com o qual já havia trabalhado no mestrado. Nos próximos sub-itens será apresentada uma breve descrição do trabalho realizado, incluindo a nova área de atuação em Linguística Computacional.

3.1 Polímeros ferroelétricos e descarga corona

Participação: Engenheirandos Valtencir Zuccolloto, Alessandra Holmo e Angélica Kondo, Mestre Nilton Guedes da Silva, Prof. Neri Alves, Prof. José Alberto Giacometti e Prof. Roberto Mendonça Faria.

O Grupo de Eletretos "Prof. Bernhard Gross" tem grande tradição no estudo de propriedades elétricas de polímeros, principalmente quando estes são submetidos à descarga corona. Dentre as principais contribuições do Grupo está o desenvolvimento dos primeiros triodos de corona com controle de corrente [17], uma técnica que foi posteriormente incorporada por vários laboratórios de pesquisa na Rússia, Estados Unidos, Portugal, Alemanha e China. Um artigo de revisão, escrito em parceria com o Prof. Giacometti [18], será publicado em breve, onde são discutidos os aspectos mais relevantes para o processo de carga de polímeros com descarga corona.

Após a minha volta ao Brasil, retomei minha colaboração com o Prof. Giacometti e orientei um aluno de mestrado na área. Este aluno, Nilton Guedes da Silva [19], desenvolveu os procedimentos experimentais para a fabricação de filmes de copolímeros de fluoreto de vinilideno com trifluoretileno (P(VDF-TrFE)), e

caracterizou estes filmes através de medidas de calorimetria exploratória diferencial de varredura (DSC), difração de Raios-X, e absorção de Infra-vermelho. Os resultados obtidos foram compatíveis com os da literatura para filmes similares, o que demonstra a adequação dos procedimentos experimentais utilizados.

Quanto ao trabalho produzido em polímeros ferroelétricos, um resultado interessante foi a descoberta de que é possível traçar curvas de histerese para estes polímeros, a partir de curvas de potencial de superfície obtidas num triodo de corona [20]. A demonstração inicial foi feita com o polímero PVDF, mas passamos posteriormente a empregar os copolímeros P(VDF-TrFE). Além de permitir a obtenção dos parâmetros ferroelétricos dos filmes, ou seja, o campo coercivo e a polarização remanente, a análise das curvas de potencial de superfície permite também testar os diferentes modelos fenomenológicos para explicar os mecanismos da polarização ferroelétrica [21,22].

Merecem destaque, também, as investigações das características elétricas de triodos de corona e sistemas similares [23,24]. Estes sistemas apresentam problemas de eletrostática interessantes, e são importantes para aplicações práticas, por serem largamente utilizados em indústrias de dispositivos de eletretos e xerografia. Como resultado relevante pode ser mencionada a elucidação da importância da componente eletrônica da descarga corona no processo de tratamento de amostras de polímeros [23].

3.2 Aspectos Fundamentais da Física

Participação: Prof. Guilherme Fontes Leal Ferreira

Da colaboração e extensiva discussão de vários aspectos fundamentais da Física com o Prof. Guilherme Fontes Leal Ferreira, surgiram alguns trabalhos que estão sendo preparados em forma de artigos. O primeiro deles foi publicado recentemente na revista Physics Essays [2], no qual é apresentado um modelo mecânico para o cálculo da tensão superficial de líquidos, que também discute como conciliar tal modelo mecânico com a Termodinâmica. Também preparamos dois artigos que discutem a utilização de entidades abstratas (como os campos) no

Eletromagnetismo, e a possibilidade de se empregar o método da ação direta à distância em problemas de Eletromagnetismo que não incluem radiação. Um desses artigos, tratando da utilização do método de ação direta para calcular a diferença de potencial de uma barra metálica que se desloca num campo magnético uniforme, já foi submetido para publicação [25]. O outro está em fase de preparação, e aborda uma revisão crítica da utilização dos campos eletromagnéticos [26].

3.3 Linguística Computacional

Participação: Bacharelandos Cláudio Yukio Nacamatsu e José Luiz Sorokin, Mestranda Maria do Carmo M. Francischetti, Profa. Sandra Maria Aluisio Caldeira (doutoranda do IFQSC), Profa. Lúcia Helena Machado Rino (doutoranda do IFQSC), Profa. Niura Maria Fontana, Profa. Ariadne M.B.R. Carvalho, Prof. Paulo César Masiero, Profa. Maria Cristina F. Oliveira.

Esta é uma área de pesquisa dentro da Ciência de Computação que trata de problemas relacionados ao uso do computador em pesquisas de Linguística Aplicada. A área engloba, entre outros, campos como o Processamento de Linguagem Natural, e o desenvolvimento de ferramentas de software para ensino de línguas e auxílio em tarefas linguísticas.

Para se compreender porque me envolvi numa área tão exótica (para um físico), faz-se necessário um breve relato de como surgiu este interesse, o que torna esta sub-seção um pouco maior do que as correspondentes na Seção III. Sempre acreditei que escrever bem textos em inglês técnico era um requisito fundamental para o sucesso de uma carreira científica, de maneira que eu procurei melhorar, na medida do possível, o meu desempenho nestas tarefas. Assim, durante o meu doutoramento, estudei não apenas a língua inglesa, mas também as estratégias de redação científica. Por pura intuição, pois na época não possuia quaisquer conhecimentos "formais" de linguística, concluí que a minha maior dificuldade (assim como de muitos estrangeiros), era de não empregar as expressões adequadas, i.e. aquelas empregadas pelos escritores nativos, para desempenhar funções específicas

num texto científico. Este problema faz com que estrangeiros utilizem a estratégia de tradução a partir da sua língua-mãe.

Esta intuição foi confirmada por estudos que mostraram que algumas das deficiências de alunos brasileiros realizando cursos de pós-graduação no exterior, estão relacionadas ao mau uso ou omissão de expressões mais ou menos convencionais que desempenham funções específicas do texto acadêmico [27]. Uma solução prática para este problema consiste na utilização de expressões aprendidas com a prática adquirida na leitura de artigos - acredito ser esta estratégia largamente difundida entre estrangeiros que precisam escrever em inglês. Ou seja, numa situação de dúvida, o escritor recorre a textos escritos por pessoas de reconhecida competência. Para otimizar o uso desta estratégia, foi feita uma compilação de expressões e sentenças extraídas de artigos e livros científicos [28]. Uma verificação surpreendente foi que um número relativamente pequeno de expressões pode ser suficiente, em alguns casos, para cobrir uma grande proporção de sentenças e frases usadas numa certa área do conhecimento. Isto ocorre porque expressões são empregadas de maneira sistemática, quando se descrevem tabelas, figuras, procedimentos experimentais, ou quando se comparam resultados. Anteviu-se portanto, a possibilidade de se criar uma ferramenta de software baseada nesta estratégia.

É importante enfatizar que existem várias ferramentas de software [29-31] para auxiliar no processo de escrita, muitas das quais já estão disponíveis comercialmente. A grande maioria delas é dedicada ao pós-processamento do texto através de análises estatísticas. Apesar de serem extremamente úteis para usuários com dificuldades linguísticas, estas ferramentas são limitadas quanto à escrita numa língua estrangeira, pois proporcionam somente mecanismos de correção e acabamento do texto, sendo que muitas vezes o usuário não é capaz de gerar um texto passível de ser apenas "melhorado". Tais ferramentas, portanto, não resolvem o principal problema dos que precisam escrever numa língua estrangeira e têm dificuldades em fazê-lo.

A proposta de um projeto de pesquisa para desenvolver ferramentas de software de auxílio à escrita foi muito bem

recebida por colegas do Departamento de Computação e Estatística do Instituto de Ciências Matemáticas de São Carlos (ICMSC), USP. Graças ao apoio destes colegas e do Prof. Jan F.W. Slaets, do DFCM, IFQSC, o projeto foi iniciado ainda em 1990, e se desenvolve com grande sucesso no momento. Uma primeira versão da ferramenta, batizada como ***AMADEUS*** (**AM**iable **A**rticle **D**evelopment **E**nvironment for **U**ser **S**upport), foi desenvolvida no ambiente gráfico XVIEW numa estação de trabalho SUN [32]. Ressalte-se que as pesquisas em Linguística Computacional do nosso Grupo de trabalho não se restringem apenas ao desenvolvimento de ferramentas de apoio. Devido à abrangência e riqueza de tópicos interdisciplinares que podem ser investigados, estamos atuando em várias sub-áreas da Ciência da Computação, para as quais produzimos artigos que discutem os aspectos da interface usuário-máquina [33] e da importância linguístico-pedagógica da estratégia utilizada no *AMADEUS* [34]. O projeto deu origem, ainda, a pesquisas em Processamento de Linguagem Natural, que estão sendo realizadas por colegas não necessariamente envolvidos na construção das ferramentas. O nosso grupo de pesquisa acredita que grandes progressos poderão ser alcançados quando as primeiras versões de ferramentas forem colocadas à disposição da comunidade científica, o que deve ocorrer em futuro próximo.

IV. Comentários Finais

Nesta seção tentarei fazer uma análise das contribuições que julgo serem as mais importantes, e das perspectivas para o trabalho no futuro. Na minha área principal, filmes Langmuir-Blodgett, ressalta-se a implantação da técnica, e formação de um grupo de pesquisa que coloca São Carlos no cenário internacional, como sendo o primeiro grupo brasileiro com contribuições na área. Este trabalho foi feito em parceria com o Prof. Roberto Mendonça Faria, que tem trabalhado com polímeros condutores. Filmes LB de polímeros condutores constituem um dos campos mais promissores não só para a aplicação da tecnologia LB, como para a Ciência dos Materiais de um modo geral. Este grupo de trabalho já demonstrou ter capacidade de atuar e competir em várias áreas de filmes LB,

como propriedades fundamentais dos filmes e polímeros condutores. No que tange aos estudos fundamentais de filmes de Langmuir e LB, meu trabalho é também fruto do aproveitamento da experiência adquirida em Bangor com modelos de potencial de superfície, já que com o meu trabalho de doutoramento, o grupo de Bangor passou a ser um dos líderes deste campo.

No trabalho com polímeros ferroelétricos, minha participação é obviamente secundária. Ela é porém decisiva, pois tenho auxiliado na interpretação e organização dos diversos resultados obtidos por colegas do Grupo de Eletretos, o que tem permitido uma melhoria na produção científica do grupo. É um ótimo exemplo de capacidade de trabalho em grupo. Nos aspectos fundamentais da Física tenho atuado basicamente como interlocutor do Prof. Guilherme F. Leal Ferreira, o que muito me honra, como físico, e ensina. Acredito que esta participação permite que o Prof. Guilherme possa estender sua atuação nessa área.

No projeto de Linguística Computacional, a minha principal participação foi na concepção da idéia do ambiente de auxílio à escrita. Tenho também contribuído para agilizar interações multidisciplinares, envolvendo vários ramos da Informática e da Linguística. O projeto se desenvolve de maneira plenamente satisfatória, e poderá ter um grande impacto na comunidade científica brasileira. O espírito de inovação e a coragem de atacar problemas em áreas altamente interdisciplinares são características fundamentais da nossa equipe de trabalho.

As perspectivas para o trabalho futuro são extremamente promissoras. Agora que já contamos com um grupo formado e atuando em filmes LB, podemos estender nossa atuação para diversos campos que utilizam a tecnologia LB, como o estudo de filmes de importância biológica e pesquisas em Eletrônica Molecular. O projeto de construção de um ambiente de auxílio à escrita está em andamento e pode abrir novas áreas de pesquisa, principalmente com relação à interação linguagem natural - computador. Espero também que a colaboração com os colegas do departamento, tanto na área de polímeros como em outras áreas da Física, possa continuar profícua como tem sido até o momento.

Resumo das Contribuições

Para sumarizar as atividades de pesquisa realizadas desde a obtenção do título de doutoramento, discrimino as diversas contribuições a seguir. A lista completa das contribuições podem ser encontradas no final deste texto.

Artigos publicados e/ou aceitos para publicação em revistas internacionais com referees 7
Artigos submetidos para publicação em revistas internacionais com referees 4
Publicação em livro 1
Artigos Completos em Congressos Internacionais 8
Resumos em Congressos Internacionais 4
Artigos Completos em Congressos Nacionais 8
Resumos em Congressos Nacionais 14
Artigos de Divulgação Científica 3

Orientação de Tese: Tese de Mestrado "Fabricação e Caracterização de Filmes de Copolímeros P(VDF-TrFE)", defendida pelo aluno Nilton Guedes da Silva em Junho/92.

Agradecimentos

O trabalho científico descrito neste texto não poderia ter sido realizado sem a inestimável colaboração dos diversos participantes mencionados nos projetos específicos. Fica aqui o meu agradecimento a todos estes colegas. Eu gostaria de agradecer, em especial, aos colegas do Grupo de Eletretos, os professores Guilherme F. Leal Ferreira, José Alberto Giacometti e Roberto Mendonça Faria, à secretária Yvone A. Biason Lopes, e aos técnicos Ademir Soares, José Roberto Bertho e Níbio J. Mangerona, não só pela colaboração mas também por propiciarem um excelente clima de trabalho. Finalmente, agradeço à minha esposa Cristina, pelo apoio e incentivo constante e pela incansável ajuda na leitura e correção de meus trabalhos.

Referências

[1] O.N.Oliveira Jr., **Langmuir-Blodgett Films: Properties and Possible Applications**, a ser publicado na Braz. J. Phys.

[2] G.F.Leal Ferreira and O.N.Oliveira Jr., Physics Essays, 5 (1992) 245-249

[3] G.F.Leal Ferreira and O.N.Oliveira Jr., **A New Approach for Interpreting Surface Pressure-Area Isotherms**, V International Conference on Langmuir-Blodgett Films, Paris, Agosto de 1991, p. B120

[4] S.Hénon and J.Meunier, Thin Solid Films, 210 (1992) 121-123

[5] D.Honig and D.Moebius, **Reflectometry under the Brewster Angle as a Tool to Determine Film Thickness, Headgroup Influence and Macroscopic Inhomogeneities of Monolayers at the air/water Interface**, V International Conference on Langmuir-Blodgett Films, Paris, Agosto de 1991, p. B06

[6] H.Mohwald, Thin Solid Films, 159 (1988) 1-15

[7] F.M.Menger, S.D.Richardson and G.R.Bromley, J.Am.Chem.Soc., 111 (1989) 6893-6894

[8] H.Morgan, D.M.Taylor and O.N.Oliveira Jr., Thin Solid Films, 178 (1989) 73-79

[9] A.Cavalli e O.N.Oliveira Jr., Anais do XV Encontro Nacional de Física da Matéria Condensada, p. 379. Tese de Mestrado de Ailton Cavalli, em preparação.

[10] O.N.Oliveira Jr., Electrical Properties of Langmuir Monolayers and Deposited Langmuir-Blodgett Films, PhD. Thesis - University of Wales, Bangor (1990).

[11] O.N.Oliveira Jr., D.M.Taylor and H.Morgan, Thin Solid Films, 210 (1992) 76-78

[12] R.J.Demchak and T.J.Fort Jr., J. Colloid Interface Sci., 46 (1974) 191-202

[13] V.Vogel, PhD. Thesis - University of Frankfurt (1987).

[14] O.N.Oliveira Jr., A.Riul Jr., L.E.Amancio and G.F.Leal Ferreira, **Surface Potentials of Mixed Langmuir Films**, a ser apresentado na IV European Conference on Organized Thin Films, em Bangor, Setembro/92.

[15] M.F.Rubner and T.A.Skotheim, **Controlled Molecular Assemblies of Electrically Conductive Polymers**, In:

Conjugated Polymers, J.L.Bredás and R.Silbey (eds.), (1991), pp. 363-403.

[16] R.M.Faria, L.H.C.Mattoso, M.Ferreira, D.Gonçalves, L.O.S.Bulhões, and O.N.Oliveira Jr., **Chloroform-Soluble Polyaniline Derivatives for LB film Fabrication**, In: 6th International Conference on Solid Films and Surfaces, Paris, França, Junho, 1992.

[17] J.A. Giacometti. **Corona with constant current: A new method for studying charge storage and transport in insulators**, Tese de Doutoramento, IFQSC, USP (1982)

[18] J.A.Giacometti and O.N.Oliveira Jr., **Corona Charging of Polymers**, a ser publicado na Digest of Literature on Dielectrics, do IEEE Trans. on Electrical Insulation.

[19] N.G.Silva, **Preparação e Caracterização de Filmes dos Copolímeros P(VDF-TrFE)**, IFQSC, USP (1992)

[20] N.Alves, J.A.Giacometti and O.N.Oliveira Jr., **Measuring hysteresis loops of ferroelectric polymers using the constant charging current corona triode**, Rev.Sci.Instrum., 62, (1991) 1840-1843

[21] N.Alves, J.A.Giacometti, O.N.Oliveira Jr., and R.M.Faria, **On the equivalence of the mechanisms governing switching and hysteresis phenomena**, VII International Symposium on Electrets ISE-7, Berlim, Alemanha, Setembro, 1991.

[22] N.Alves, J.A.Giacometti, G.Minami and O.N.Oliveira Jr., **Ferroelectric Behavior of P(VDF-TrFE) Copolymer Samples**, a ser apresentado na 1992 CEIDP, organizada pelo IEEE (EUA), em Victoria, Canadá.

[23] D.L.Chinaglia, G.F.Leal Ferreira, J.A.Giacometti and O.N.Oliveira Jr., **Corona-triode characteristics: on effects possibly caused by the electronic component**, In: VII International Symposium on Electrets, ISE-7, Berlim, Alemanha, Setembro, 1991.

[24] J.S.C.CAMPOS, J.A.Giacometti and O.N.Oliveira Jr., **Electrical Characteristics of Point to Plate Corona Systems with a Biased Cylinder**, a ser apresentado na 1992 CEIDP, organizada pelo IEEE (EUA), em Victoria, Canadá.

[25] G.F.Leal Ferreira and O.N.Oliveira Jr., **Is it Sound to Carry on Using Abstract Entities?**, submetido para publicação na revista Galilean Electrodynamics

[26] G.F.Leal Ferreira and O.N.Oliveira Jr., **Forces and Fields in Electromagnetism**, a ser submetido para publicação.

[27] N.M.Fontana e O.N.Oliveira Jr., "O Texto Acadêmico em Inglês como Língua Estrangeira - Dificuldades e Perspectivas", Anais do IX Simpósio Nacional de Ensino de Física, São Carlos, S.P., Janeiro, 1991.

[28] O.N.Oliveira Jr., S.M.A.Caldeira and N.Fontana, "Chusaurus: A Writing Tool Resource for Non-native Users of English", XI International Conference of the Chilean Computer Science Society, pp. 59-70, Santiago, Chile, 1991. A ser publicado também no livro **Computer Science: Research and Applications**, editado por R.Baeza-Yates e U.Manber, a ser publicado em Julho/92 pela Plenum Press.

[29] P.A.Carlson, "Cognitive Tools and Computer-Aided Writing", AI Expert, pp. 100-105, October 1990.

[30] J.Matzkin, "Grammar Checkers Improve, But Won't Replace Your English Teacher", PC Magazine, p. 46, March, 13, 1990.

[31] L.Cherry, "Writing Tools", IEEE Trans. Commun., Vol. Com-30, pp. 100-105, January, 1982.

[32] S.M.A.Caldeira, M.C.F. de Oliveira, N.M.Fontana, C.Y.Nacamatsu and O.N.Oliveira Jr., "Writing tools for non-native users of English", a ser apresentado no XVIII Latinamerican Informatics Conference, Las Palmas, Ilhas Canárias, Espanha, Setembro de 1992.

[33] M.C.F. De Oliveira, S.M.A. Caldeira, P.C. Masiero and O.N.Oliveira Jr., "A Discussion on human-computer interfaces for writing supportt tools", a ser apresentado na XI International Conference of the Chilean Computer Science Society, Santiago, Chile, Novembro de 1992.

[34] N.M.Fontana, S.M.A.Caldeira, M.C.F. De Oliveira and O.N.Oliveira Jr., Computer Assisted Writing - Applications to English as a Foreign Language, a ser submetido para publicação na revista CALL (Computer Assisted Language Learning).

Lista das Contribuições Após o Término do Doutoramento

1. Trabalhos Publicados em Revistas Especializadas

ALVES, N.; GIACOMETTI,J.A.; OLIVEIRA JR.,O.N. - Measuring hysteresis loops of ferroelectric polymers using the constant charging current corona triode. Rev.Sci.Instrum., 62, 1840 (1991).

LEAL FERREIRA,G.F. & OLIVEIRA JR.,O.N. - Force, energy and mechanical models for surface tension, Physics Essays, 5, 245 (1992).

OLIVEIRA JR.,O.N.; TAYLOR,D.M.; MORGAN,H. - Modelling the surface potential-area dependence of a stearic acid monolayer. Thin Solid Films, 210, 76 (1992).

OLIVEIRA JR.,O.N.; TAYLOR,D.M.; STIRLING,C.J.M.; TRIPATHI,S.; GUO,B.Z. - Surface potential studies of Langmuir monolayers and Langmuir-Blodgett deposited films of *p*-$MEC_6H_4S(O)-(CH_2)_{11}-S-(CH_2)_{10}-COOH$, Langmuir, 8, 1619 (1992).

OLIVEIRA JR.,O.N., Langmuir-Blodgett Films: Properties and Possible Applications, a ser publicado na revista Braz. J. Phys.

GIACOMETTI,J.A.; OLIVEIRA JR.,O.N.; Corona Charging of Polymers, a ser publicado na revista Digest of Literature on Dielectrics, do IEEE (USA).

FARIA,R.M; MATTOSO,L.H.C.; FERREIRA,M.; GONÇALVES,D.; BULHÕES,L.O.S.; OLIVEIRA JR.,O.N.; Chloroform-Soluble Poly(o-metoxyaniline) for Ultra-thin Film Fabrication, a ser publicado na revista Thin Solid Films.

CHINAGLIA,D.L.; LEAL FERREIRA,G.F.; GIACOMETTI,J.A.; OLIVEIRA JR.,O.N.; Corona Triode Current-Voltage Characteristics: On Effects Possibly Caused by the Electronic Component, submetido para publicação na revista J.Phys. D: Appl. Phys.

GONÇALVES,D.; FARIA,R.M.; OLIVEIRA JR.,O.N.; SWORAKOWSKI,J.; Langmuir-Blodgett Films of Poly(o-anisidine), submetido para publicação na revista Synthetic Metals.

FARIA,R.M.; GUIMARÃES NETO,J.M.; OLIVEIRA JR.,O.N.; Thermal Studies on VDF/TrFE Copolymers, submetido para publicação na revista J.Mat.Sci.

LEAL FERREIRA,G.F. & OLIVEIRA JR.,O.N.; Is it Sound to Carry on Using Abstract Entities, submetido para publicação na revista Galilean Electrodynamics.

2. Publicação em Livro

OLIVEIRA JR.,O.N., CALDEIRA,S.M.A.; FONTANA,N. - CHUSAURUS: A writing tool resource for non-native users of English. In: Computer Science: Research and Applications, eds. U.Manber and R.Baeza-Yates, Plenum Press. A ser publicado em Julho/92

3. Trabalhos Publicados em Revistas de Divulgação

OLIVEIRA JR.,O.N. & TAYLOR,D.M. - O Largo Potencial dos Filmes Finos, Ciência Hoje, no. 67, Outubro de 1990.

OLIVEIRA JR.,O.N. - O desafio da Eletrônica Molecular, J.Alta Tecnol., São Carlos, 4, 15 (1991).

OLIVEIRA JR.,O.N. - A importância da Redação Científica, Jornal da USP, no. 212, 13-26 de Abril, (1992).

4. Comunicações em Congressos e Simpósios

4.1 Nacionais

FONTANA,N., OLIVEIRA JR.,O.N. - O Texto Acadêmico em Inglês como Língua Estrangeira - Dificuldades e Perspectivas. In: IX Simpósio Nacional de Ensino de Física, São Carlos-SP, Janeiro, 1991.

OLIVEIRA JR.,O.N. - A Escrita Científica no Ensino de Física, In: IX Simpósio Nacional de Ensino de Física, São Carlos-SP, Janeiro, 1991.

CALDEIRA,S.M.A., CARVALHO,A.M.B.R., OLIVEIRA JR.,O.N. - Um Ambiente para a Criação de Textos em Inglês. In: IX Simpósio Nacional de Ensino de Física, São Carlos-SP, Janeiro, 1991.

OLIVEIRA JR.,O.N., FARIA,R.M., FERREIRA,M. - Propriedades elétricas de filmes Langmuir-Blodgett obtidos de polipirrol. In: XIV Encontro Nacional de Física da Matéria Condensada, SBF, Caxambú-MG, Maio, 1991.

ALVES,N., GIACOMETTI,J.A., OLIVEIRA JR.,O.N., FARIA,R.M. - A equivalência dos mecanismos que governam os fenômenos de chaveamento e histerese. In: XIV Encontro Nacional de Física da Matéria Condensada, Caxambú-MG, Maio, 1991.

ALVES,N., GIACOMETTI,J.A., OLIVEIRA JR.,O.N. - Medidas da curva de histerese em polímeros ferroelétricos usando o triodo de corona com corrente constante. In: XIV Encontro Nacional de Física da Matéria Condensada, Caxambú-MG, Maio, 1991.

OLIVEIRA JR.,O.N. - Aplicação do modelo de Demchak-Fort ao potencial de superfície de filmes de Langmuir. In: XIV Encontro Nacional de Física da Matéria Condensada, Caxambú-MG, Maio, 1991.

OLIVEIRA JR.,O.N. - Estudo de filmes Langmuir-Blodgett através de medidas de potencial de superfície. In: XIV Encontro Nacional de Física da Matéria Condensada, Caxambú-MG, Maio, 1991.

SILVA,N.G., OLIVEIRA JR.,O.N., GIACOMETTI,J.A., ALVES,N. - Preparação e caracterização de filmes do copolímero P(VDF-TrFE). In: XIV Encontro Nacional de Física da Matéria Condensada, Caxambú-MG, Maio, 1991.

OLIVEIRA JR.,O.N.; AMANCIO,L.E. - Simulação por computador de curvas de potencial de superfície de filmes de Langmuir. In: XIV Encontro Nacional de Física da Matéria Condensada, Caxambú-MG, Maio, 1991.

CALDEIRA,S.M.A., OLIVEIRA JR.,O.N. - Proposta de um ambiente para auxiliar na produção de textos científicos em inglês. In: Congresso Nacional de Informática, 24., São Paulo-SP, Setembro, 1991.

SILVA,N.G., OLIVEIRA JR.,O.N., GIACOMETTI,J.A., ALVES,N. - Preparação de Filmes do Copolímeros P(VDF- TrFE). In: I Congresso Brasileiro de Polímeros, São Paulo-SP, Setembro, 1991.

ALVES, N., GIACOMETTI, J.A., SILVA, N.G., OLIVEIRA JR., O.N. - Estudo das propriedades da polarização ferroelétrica em polímeros de fluoreto de polivinilideno (PVDF) e seus copolímeros com trifluoretileno P(VDF-TrFE). In: Congresso Brasileiro de Polímeros, São Paulo-SP, Setembro, 1991.

OLIVEIRA JR.,O.N. - Aplicação do modelo de Demchak-Fort ao potencial de superfície de filmes de Langmuir. In: XIV Encontro Nacional de Física da Matéria Condensada, Caxambú-MG, Maio, 1991.

OLIVEIRA JR.,O.N. - Estudo de filmes Langmuir-Blodgett através de medidas de potencial de superfície. In: XIV Encontro Nacional de Física da Matéria Condensada, Caxambú-MG, Maio, 1991.

SILVA,N.G., OLIVEIRA JR.,O.N., GIACOMETTI,J.A., ALVES,N. - Preparação e caracterização de filmes do copolímero P(VDF-TrFE). In: XIV Encontro Nacional de Física da Matéria Condensada, Caxambú-MG, Maio, 1991.

OLIVEIRA JR.,O.N.; AMANCIO,L.E. - Simulação por computador de curvas de potencial de superfície de filmes de Langmuir. In: XIV Encontro Nacional de Física da Matéria Condensada, Caxambú-MG, Maio, 1991.

CALDEIRA,S.M.A., OLIVEIRA JR.,O.N. - Proposta de um ambiente para auxiliar na produção de textos científicos em inglês. In: Congresso Nacional de Informática, 24., São Paulo-SP, Setembro, 1991.

SILVA,N.G., OLIVEIRA JR.,O.N., GIACOMETTI,J.A., ALVES,N. - Preparação de Filmes do Copolímeros P(VDF- TrFE). In: I Congresso Brasileiro de Polímeros, São Paulo-SP, Setembro, 1991.

ALVES, N., GIACOMETTI, J.A., SILVA, N.G., OLIVEIRA JR., O.N. - Estudo das propriedades da polarização ferroelétrica em polímeros de fluoreto de polivinilideno (PVDF) e seus copolímeros com trifluoretileno P(VDF-TrFE). In: Congresso Brasileiro de Polímeros, São Paulo-SP, Setembro, 1991.

GONZALEZ, J.P.D.; NASCIMENTO, O.R.; OLIVEIRA JR.; O.N. - Os laboratórios de Física: um novo método de avaliação. In: Encontro: Experiências Inovadoras de Ensino na Universidade de São Paulo, São Paulo-SP, Outubro, 1991.

RIUL JR., A; AMANCIO, L.E.; OLIVEIRA JR., O.N.; LEAL FERREIRA, G.F., Simulação por Computador de Curvas de Potencial de Superfície de Filmes de Langmuir Mistos. In: XV Encontro Nacional de Física da Matéria Condensada, Caxambú-MG, Maio, 1992.

CAVALLI, A.; OLIVEIRA JR., O.N., Homogeneidade de Filmes de Langmuir, In: XV Encontro Nacional de Física da Matéria Condensada, Caxambú-MG, Maio, 1992.

CONSTANTINO, C.J.L.; FERREIRA, M.; CURVELO, A.A.S.; OLIVEIRA JR.; O.N., Filmes de Langmuir de Ligninas, In: XV Encontro Nacional de Física da Matéria Condensada, Caxambú-MG, Maio, 1992.

OLIVEIRA JR., O.N., Possíveis Aplicações de Filmes Langmuir-Blodgett, In: XV Encontro Nacional de Física da Matéria Condensada, Caxambú-MG, Maio, 1992.

FERREIRA, M.; MATTOSO, L.H.C.; GONÇALVES, D.; OLIVEIRA JR., O.N.; FARIA, R.M., Filmes Langmuir-Blodgett de Poli(o-metoxianilina), In: XV Encontro Nacional de Física da Matéria Condensada, Caxambú-MG, Maio, 1992.

ALVES, N.; HOLMO, A.C.; GIACOMETTI, J.A.; OLIVEIRA JR., O.N., Dependência da Polarização Remanente de Filmes de P(VDF-TrFE) com a Cristalinidade de Filmes Preparados por Solução, In: XV Encontro Nacional de Física da Matéria Condensada, Caxambú-MG, Maio, 1992.

CAVALLI, A; OLIVEIRA JR.; Potencial de Superfície de filmes de Langmuir de Fosfolipídios, Congresso de Pós-Graduação em Ciência e Engenharia de Materiais, São Carlos-SP, Junho, 1992.

SILVA, N.G.; ALVES, N.; OLIVEIRA JR., O.N., Caracterização Térmica dos Copolímeros P(VDF-TrFE) por Calorimetria Exploratória Differencial de Varredura (DSC), Congresso de Pós-Graduação em Ciência e Engenharia de Materiais, São Carlos-SP, Junho, 1992.

4.2 Internacionais

OLIVEIRA JR.,O.N., TAYLOR,D.M., MORGAN,H. - Modelling the surface potential-area dependence of a stearic acid monolayer, In: V International Conference on Langmuir-Blodgett Films, Paris, França, Agosto, 1991.

LEAL FERREIRA,G.F. & OLIVEIRA JR.,O.N. - A new possible approach for interpreting surface pressure-area isotherms, In: V International Conference on Langmuir-Blodgett Films, Paris, França, Agosto, 1991.

CHINAGLIA,D.L.; LEAL FERREIRA,G.F.; GIACOMETTI,J.A.; OLIVEIRA JR.,O.N. - Corona-triode characteristics: on effects possibly caused by the electronic component. In: VII International Symposium on Electrets, ISE-7, Berlim, Alemanha, Setembro, 1991.

ALVES,N.; GIACOMETTI,J.A.; OLIVEIRA JR.,O.N.; FARIA,R.M. - On the equivalence of the mechanisms governing switching and hysteresis phenomena. VII International Symposium on Electrets ISE-7, Berlim, Alemanha, Setembro, 1991.

OLIVEIRA JR.,O.N.; CALDEIRA,S.M.A.; FONTANA,N. - CHUSAURUS: A writing tool resource for non-native users of English.

In: International Conference of the Chilean Computer Science Society, Santiago, Chile, Outubro, 1991.

FARIA, R.M., MATTOSO, L.H.C., FERREIRA, M., GONÇALVES,D., BULHÕES,L.O.S. AND OLIVEIRA JR.,O.N., Chloroform-Soluble Polyaniline Derivatives for LB film Fabrication", In: 6th International Conference on Solid Films and Surfaces, Paris, França, Junho, 1992.

MATTOSO, L.H.C., FERREIRA, M., GONÇALVES, D., BULHÕES,L.O.S., OLIVEIRA JR., O.N. AND FARIA, R.M., Langmuir Monolayers and Deposited LB Films of Poly(o-Metoxyaniline), In: International Conference on Science and Technology of Synthetic Metals", Gotemburgo, Suécia, Agosto, 1992.

CALDEIRA, S.M.A.; DE OLIVEIRA, M.C.F.; FONTANA, N.M.; NACAMATSU, C.Y.; OLIVEIRA JR., O.N., Writing Tools for Non-native Users of English, XVIII Latinamerican Informatics Conference, Las Palmas, Ilhas Canárias (Espanha), Setembro, 1992.

ALVES, N.; GIACOMETTI, J.A.; MINAMI, G., OLIVEIRA JR., O.N., Ferroelectric Behavior of P(VDF-TrFE) Copolymer Samples, a ser apresentado na 1992 CEIDP, organizada pelo IEEE (EUA), em Victoria, Canadá.

ALTAFIM, R.A.C.; NUNES, V.A.A.; GIACOMETTI, J.A.; OLIVEIRA JR., O.N., Electrical Discharges in Small Air Gaps, a ser apresentado na 1992 CEIDP, organizada pelo IEEE (EUA), em Victoria, Canadá.

CAMPOS, J.S.C.; GIACOMETTI, J.A.; OLIVEIRA JR., O.N., Electrical Characteristics of Point to Plate Corona Systems with a Biased Cylinder, a ser apresentado na 1992 CEIDP, organizada pelo IEEE (EUA), em Victoria, Canadá.

DE OLIVEIRA, M.C.F.; CALDEIRA,S.M.A.; MASIERO,P.C.; OLIVEIRA JR.,O.N. - A Discussion on Human-computer Interfaces for Writing Support Tools, In: XI International Conference of the Chilean Computer Science Society, Santiago, Chile, Novembro, 1992.

APÊNDICE

A seguir são anexadas cópias dos artigos de revistas internacionais com referees, uma cópia do artigo a ser publicado em um livro da Plenum Press e um artigo de Conferência que descreve o ambiente de auxílio à escrita de textos científicos.

ALVES, N.; GIACOMETTI, J. A.; OLIVEIRA JUNIOR, O. N. Measuring hysteresis loops of ferroelectric polymers using the constant charging current corona triode. **Review of Scientific Instruments**, New York, v.62, n.7, p.1840-3, July 1991.

LEAL FERREIRA, G. F.; OLIVEIRA JUNIOR, O. N. Force, energy, and mechanical models for surface tension. **Physics Essays**, Ontario, v. 5, n. 2, p. 245-249, 1992.

OLIVEIRA JUNIOR, O. N.; TAYLOR, D. M.; STIRLING, C. J. M.; TRIPATHI, S.; GUO, B. Z. Surface potential studies of langmuir monolayers and langmuir-blodgett deposited films of *p*-$MeC_6H_4S(O)(CH_2)_{11}S(CH_2)_{10}COOH$. **Langmuir**, Washington, v.8, n.6, p.1619-26, 1992.

Langmuir-Blodgett Films - Properties and Possible Applications

Osvaldo N. Oliveira Jr.

Instituto de Física e Química de São Carlos, Universidade de São Paulo
Caixa Postal 369, São Carlos, 13560, S.P. - Brasil

Received , 1992

Langmuir-Blodgett (LB) films are ultra thin organic films obtained from the successive deposition of monolayers from the water surface onto a solid substrate. They possess interesting properties such as controllable thickness, surface uniformity and a high degree of orientational order, which make them potential candidates for application in electronic devices and sensors.

I. Introduction

One of the most demanding challenges in materials science today is the development of new materials with tailored properties to suit specific applications. The ultimate goal is the engineering of molecules which would be the building blocks for sensors and electronic devices, in the emerging field of molecular electronics. Such ambitious endeavors will only be achieved if experimental techniques are available which allow the assembling of molecules to form two or three dimensional structures. The Langmuir-Blodgett (LB) technology is perhaps the most promising of such techniques because it allows the fabrication of ultra thin, highly ordered organic films. In the LB method, a one molecule thick layer (Langmuir monolayer) spread at the air/water interface is transferred onto a solid substrate, a process that can be repeated several times with the same substrate to form multilayer films.

In this paper, several aspects of LB films and Langmuir monolayers will be reviewed. In Section II, following a brief hystorical note the experimental procedures for the film fabrication are described. The most important LB forming materials are discussed in Section III, while Section IV deals with the characterization of Langmuir monolayers as well as LB deposited films. The many possible applications of LB films are discussed in Section V in which a special subsection has been provided for introducing the topic of molecular electronics. Section VI closes the paper with the state of the art. Because literature on LB films and Langmuir monolayers is abundant ([illegible] only) a few papers will be listed here which may be starting points for those who wish to further their knowledge in the field.

II. Langmuir Monolayer and LB Film Fabrication

Insoluble monolayers are formed on the surface of a clean liquid which has a high surface tension (e.g. water) by the spreading of insoluble, non-volatile substances over the surface. Spreading occurs when the molecules of the substance, generally possessing a hydrophilic head and a long hydrophobic tail (see Section III), are attracted to the water more than they attract each other. A one molecule thick film, termed Langmuir monolayer, is formed provided that the area of the surface is sufficient to accommodate all the molecules spread. The history of insoluble monolayers can be traced back to ancient times, for Aristotle in ancient Greece was reported to have noted the calming effect of oil on a water surface. Following studies from the end of last century by Agnes Pockels and Lord Rayleigh - the latter was the first to suggest that the oil film could be one molecule thick - Langmuir in 1917 introduced new theoretical concepts and experimental methods which were to prove of major importance to the study of these films. Today, the subject of insoluble monolayers at the air/water interface is a well-established topic addressed in the majority of texts of Physical Chemistry of Surfaces.

The equipment used for the production of Langmuir monolayers and/or LB deposited films has become traditionally referred to as a Langmuir trough (Figure 1). Basically it consists of a container which holds a liquid subphase on which the monolayer is spread, barriers to enable film compression and other measuring apparatus for monolayer characterization. Included in these are a surface pressure sensor and a position detector attached to the barriers to measure the surface area of the film. The container must be made from an inert material such as Teflon which does not contaminate the aqueous subphase. The trough and barrier arrangement must

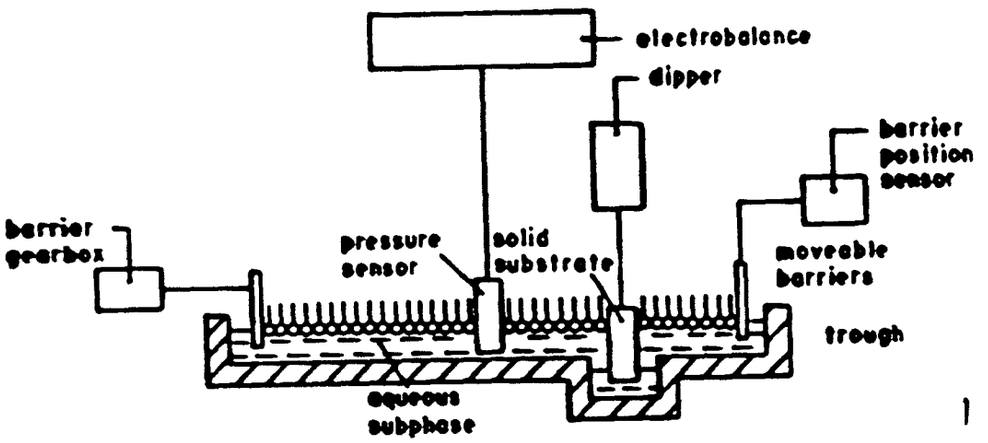

Figure 1: Langmuir trough. The monolayer is spread on the surface of an aqueous subphase, and then compressed by means of moveable barriers. A pressure sensor/electrobalance arrangement measures the surface pressure, and the area per molecule is obtained from the total area given by the barrier position sensor. The dipper controls the immersion and withdrawal of the solid substrate for monolayer deposition.

provide a means for constraining and compressing the monolayer.

The material is dissolved in an appropriate organic, volatile solvent (e.g. chloroform) and dispensed onto the surface of an aqueous subphase. The solvent evaporates within a short time and the molecules then left spread over the whole water surface. The monomolecular layer, so-called Langmuir monolayer, is compressed until the molecules are aligned in a regular arrangement. Langmuir-Blodgett films are fabricated by immersing a clean substrate into the monolayer-covered aqueous subphase, as illustrated in Figure 2. Repeated dippings of the substrate result in the deposition of a multilayer structure, which in some cases can be up to hundreds of monolayers. A good deposition will depend not only on the nature of the monolayer molecules themselves, but also on subphase conditions such as pH, temperature, and ionic contents, on the speed of immersion and withdrawal of the substrate (dipping speed) and on whether the substrate is hydrophilic or hydrophobic.

LB films usually deposit in a symmetrical mode, referred to as Y-type films, in which the molecules in successive layers adopt a head-to-head and tail-to-tail arrangement as shown in Figure 3a. In the Y-type deposition on a hydrophilic substrate, a monolayer is not picked up by the substrate during the first immersion of the substrate (downstroke), but in subsequent trips deposition always occurs both in the downstrokes as well as in the upstrokes. There are two other types of deposition, the so-called X and Z-types shown schematically in Figures 3b and 3c, where deposition occurs only in the downstrokes or in the upstrokes, respectively. Super-lattices can also be built in which monolayers of different materials are deposited on the same substrate.

In addition to the commonly used vertical dipping method described above, deposition can also be made by surface contact using the horizontal lifting method. Almost any type of solid substrate can be employed in LB deposition, though deposition will only be successful if a number of requirements are met. The most used materials are glass slides, or metal evaporated-glass slides and semiconductor wafers. Prior to deposition, substrates must be thoroughly cleaned and usually rendered either highly hydrophilic or hydrophobic depending on the specific type of deposition that is aimed at.

It is essential that the most stringent cleaning procedures are adopted in the LB work. The Langmuir trough and its accessories need to be free of surface-active materials and greases. Glassware must be scrupulously washed and rinsed copiously with ultra pure water. High purity solvents must be used to avoid any residues being left on the cleaned surface. Also, the water must be of very high purity and be changed at regular intervals, preferably for each new monolayer spread, to avoid bacterial growth known to occur when water is left in the trough for several days.

Ultra pure water is usually supplied by commercially available purification systems, based on ultra filtration and ion exchange techniques. Though these systems are provided with a resistivity meter which allows continuous assessment of the quality of the water, non-ionizable impurities may still pass undetected which will affect monolayer behavior. Surface potential and lateral conductance measurements have been proven to be extremely sensitive to minor concentrations of impurities and may therefore be used to ensure that only

high purity water is employed in Langmuir monolayer and LB film studies.

It is also widely recognised that a dust-free environment is an essential requirement for the production of high quality Langmuir monolayers and LB deposited films. Ideally, the LB apparatus should be housed in a semiconductor clean room with temperature and relative humidity control. To gain access to such a clean room researchers should wear overshoes and special coats and hats aimed at preventing any dust from contaminating the environment.

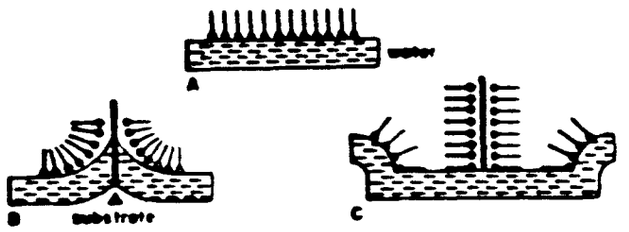

Figure 2: Monolayer deposition. A monolayer is not picked up by the substrate during the first immersion of the substrate (downstroke), but in subsequent trips deposition always occurs both in the downstrokes as well as in the upstrokes.

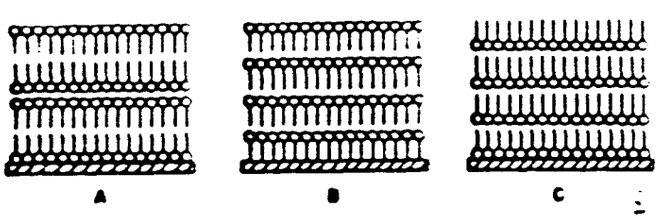

Figure 3: Types of LB deposition. a) Y-type; b) X-type; c) Z-type.

III. LB Forming Materials

The main class of compounds which form stable monolayers on the water surface are those referred to as amphipathic or amphiphilic. Molecules of these compounds possess a highly polar group, which is attracted to the water, and a sufficiently large non-polar moiety (generally a long hydrophobic tail) which prevents the monolayer from dissolving into the water. The polar group is usually located at one end of the molecule so that the molecules can be made to align parallel to each other with the hydrophobic tail protruding from the water surface. The simplest amphiphilic materials are the long chain alkanoic acids, e.g. stearic acid, and their derivatives which have been the most widely investigated compounds. (For a review on LB forming materials, see [13]). Chains containing one or more double bonds can replace the alkyl chain of fatty acids yielding monolayers that are amenable to polymerization. A good example of this type of compound is ω-tricosenoic acid (a 24 carbon fatty acid with a double bond at the end of the hydrocarbon chain) that has been used in LB resists for electron beam litography. Aromatic materials such as the long-chain anthracenes and azobenzenes have also been employed in the fabrication of LB films.

LB films of these simple molecules, however, are usually fragile and have poor thermal stability and mechanical properties. This has prompted the study of LB films made from polymerizable materials and also preformed polymers in a work pioneered by Tredgold and his collaborators in the United Kingdom[14]. Examples of recent use of polymers for LB film fabrication include films made from polyimides, polyglutamate, polydiacetylene, polyisocyanides, octadecyl esters of polyamic acids, and mixed films of hydrophilic and hydrophobic block copolymers. Polymerizable films of a styrene functionalized surfactant, phospholipids and long-chain derivatives of alpha- amino acids and diynoic, trienoic and acrylic acids have also been reported.

The last 2 or 3 years have seen a spectacular increase in the interest in conducting polymer LB films, as the ability to engineer supermolecular structures of a number of conducting polymers has been demonstrated[15]. The wide variety of possible applications together with their excellent mechanical and electroactive properties make the conducting polymers perhaps the current most important class of materials for fabricating LB films. Three main families of conducting polymers have been used so far, namely the poly-alkyl thiophenes, the polypyrroles and the polyanilines. It is worth mentioning that conducting LB films have also been made from non-polymeric materials such as the tetracyanoquinodimethane (TCNQ) salts and the tetrathiafulvalene derivatives.

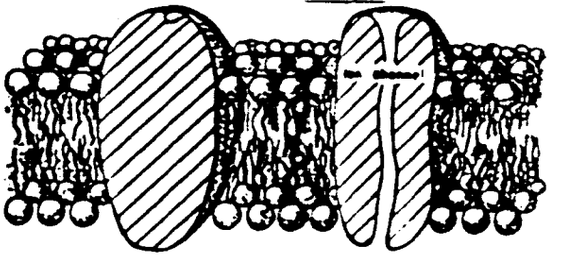

Figure 4: Schematic diagram of a cell membrane. The lipid bilayer is responsible for the structural integrity of the membrane which is traversed by proteins and other constituents. In the picture an ion channel is shown to illustrate how charge transport through the membrane can occur.

Another important class of LB materials comprises

those which are relevant because of their biological implications. According to the fluid mosaic model of Singer and Nicholson shown schematically in Figure 4, the structural framework of a biological membrane is formed from a lipid bilayer, or essentially a two-layer LB film: two parallel monolayers with their headgroups on the outside surfaces and the tails pointing inward; and containing a variety of proteins and lipopolysaccharides (LPS). The lipid molecules, such as cholesterol and phospholipids are the most numerous and are responsible for the structural integrity of the membrane. If proteins and other cell membrane constituents are successfully incorporated into LB films, such structures could serve as realistic models of biological systems on which useful devices could be based. For instance, protein LB films have been suggested for biosensors, and the incorporation of Gramicidin A into DPPC (dipalmitoyl phosphatidylcholine) LB films has been used in high spatial resolution of ionic channels using scanning tuneling microscopy.

There has been renewed interest in the synthesis of novel compounds with specifically tailored electrical and optical properties. Accordingly, sulphoxide-containing compounds and organo-ruthenium complexes with a fatty acid have been used in pyroelectric LB films, and dye-impregnated LB films have been fabricated aimed at a variety of applications such as pn junctions, nonlinear optical films, energy transfer, and coating of optical fibres. The macrocyclic porphyrin and phthalocyanine derivatives have been extensively studied for applications that range from gas sensing devices to electrochromism. Novel materials yielding LB films with unusual, almost unexploited properties have also been studied. Included in these are the ferroelectric side chain polymers, the liquid crystals, and the amphiphilic orthophenanthroline thiocyanato from which magnetic LB films have been deposited.

Some of the materials mentioned in this section are available from chemical suppliers but others have to be synthesized from basic materials. It is often the case that some materials are not suitable for transfer onto a solid substrate because they form monolayers which collapse at relatively low surface pressures. However, in many cases long hydrocarbon chains can be chemically attached to the molecules of interest to improve their stability on the water surface. Some polymer monolayers, on the other hand, are extremely rigid and consequently deposition is not always successful, but this problem can be usually overcome if mixtures of conducting polymers and fatty acids are used, or if appropriate functional groups are added to the polymer molecules.

IV. Characterization

4.1 Langmuir Monolayers

The fabrication and characterization of Langmuir monolayers constitute a field of research in its own right because of the rich variety of electrical, optical, thermodynamical and rheological properties of monolayers which have been under investigation through a variety of experimental techniques. The upsurge of interest in LB films has added a new dimension to the subject of Langmuir monolayers, for the properties of LB films depend on the monolayer characteristics. Important issues in the monolayer characterization are related to the effects of subphase conditions on the monolayer properties, and also its homogeneity and stability on the water surface.

Among the many techniques employed in the characterization of Langmuir monolayers, the surface pressure and the surface potential methods have been the most widespread. After discussing these measurements at some length, other techniques which have also provided relevant information on monolayer behavior wil be discussed briefly.

Surface pressure is defined as the decrease in the surface tension of the liquid owing to the presence of the monolayer. It is normally measured using a Wilhelmy plate/electrobalance arrangement that monitors the force required for the sensing plate to be kept stationary against changes in surface tension. The pressure-area (π-A) isotherm, obtained by compressing the monolayer, is the most commonly used characteristic in the description of a monolayer. Figure 5 (i) shows a typical π-A curve for stearic acid, where A is the average area occupied on the liquid surface by the molecules forming the monolayer. When the monolayer is compressed beyond the steep increase in surface pressure, collapse occurs and the molecules are forced out of the monolayer forming lenses.

The almost featureless π-A curve shown in Figure 5 is characteristic of simple, monofunctionalized molecules and can be interpreted unambiguously, at least qualitatively. For more complex molecules, there is usually the formation of expanded monolayers which is dependent upon factors such as the presence of a second polar group which interfere with the tendency of the chains to pack closely. This is illustrated in Figure 6 for a bi- polar compound that possesses two hydrophilic groups at each end of the molecule. The carboxylic group (COOH) is anchored to the water surface while the *p*-tolyl sulphoxide group is removed from the water surface as the monolayer compression proceeds.

Although a qualitative explanation for the shape of π-A curves can be offered in many cases, a quantitative analysis is much more difficult to be achieved, even for the simplest long- chain alkanoic monolayers. Theoretical studies have been presented in the literature which have attempted to describe phase transitions in fatty acid and phospholipid monolayers quantitatively. These studies encompass thermodynamical analyses based on statistical mechanics and computer simulation techniques.

The surface potential technique is the second most

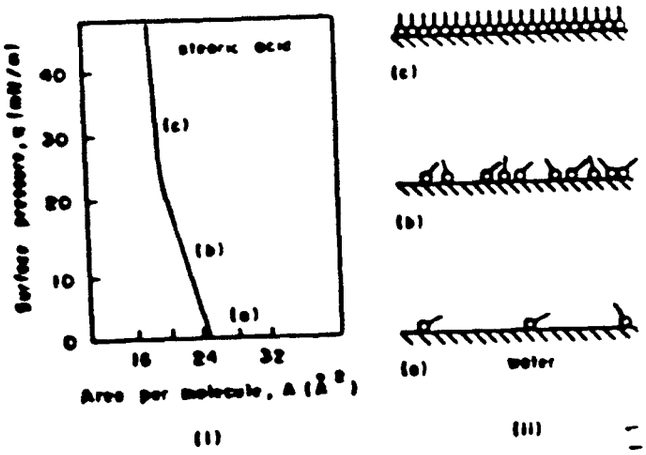

Figure 5: Pressure-area isotherm and molecular configuration. (i) characteristic for a monolayer of stearic acid on ultrapure water. (ii) molecular configuration in the three regions marked in the π-A curve, (a) gaseous phase, (b) liquid-expanded phase, and (c) condensed phase. From ref. [17].

frequently used method for characterizing floating Langmuir monolayers. The surface potential of a monolayer, ΔV, is defined as the difference in potential between a monolayer-covered surface and a clean aqueous surface. In most cases, it is measured using a Kelvin probe. The technique provides valuable information on a number of monolayer effects, especially for identifying phase transitions resulting from molecular orientation during monolayer compression.

The interpretation of surface potential measurements, however, has been plagued with two main types of problem. First, although it has long been established that ΔV arises mainly from the molecular dipoles of the film-forming molecules, discrepancies exist between the measured and the expected values for these dipole moments. Second, the measured monolayer surface potentials for large areas per molecule are usually not reproducible, changing drastically even for consecutive compressions of the same monolayer. Over the last four years these problems have been overcome to a great extent as explained in the following.

The measured ΔV can now be successfully related to the group dipole moment of individual molecules if the monolayer is treated as a 3-layer parallel plate capacitor. In this so-called Demchak and Fort model[16], the measured surface potential is assumed to arise from three main contributions: a moment μ_1 which is caused by the reorientation of water molecules induced by the presence of the monolayer; a moment μ_2 due to the dipoles of the hydrophilic headgroups; and a moment μ_3 assigned to the hydrophobic tails. Each of the 3 layers has a different relative permittivity to account for the different polarisabilities of the medium immediately surrounding the dipoles (Figure 7). When a monolayer is ionised, an additional contribution to the measured surface potential arises from the Gouy-Chapman electrical double layer.

Quantitative agreement between theory and experiment has now been obtained for condensed monolayers of a number of aliphatic compounds by Taylor and coworkers at Bangor, U.K. [16]. An alternative, slightly different model has been suggested by Vogel and Mobius from Goettingen in Germany, in which a 2-layer rather than a 3-layer capacitor is used, and the local permittivities are not considered explicitly. Despite the success of these models, so far they have been applied only to a limited class of compounds and still contain several arbitrary assumptions whose validity needs to be confirmed.

The non-reproducibility of surface potential data for expanded monolayers was a major problem for a long time. The large fluctuations usually observed in the surface potential was attributed to non-homogeneity in the monolayer with the formation of clusters and islands. This non-homogeneity has been identified as originated from extremely low amounts of impurities present in the water surface, and it has been demonstrated that reproducible results can now be obtained for expanded monolayers provided that adequately purified subphase water is employed. While this may be taken as indicator of a (macroscopically) homogeneous monolayer, it has been unequivocally established, on the other hand, that the monolayers are not homogeneous at the microscopic level. Domains of the order of tens of microns have been observed in monolayers of fatty acids by phase contrast microscope and reflectometry under the Brewster angle, and in monolayers of phospholipids and porphyrin-fatty acids by means of fluorescence microscopy. The existence of domains has also been predicted in molecular dynamics simulations for fatty acid monolayers.

Another recent important finding relating to monolayer structuring has been obtained by measuring directly the lateral conductance of phospholipid and fatty acid monolayers. The conductance was shown to occur only when the molecules are packed at or below a critical area per molecule, and has been suggested to arise from proton hopping through a hydrogen-bonded network at the water/monolayer interface. The existence of a critical area has also been confirmed by surface potential, ellipsometry and microscopy measurements, and appears to be related to the growth of the monolayer domains.

Surface pressure, surface potential, and lateral conductance measurements provide only information on the collective behavior of the assembled molecules, and so do some other measurements like surface viscosity and ellipsometry which have also been used in the characterization of Langmuir monolayers. In recent years,

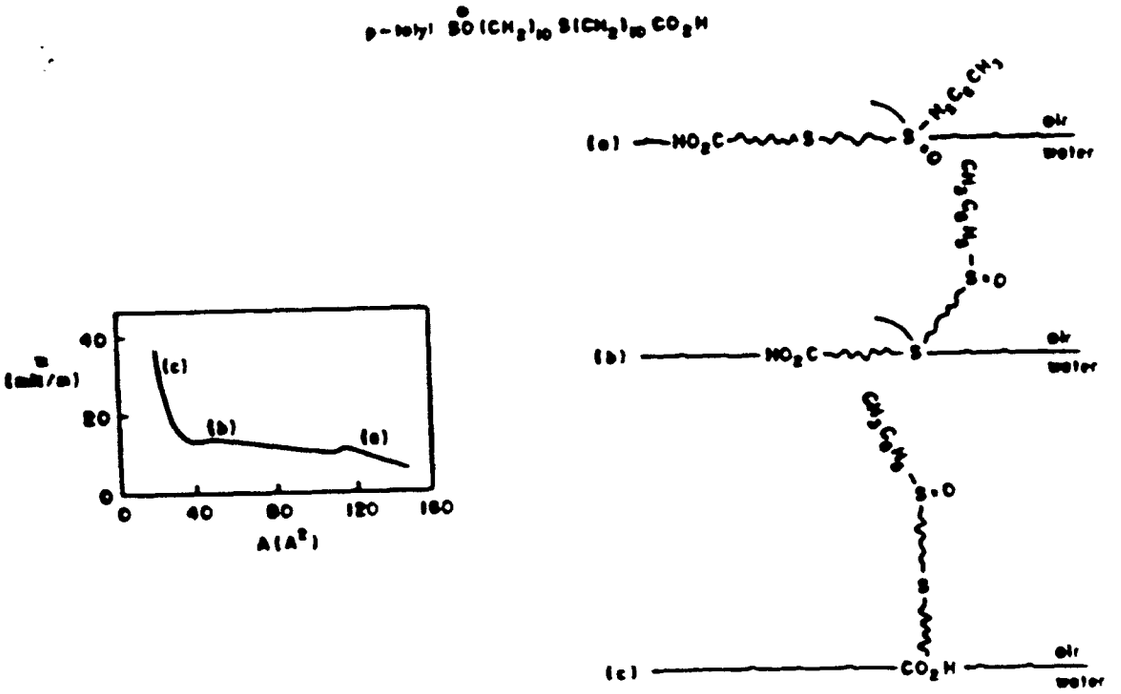

Figure 6: Bipolar compound. (i) π-A characteristic for a monolayer of p-tolyl sulphoxide acid (TSA) on ultrapure water. (ii) possible molecular configuration in the three regions marked in the π-A curve. From ref [17].

molecular ordering has been investigated in which non-linear optical techniques, synchrotron X-ray diffraction and reflection and neutron reflection have been used. These latter methods provide detailed information on chain orientation and packing characteristics, and allow the thickness of the monolayer to be measured to an accuracy of one angstrom.

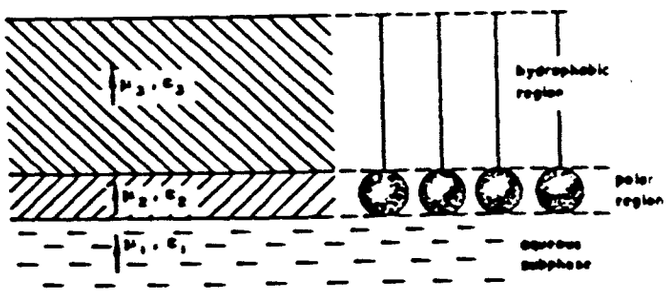

Figure 7: The Demchak and Fort model. The 3-layer capacitor model of a condensed monolayer at the air/water interface. The contribution of the dipoles in each layer, μ_i, to the surface potential, ΔV, depends on the local permittivity, ε_i, of each layer. From ref. [17].

4.2. Langmuir-Blodgett Deposited Films

There are a number of characteristics which need to be investigated before the properties of LB films can be used in actual applications. First of all, it is necessary to establish whether deposition really took place and whether the film deposited is indeed a genuine LB film or simply a sample prepared using the LB method. By measuring the transfer ratio of a particular monolayer in successive depositions, it is usually possible to know the type of film deposited (Y, X or Z) and also investigate which parameters affect deposition. However, the measurement of the transfer ratio on its own cannot ensure whether the film is uniform or highly ordered. Several other techniques must be used in order to gain such information. The thickness of the LB film and the intermolecular distances may be determined by ellipsometry, surface plasmon resonance, X-ray diffraction and neutron diffraction and reflection, and electron diffraction. Synchrotron X-ray reflection, for instance, allows the thickness to be determined to an accuracy of one angstrom. The thickness can also be obtained when the film is part of a MIM structure by measuring the capacitance of the structure.

Some of the techniques mentioned above can be used to study the orientational order of the molecules in the film, but this can also be investigated by Raman scattering, electron spin resonance, Near Edge X-ray Absorption Fine Structure (NEXAFS), linear dichroism and FTIR spectroscopy. Film texture and the presence of defects can be investigated using scanning electron

microscopy (SEM), transmission electron microscopy (TEM), scanning tunneling microscopy (STM), atomic force microscopy (AFM) and optical microscopy. Possible reasons for non- homogeneities in LB films are the reorientation of the molecules during deposition or after it, or even non-homogeneity on the monolayer at the air/water interface. At the molecular level, non-homogeneities are bound to exist since domain structures have been reported for fatty acid and phospholipid Langmuir monolayers. Surprisingly, however, regular arrangement (to an accuracy of the order of angstroms) of fatty acid molecules has been observed in STM measurements.

For conducting LB films, the in-plane conductivity has been measured using mechanically pressed contacts, conducting paste or evaporated gold electrodes, but has also been obtained through Hall effect and surface acoustic wave (SAW) devices. Though some attempts have been made to investigate the mechanisms responsible for the conductivity in LB films, considerable theoretical work is still required for these mechanisms be established.

The characterization of LB films can be a rather complex matter. Structural differences may exist between the first and subsequent layers, including tilt of the chains in relation to the substrate. Some authors have reported that the structural arrangement of fatty acid films may change from hexagonal to orthorhombic at thicknesses greater than a monolayer. These differences probably arise from substrate-film interaction which tend to die off with the increase in the number of layers. Capacitance-voltage measurements, on the other hand, have shown that in some films the thickness is proportional to the number of layers, which would indicate that within the accuracy of the measurements all layers were equivalent.

Stability is a major problem for applications of LB films. In addition to the poor thermostability of films built from aliphatic compounds, there have been reports of changes in film properties with time. The surface potential of sulphur- containing LB films has been shown to decrease by 40% in a month of deposition when they are stored in ambient conditions. Films stored in a dry air atmosphere presented a much smaller decrease which shows that storage conditions are important for film stability[17]. Also, Z and X-type films have been observed to relax to the more stable Y-type, indicating that structural changes may occur as well.

Apart from the experimental methods already mentioned in this section, other techniques which have also been used in the characterization of LB films include thermo and photodesorption measurements, electron spin resonance, Penning ionisation electron spectroscopy, surface plasmon resonance, Auger electron spectroscopy, cyclic voltammetry, photoacoustic spectroscopy and Stark spectroscopy.

V. Possible Applications

The multitude of possible applications which have been suggested over many years are a legacy from the pioneering work of Prof. Kuhn and his collaborators in Goettingen, Germany, where charge and energy transfer in LB films were studied. An extensive review of the possible applications of LB films has recently been provided by Petty[18].

The potential applications of LB films stem from their unique blend of features: they are ultra thin films (of the order of nm) and possess a high degree of structural order. Also, some films have interesting optical, electrical and biological properties characteristic of organic compounds. The LB technology offers the possibility of tailoring material properties either by molecular engineering of the individual molecules using modern methods of organic chemistry or the control over the architecture of the films as shown in Figure 8. This latter control permits the observation in LB film form of useful physical properties of organic compounds which is not possible for the same material in its bulk crystalline form because of structural restrictions. For example, most organic materials crystallize with a centre of symmetry and therefore second order nonlinear phenomena such as second harmonic generation and pyroelectricity cannot be observed, but may be present in LB films made from these very materials.

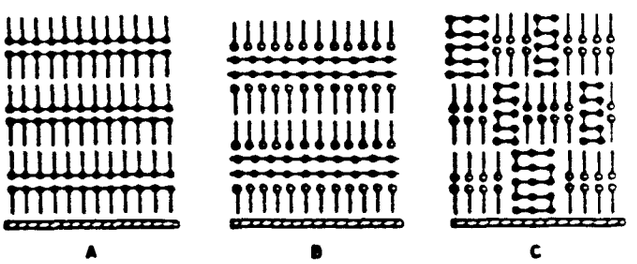

Figure 8: Supermolecular structures. Different possible structures for LB films of conducting polymers. From ref. [15].

A great number of possible applications of commercial interest have been suggested for LB films. The films may be used as passive layers in MIS (metal-insulator-semiconductor) structures, in resists for submicrolitography, in the passivation of n-GaAs surfaces, in surface acoustic wave (SAW) devices, and in the lubrication of thin film magnetic disks to enhance the useful life of high density hard disks. Many other possible applications include non-linear optical devices, pyro- and piezoelectric devices, chemical and biological sensors, photodiodes, conducting films for electrode materials, thermochromic devices, coating of optical fibers for nonlinear optical properties, ultrafiltration membranes and the building of molecular electronic devices.

This latter possible application has brought so much excitement to the scientific community that a special subsection has been reserved for molecular electronics in this paper.

Among the many classes of materials that have been used for LB film formation, the conducting polymers deserve special attention. Perhaps the most exciting development in the area in recent years has been the demonstration of the use of a conducting polymer based LB film as the active element of an electronic device. FETs have been fabricated by Stubb's group in Finland, and also by Rubner's group in the USA, in which mixed LB films of different conducting polymers have been used [18].

5.1. Molecular Electronics

The research on the possible fabrication of Molecular Electronic Devices (MED) has raised hopes for the development (perhaps in the not very distant future) of the so-called nanotechnology, whereby devices will have nanometric dimensions. Such an achievement would certainly provoke a revolution in electronic devices, information technology and in science and technology as a whole. These systems will be fabricated in such a way as to make use of specific interactions between molecules, interactions that will lead to functions being performed similar to those now realized by semiconductor and magnetic materials. The realization of such systems will only be possible if suitable techniques are developed for assembling molecular structures. Of the many possible approaches, the Langmuir-Blodgett (LB) technology is certainly one of the most important, for it provides not only a method of assembling molecular systems in a controlled manner but can also take advantage of the self-assembling nature of certain molecular species.

The first requirement for building an MED is the development of a molecular switch capable of shifting information, reversibly, from one stage to the other. This achievement would be equivalent to the discovery of the transistor in conventional microelectronics[19]. The information must be accessible at the molecular level, so that the "state" of the switch can be determined. The information must be transported over distances by molecular wires and/or molecular networks. Finally, the switches and networks need to be assembled in three dimensional structures or arrays that will ultimately lead to the MED. Work on LB films has encompassed all the different stages mentioned. Both optical and electrically reversible switching, for example, have been observed in LB films in which the switching function originated from a number of different processes such as electrochromism, photodimerization and electron transfer. Figure 9 illustrates a porphyrin-phthalocyanine arrangement in which electron transfer can occur upon excitation by visible laser light[20]. Three- dimensional molecular memories have been suggested based on electron motion perpendicular to LB multilayers of macrocyclic compounds.

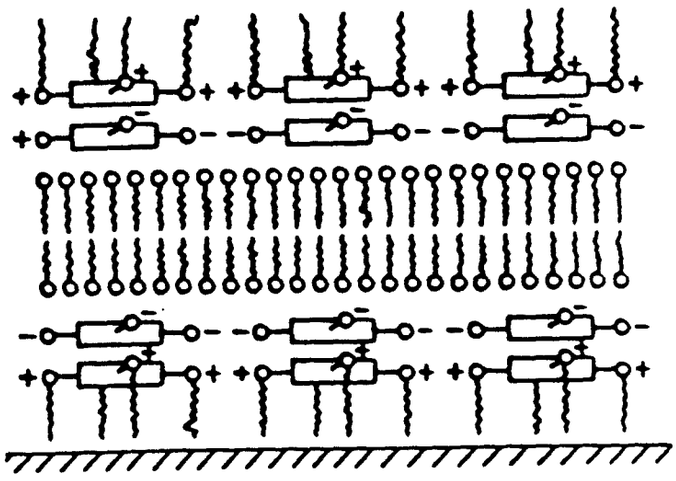

Figure 9: Electron transfer. LB film of porphyrin-phthalocyanine heterodimers in which electron transfer can occur parallel to the substrate by exposing the film to visible laser light. From ref. [20].

The need to access individual molecules in order to store and retrieve data is a problem which appeared to be almost unsurpassable until very recently. Now that instruments such as the scanning tunneling microscope (STM) and atomic force microscope (AFM) are available it is possible to probe surface properties of LB films down to atomic dimensions. Accordingly, these techniques have been used for molecular resolution images of LB films which paves the way for investigations on the access of individual molecules.

Despite the worldwide effort of interdisciplinary teams working on the different aspects of M.E., real applications remain something for the future. Several issues are yet to be addressed including the need to detect and repair failures in components that do not perform correctly. Additionally, the interpretation of some of the most important recent results is still open to discussion. For instance, organic molecular rectifiers based on LB films have been built but there has been some debate as to whether the observed rectifying function is molecular in origin[16]. Also, it cannot be claimed at the moment that the STM and AFM data are completely free from experimental artefacts.

VI. The State of the Art

Conducting polymers are now at the forefront of research in LB films because of their improved mechanical and thermal properties, and also because some of them are electroactive and therefore suitable for fabricating electronic devices. For the characterization of Langmuir monolayers on the water surface and LB deposited films

there is a trend towards the use of experimental methods that are capable of providing information at the molecular level. The tilt of molecules and structuring of the monolayer have been observed by synchrotron X-ray and Neutron diffraction and reflection measurements, while the advent of the STM and AFM technologies has made it possible to probe LB deposited films with molecular resolution. Another important development is the use of sophisticated theoretical methods, e.g. Monte Carlo and molecular dynamics, to simulate Langmuir monolayers and LB films, and the computer aided design of special molecules to suit a particular application. Nevertheless, theoretical analyses of LB and Langmuir films are still at an embrionic stage.

Almost two decades of extensive research on LB films and on their possible applications have elapsed, and these films continue to be referred to only as "promising" for technological applications. It appears that, so far, the only commercial application of an LB-based device is a low-level radiation source to act as standard for calibrating tritium detectors, which was developed by Martin Taylor's group at Bangor University in the United Kingdom. The source consists of LB films from palmitic acid mixed with small amounts of tritiated palmitic acid deposited on an aluminium plate.

In fact, if one inspects the special issues of scientific journals dedicated to LB films one may say that some possible applications have been mentioned over the last 15 years, without any major breakthrough towards making them a reality. One may wonder, then, whether LB films will ever be used in commercially available devices. In this respect, an important point must be borne in mind: technology is about concentrating research and development efforts into specific final products, e.g. a device made from a specific material that performs a specific function. Research on LB film, however, has been more akin to fundamental science, in particular because the background knowledge of property-structure correlations is yet to be established for these films. Fundamental science is about opening up new possibilities and extending horizons, and this is precisely what has been done in the LB field as demonstrated by the large number of different types of molecule and molecular assembly investigated for LB film formation and also by the immense number of different applications. Before the feasibility of a specific commercial device is demonstrated so that the research efforts may be directed towards it, the potential of LB films are likely to remain unfulfilled.

Many problems must be solved before LB films can be used in real applications, the most important of which are the lack of thermal stability and the poor molecular alignment in many films[18]. The LB technology will also have to be adapted for the cost-effective mass production of LB-based devices. Langmuir troughs, albeit in some cases fully automated and highly sophisticated, are designed with the specific purpose of being used in research and development. They usually allow for the incorporation of experimental techniques for monolayer characterization, dipping facilities for alternate layers and for a variety of substrates, etc. For device mass production, trough design will have to change drastically; troughs may need to be miniaturised, and a number of them placed in an assembly line harmoniously linked to other industrial processing unities.

As far as molecular electronics is concerned, the capability for storing optical and electrical data has been clearly demonstrated, and there is now the hope that data can be accessed at the molecular level with the use of STM and AFM techniques. While it is almost certain that some of the devices are to be built using the LB technique, chemisorption methods such as the one developed by Sagiv[21] may also be employed. Like the LB technology, chemisorption can also allow the deposition of monomolecular films on solid substrates and take advantage of the self-assembling nature of some of the molecules. Incorporation of biological molecules capable of self-assembling into electronic devices may lead to the fabrication of so-called biochips and ultimately to the development of the biological computer. Again, the study of fundamental properties of the deposited films is essential for further progress to be made.

Any major achievement in the field is likely to depend on the cooperative work of multidisciplinary teams composed of Chemists, Biochemists, Biologists, Electronic Engineers and Physicists.

Acknowledgments

I thank FAPESP and CNPq which are sponsoring the LB work in São Carlos.

References

1. G.G.Roberts, Langmuir-Blodgett Films (Plenum Press, N.Y. 1990).
2. O.N.Oliveira Jr. and D.M.Taylor, Ciência-Hoje 67, 18 (1990).
3. A.Ulman, J.Mater.Educ., 11, 205 (1989).
4. I.R.Peterson, J.Phys.D: Appl.Phys., 23, 379 (1990).
5. A.Barraud, Thin Solid Films, 175, 73 (1989).
6. R.H.Tredgold, Rep.Prog.Phys., 50, 1609 (1987).
7. V.K.Agarwal, Physics Today, 41, 40 (1988).
8. M.B.Biddle and S.E.Rickert, Ferroelectrics, 76, 133 (1987).
9. T.Moriizumi, Thin Solid Films, 160, 413 (1988).
10. M.Vandevyver, Thin Solid Films, 159, 243 (1988).
11. R.H.Tredgold, Advances in Physics, 26, 79 (1977).
12. M.Sugi, J.Mol. Electronics, 1, 3 (1985).
13. R.A.Hann, Phil. Trans. R.Soc. Lond. A 330, 141 (1990).

14. P.Hodge, F.Davis and R.H.Tredgold, Phil. Trans R.Soc. Lond A330, 163 (1990).
15. M.F.Rubner and T.A.Skotheim, in Conjugated Polymers, J.L.Brédas and R.Silbey (eds.), pp.363 (1991).
16. D.M.Taylor, O.N.Oliveira, Jr. and E.Morgan, J.Coll and Interface Sci., 139, 508 (1990).
17. O.N.Oliveira Jr., "Electrical Properties of Langmuir Monolayers and LB-Deposited Films", PhD. Thesis, University of Wales, Bangor, U.K., 1990
18. M.C.Petty, "Possible Applications for Langmuir-Blodgett Films", Thin Solid Films in the press.
19. J. de Rosnay, "Molecular Information Processing and Molecular Electronic Devices", Proc. 5th International Conference on Langmuir-Blodgett Films, (Paris, August 1991) p. A1.
20. J.F.Lipskier, T.B.Tran-thi, S.Palacin, S.Gaspard, D.Houde and C.Pepin, Proc. 5th International Conference on Langmuir- Blodgett Films (Paris, August 1991) p. CO2.
21. J.Sagiv, J.Am.Chem.Soc. 102, 92 (1980).

REVIEW

Corona Charging of Polymers

José A. Giacometti
and Osvaldo N. Oliveira Jr.
Instituto de Física e Química de São Carlos,
Universidade de São Paulo, São Carlos, SP Brasil

ABSTRACT

A review of the corona charging of polymers is presented. After providing a brief account of the corona discharge process and of its application for charging materials, the paper focuses on the evolution of corona triodes that allow the sample surface potential to be monitored during the charging process. Particular emphasis is given to the main contributions arising from research, basically on Teflon FEP and ferroelectric polymers, in which a constant-current corona triode was used. Such a triode system has become a powerful tool in the study of charge transport and ferroelectric properties of polymers, because keeping the charging current constant facilitates matching of the experimental results to a number of theoretical models.

1. INTRODUCTION

INTEREST in the corona charging of material surfaces has arisen from the need to charge materials electrically which operate in open circuit, for applications in electrophotography and electrets. In the very beginning, surfaces were charged by direct exposure to a corona point or wire, but in this procedure one had little control over the potential to which the surface was charged, and over the charge uniformity. The insertion of a grid between the point (or wire) and the sample changed this state of affairs, because a much better control could be achieved. These three-electrode systems, now traditionally called corona triodes, were further refined so as to allow the monitoring of the charging process itself, and now some of them operate under constant charging current condition. The constant current triodes have been extensively used in the study of charge storage and charge transport of polymers and will be the focus of the present paper.

The experimental setup and procedures adopted in the constant current corona triodes are discussed in Section 5, while Section 6 deals with the main results presented in the literature deriving from work in one of such triodes. In an attempt to provide some background knowledge of corona charging, we include three more sections. Section 2 presents a brief review on corona discharge, Section 3 lists the main applications of the corona discharge for charging materials, and in Section 4 presents the general properties of corona charged materials. Because discussion in these three sections will be restricted to general ideas, the reader wishing to further his/her knowledge in

any particular aspect is referred to a number of papers which are listed in the bibliography.

2. THE CORONA DISCHARGE

CORONA is a self-sustainable, non-disruptive electrical discharge which occurs when a sufficiently high potential difference exists between asymmetric electrodes such as a fine wire or a point and a plate or cylinder. Because of the high electric field near the emitting electrode (point or wire), the air that is normally insulating becomes ionised and the resulting ions are driven towards the low-field electrode. The threshold for the corona discharge depends upon the availability of a free electron that can trigger an avalanche responsible for ionising the gas. Electrons are efficient ionising agents because upon impact they transfer all their energy acquired from the electric field to gas molecules.

Different regimes exist for the corona discharge. Just above the threshold both positive and negative coronas are pulsating, in the so-called autostabilisation regime [1]. On increasing the corona voltage, the positive corona becomes a continuous glow discharge while the negative corona reaches the regular Trichel pulses regime. At very high corona voltages the negative corona also becomes a continuous glow discharge. At yet higher voltages streamers are formed in both positive and negative coronas until breakdown occurs.

All ref numbers are renumbered Also in the figure caption Please check and correct

Figure 1.

Corona discharge in the point-to-plane geometry. The ionisation is limited to a region close to the point (high field electrode) and the drift region extends towards the plane (low field electrode). Also shown are the field and ion flow lines. The angle θ is used in the Warburg's law.

The corona discharge may be classified as a glow discharge in which the ionization is confined to regions close to the high-field electrode, being much smaller than the conduction region as can be seen in Figure 1 for the point-to-plane geometry. That is, luminescence is observed only in a small portion of the gap. The conduction region is characterized by the presence of charge carriers of only one polarity, and since the mobility of these carriers is low (of the order of cm^2/Vs), the corona current always increases with increasing corona voltage, *i.e.* the process has a positive differential resistance. This is why the discharge is controllable and thus easily applied to generate thermalized ions in order to charge dielectrics. By convention, the discharge is said to have the same polarity as the high-field electrode. Also in Figure 1 are shown schematically the electric field lines which correspond roughly to the trajectory of ions. The current density distribution over the plane obeys the socalled War-

Original must be 80–83 (< 85) mm wide. 1:1 scale for printing. SEND NEW ORIGINAL. All 18 figure are missing!

burg law [2], and in the point-to-plane geometry the current density $\propto \cos^5 \theta$, where θ is the angle shown in Figure 1.

The glow near the point can also produce neutral activated species which in the charging process of polymers are carried to the sample surface by the corona wind [3]. This electrical wind originates from the kinetic energy the molecules of the gas acquire from the charged species that traverse the gap. The chemical activity of these neutral species may play an important role in the electrochemical processes on polymer surfaces, a point which we shall return to in Section 4.

The types of ion generated in positive and negative coronas have been determined by several authors [4,5] using mass spectrometer techniques, and were found to depend strongly on the gas. In air, the dominant species for positive corona are hydrated ions with the general formula $(H_2O)_nH^+$, where n is an integer that increases with increasing relative humidity. At low relative humidity other ion species, such as $(H_2O)_nNO^+$ and $(H_2O)_n(NO_2)^+$, become dominant. For negative coronas, the most important ions are CO_3^- ions; at 50% of relative humidity about 10% of the ions are in the hydrated form $(H_2O)_nCO_3^-$. The ion species and their dependence on the air humidity can be important parameters in corona treating solid surfaces [6].

Under the conditions corona discharges are normally employed in actual applications (electrode spacings of the order of cm, and dc corona voltages of the order of kV), the negative corona is in the so-called Trichel pulse regime [1] whereas the positive corona is in the continuous glow regime [7].

There are several cases in which the corona discharge is unwanted, as in corona losses and radio interference. However, it has found a number of industrial applications in electrostatic precipitators, electrophotography, treatment of plastic surfaces, electrostatic printing, fabrication of electrets, radiation detectors and dosimeters. Owing to its many applications, the corona discharge has been extensively studied and the present understanding of the physical processes involved in the discharge has been summarised in a number of excellent review papers and books [8–13].

3. APPLICATIONS IN CHARGING MATERIALS

ONE of the most traditional applications of the corona discharge is in the electrophotographic process proposed by Carlson in 1938 [14]. It consists of forming electrostatic images by a photoconductive discharge of an electrostatic charged surface. These images are later developed by electrical attraction of fine particles onto

the surface. Corona discharge is used in the first step of the process, *i.e.* in the sensitising of the xerographic plate in which ions are deposited uniformly over a photoconductive film; uniformity usually being achieved by moving the corona source over the plate surface. Sensitising by the corona discharge has been proven to be more effective than other methods that use radioactive sources, electrostatic induction or conductive rubber rollers [15].

Different experimental arrangements have been used for corona sensitising [15]. In the so-called 3-wire corotron, three parallel corona wires are situated above the xerographic plate and below a grounded electrode strip; this technique allows very rapid charging The scorotron is a slightly modified version of the corotron, in which a control metallic grid is inserted between the corona wires and the plate. The grid is biased to a voltage that approximates the potential required for the photoconductive plate, normally $\sim$ 400 V, therefore much lower than the voltage of the corona wires. (The scorotron is, in fact, a three-electrode system analogous to the corona triode to be presented in Section 5. A third possible arrangement is the shielded corotron which consists of a single corona wire mounted in a grounded metal shield.

Corona discharge has been used in the electrical separation of particles from gases, a process which already had been suggested by Hohlfeld [16] as long ago as 1824. Because the corona discharge also can be used in the retention and collection of the charged particles, corona-based electrostatic precipitators have found widespread application in the treatment of contaminated gas in heavy industries [17,18]. Other means such as radioactivity can be employed for particle charging, but none have been able to compete, in terms of costs, with the corona method.

Electret production using the corona method has had a tremendous impact on the fabrication costs of a number of devices which range from microphones to motors [19]. An electret is a solid dielectric material which generates a permanent electric field. The first electret material used in commercial applications was carnauba wax that possessed poor stability, but the advent of polymer film electrets, *e.g.* Teflon™ FEP (fluorethylene propylene), made a number of new applications possible [20]. Film electret microphones, for instance, have been highly successful because of the stability of the charge in Teflon FEP, and also because of their excellent acoustic properties. Other electret devices include gas filters, motors, relay switches, optical display systems, underwater transducers and radiation dosimeters [21]. Electrets can be produced using other charging techniques [22] such as liquid contact [23], voltage breakdown [24] and electron beam [25] but the corona discharge has been preferred because it is simpler, gives better surface charge uniformity, and allows large scale production [26] at low cost.

In addition to being used for charging the majority of the devices mentioned above, corona discharge is also employed for polarising polymer materials such as polyvinylidene fluoride (PVDF) and its copolymers with tetrafluorethylene P(VDF- TrFE) [27]. In commercial applications, use is made of the piesoelectric and pyroelectric properties these materials are known to possess. Perhaps the most important application, in this respect, has been the fabrication of piesoelectric transducers for biomedical instrumentation [28]. Here the advantages of the corona charging lie on the possibility of obtaining the high electric field required for poling the sample without major breakdown, and again the possibility of low cost, large-scale production [29].

A novel application of corona charging has been in the poling of doped polymeric materials for non-linear optics (NLO) [30-33]. The polymer samples are initially doped with nonlinear optical dopants such as disperse orange 3 (an NLO dye), and then corona poled for orienting the dopants in a noncentrosymmetric fashion as required for the observation of second harmonic generation.

Commercial applications of electrets have relied heavily on the availability of charge storage data for a number of polymer films. It is fair to say, therefore, that fundamental research on the electrical properties of polymers has been essential for technological developments. In this context, the corona charging of polymers has played a two-fold role. In addition to serving as a means for charging polymers to be studied later using other experimental techniques (see Section 4), it also has been employed in corona triodes that allow study of charge transport and ferroelectric properties to be made during the charging process This latter application of corona charging is discussed at some length in Section 6.

4. GENERAL PROPERTIES OF CORONA CHARGED SURFACES

THE previous Section illustrated the many possible uses of the corona discharge in the charging process and polarization of solid materials. In this Section we shall elaborate on the relevant properties which corona-charged samples are required to possess for specific applications. In electrophotography, for instance, charges deposited on the photoconductive surface are expected to be removed by exposure to light; in electrets one usually envisages charge stability which determines the useful life of devices. In summary, the relevant issues relate to charge storage and transport in these solid materials.

Usually, these topics are investigated by measuring the surface potential $V(t)$ under open circuit condition, *i.e.* measuring the equivalent surface charge density $\sigma(t)$ of the dielectric. The surface potential is defined by assuming that the electric field $E(x,t)$ exists only inside the

Figure 2.

Schematic diagram for the definition of the sample surface potential under the open circuit condition. The planar symmetry is assumed since the sample thickness L is much smaller than the lateral dimensions of the sample. (The thickness is exaggerated in the drawing). The electric field $E(x,t)$, from which the surface potential is determined, is then restricted to the interior of the sample, vanishing outside it.

dielectric (see Figure 2). Then, its value is given by

$$V(t) = \int_0^L E(x,t)dx \qquad (1)$$

where L is the dielectric thickness. Its value is related to the equivalent surface charge density by $V(t) = L\sigma(t)/\epsilon$, where ϵ is the dielectric permittivity.

Figure 3.

Simple version of a corona triode. A metallic point is connected to a HV supply, V_c to produce corona ions which are driven towards the sample. A grid, biased by a voltage supply, V_g, is inserted into the point-to-sample gap. The charging current, I, can also be measured and will decrease to zero when the sample surface potential is equal to V_g.

In the early days the polymer sample surfaces were exposed directly to a corona point or wire discharge. High surface charges can be attained using this procedure, but the final sample voltage and the surface charge uniformity are not easily controlled. An important improvement was the advent of the corona triode [34] which consists basically of a corona tip, a metallic grid and a sample holder (Figure 3). Using a corona triode, one can choose the potential at which the sample is to be charged, and also achieve a uniform charge distribution at the end of the charging procedure. Unlike the constant current corona triodes to be discussed in the next Section, the corona triodes normally used do not allow the surface potential of the sample to be monitored during the charging process.

Information on charge storage and charge transport can be obtained by measuring the surface charge (potential) decay after the charging process, by means of an electrostatic voltmeter or other techniques such as the thermally stimulated current (TSC) or thermally stimulated depolarization (TSD) [35], heat pulse technique [36,37], laser induced pressurel Pulse (LIPP) [38–40], piesoelectric pressure step (PPS) [41] and laser intensity modulated method (LIMM) [42]. The TSC and TSD techniques have been the favorite ones in the study of charge stability of electrets.

Though the procedure for corona charging a photoconductive film in electrophotography is straightforward, the mechanisms involved in the surface charge storage and dissipation can be quite complex [15]. Photosensitive materials such as ZnO (zinc oxide) and amorphous selenium are evaluated according to their performance with regards to the maximum surface charge density that can be applied to a layer in the dark, the charge decay in the dark and upon excitation by a pulse of light or by continuous illumination, and the residual potential which remains after exposure to light [15]. The most important parameters in these studies are the mobility of the charge carriers, the efficiency of the photoinjection process [43] and breakdown effects [44]. The theoretical models used to describe these phenomena [45] are employed also for charge storage and transport in organic crystals [46], amorphous materials [47] and polymers [48].

Figure 4.

Surface potential decay for samples of polyethylene illustrating the crossover effect. Samples from a 0.015 mm thick polyethylene film were corona charged to various different final surface potentials and had their surface potential decay monitored. From [49].

As far as polymers are concerned, a number of charge decay studies have concentrated on polyethylene (PE) [48] probably because of the crossover phenomenon observed in this polymer [49]. By crossover effect is meant the experimental observation that the surface potential of samples initially charged to higher potentials decay faster and reach lower final potentials, as shown in Figure 4. This phenomenon was first attributed to the field-dependence of parameters such as the carrier mobility and the trapping time. However, it has recently been proven [50] that field-dependency by itself is not sufficient to explain the effect and it seems that a probable explanation is based on the partial charge injection when large amounts of charge are deposited on the polymer surface [51]. Other possibilities relate to the corona treatment of the polymer surface which will be discussed at the end of this Section.

Polymers are known to possess traps for electric charges which may originate from defects in the polymer structure or even in the boundaries between crystalline and amorphous regions of the polymer [52]. In Teflon FEP (fluorethylene propylene) and PTFE (polytetrafluoroethylene), the intrinsic conductivity can usually be neglected as can the polarisation effects. Dynamics of the transport of extrinsic charge in polymeric dielectrics containing no intrinsic carriers, is then dominated by the transport of free charge and by charge trapping. In this context, relevant parameters are trap density, depth in energy of these

traps, trapping and detrapping times, and mobility of the charge carriers once they are released from the traps. The determination of trap distributions in Teflon, both spatially over the sample thickness as well as in energy, is a legacy from the work of von Seggern [53,54]. By comparing TSC thermograms of polymer samples charged by corona discharge and by an electron beam, he was able to identify shallow surface traps on the polymer surface and two levels (in energy) of deep traps which are probably distributed over the whole bulk of the sample. This model for trap distribution has also been successfully employed in the interpretation of surface potential measurements in constant-current corona triodes.

Corona charging can be used for inducing phase transitions in PVDF, from the non-polar α form to the polar α, and β [55], which requires that high electric fields are applied to the polymer sample. High electric fields with corona charging can be achieved before electric breakdown takes place because dielectric failures are normally due to localised defects [56]. Since the surface exposed to the corona discharge is non-metalised, defects in corona-charged samples tend to remain local as long as the surface conductivity is negligible [57].

The corona discharge can not only deposit electric charges on the surface of the polymer but also cause morphologic changes of the surface itself [58] and of its trapping capability [59]. Corona treatment has been used for improving adhesion to electrodes and wettability of polymers such as PE (polyethylene), PET (polyethylene terephthalate) and PP (polypropylene) [60]. With regards to trapping capability, corona treatment effects are most prominent when high charging currents are employed and the point-to-sample distance is small. Corona treatment has been suggested to cause the decrease in thermal stability of negative charges stored in Teflon FEP [61], the appearance of the crossover phenomenon in lowdensity polyethylene [62], and charge injection in several polymers such as LDPE, PTFE and PE [63,64]. This charge injection has been attributed to the action of excited neutral molecules [63], but a possible alternative explanation has been suggested by Dias *et al.* [61]. The latter authors suggest that the potential decay observed may not be caused by charge injection but rather arise from a surface charge compensation by the arrival of ions of opposite polarity onto the sample surface. That ions of opposite polarity can reach the sample surface has been confirmed recently by Chinaglia *et al.* [65] who showed that the plate current for negative corona in a corona triode can become positive when the point-to-grid distance is < 15 mm and the grid is biased positively. The occurrence of charge injection in polyethylene also has been put under suspicion by Das Gupta [66] on the basis of studies in LDPE.

Figure 5.

Experimental setup used by Weinberg *et al.* [67] to measure the surface potential of the polymer sample during the charging process. Ions from a corona source were made to impinge onto two surfaces, the insulating film surface and a metal reference plate. A voltage V_b is applied to the conducting substrate so as to maintain the current I_i equal to I_m.

5. CONSTANT CURRENT CHARGING CORONA TRIODES

For a long time, corona discharge was used simply as a means of charging polymer samples which would be later studied by other methods. In order to monitor the charging process to some extent, a few experimental arrangements have been developed. To our knowledge, the first of such attempts was a comparison method presented by Weinberg *et al.* [67]. In their setup, depicted schematically in Figure 5, the steady-state potential difference across a polymer sample could be measured during the corona charging. It consisted of a corona system with two identical metal plates, one of which worked as a reference and the other as the sample holder. The corona ions impinged on both surfaces, and while the sample became charged, the sample holder had to be biased with a voltage V_b, for the charging current I_i to be kept equal to the current I_m, that reached the bare metal plate. The sample potential was then given by $-V_b$ and therefore the characteristics curves for the charging current *vs.* the surface potential could be obtained.

Figure 6.

Corona triode developed by Moreno and Gross [34]. A corona voltage V_c was applied to the point P placed above the grid and the sample in the triode chamber. The grid was connected to ground while the sample holder was biased with the voltage V_g. The sample was vibrated by a loudspeaker L driven by the oscillator. The measuring circuit consisted of two branches: (1) the dc branch in which the charging current passing through the resistor R was measured with an electrometer E. (2) the ac branch consisting of a capacitor C and a resistor R_1, from which the ac signal was measured with a lock in amplifier. The transducer, T, served as a decoupling agent for the two branches. The ac signal corresponding to the surface potential, and the charging current were then monitored by the recorder.

Having realized that relevant information was lost during the charging process, Gross conceived a corona triode which was to become a hallmark in the study of charge transport in polymers. He and his co-worker, Moreno

[34], developed a three-electrode system, called corona triode, that allowed simultaneous measurement of the charging current and the sample surface potential. Figure 6 shows their experimental arrangement including the triode chamber and the measuring circuit. The surface potential was measured using the vibrating capacitor or modified Kelvin method [68], the two plates of the capacitor being the grid and the sample. Vibrating the sample with a loudspeaker (frequency of ~ 300 Hz) generates an ac signal which is measured with a lock-in amplifier. The signal V_R in the central electrode of the sample holder comprises contributions from the current I traversing the gap between the sample and the grid, the displacement current and others that originate from vibrating the sample. It is given by

$$V_R = RI + k\frac{dV(t)}{dt} + K\omega[V_g - V(t)]\cos\omega t - K\frac{dV(t)}{dt}\sin\omega t \tag{2}$$

where ω is the frequency, and k and K are constants which depend on geometric factors, on the circuit parameters and on the amplitude of the vibration [34]. R is the resistor in which the charging current is measured.

Figure 7.

Plots of surface potential and charging current versus time. The triode by Moreno and Gross was used to charge a Teflon FEP film 25 μm thick. As the surface potential approached the grid voltage, the charging current went to zero. From [34].

The measuring circuit has two branches in order to separate the ac signal due to the sample vibration from the dc signal that gives the charging current. Alternating signals with frequency are measured in the ac branch, one of which is proportional to the potential $(V_g - V(t))$ yielding the surface potential, and the other is proportional to $dV(t)/dt$. The coefficient of the $dV(t)/dt$ term, however, is ~ 1000 x smaller than that of the $(V_g - V(t))$ term, and could then be neglected. The total current is measured in the dc branch, and since constant voltages are applied to both the grid and the corona tip, it decreases when the sample voltage increases as shown in Figure 7.

The change in the charging current was clearly a limitation which prompted the development of special versions of the corona triode [69] in which the current is controlled and kept constant at a desired value. Such systems resemble a low energy electron gun, which also operates at constant charging current, but has the advantage of providing for positive as well as for negative currents. As will be shown in the next Section, the constant current condition is essential for some charge transport equations to be solved, either numerically or analytically. There are two ways in which current control can be achieved,

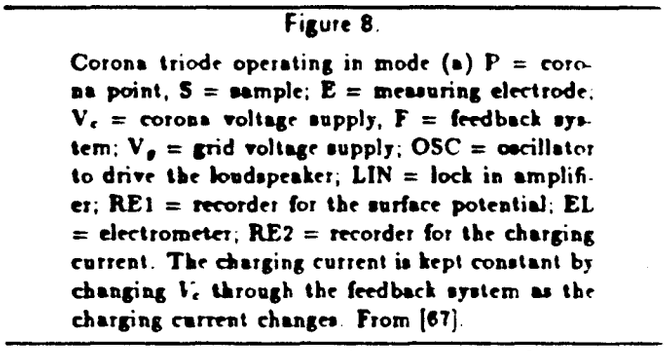

Figure 8.

Corona triode operating in mode (a) P = corona point, S = sample; E = measuring electrode; V_c = corona voltage supply, F = feedback system; V_g = grid voltage supply; OSC = oscillator to drive the loudspeaker; LIN = lock in amplifier; RE1 = recorder for the surface potential; EL = electrometer; RE2 = recorder for the charging current. The charging current is kept constant by changing V_c through the feedback system as the charging current changes. From [67].

5.1 CONSTANT GRID VOLTAGE MODE

The corona current is increased by increasing the tip voltage in order to compensate for the decrease of the charging current when the sample potential rises. The first constant current corona triode [69, 70] shown schematically in Figure 8, operated in this mode, where a feedback system F controlled the tip voltage V_c. Analogously to the triode in [34], the sample surface potential was measured using the modified Kelvin method [68] with the vibration of the sample holder (Equation 2).

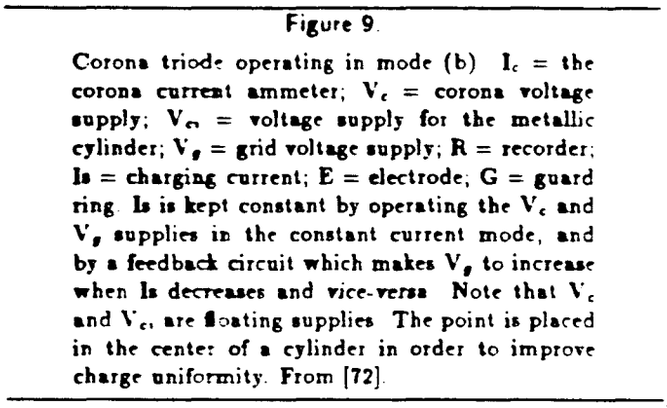

Figure 9.

Corona triode operating in mode (b) I_c = the corona current ammeter; V_c = corona voltage supply; V_{cc} = voltage supply for the metallic cylinder; V_g = grid voltage supply; R = recorder; Is = charging current; E = electrode; G = guard ring. Is is kept constant by operating the V_c and V_g supplies in the constant current mode, and by a feedback circuit which makes V_g to increase when Is decreases and *vice-versa*. Note that V_c and V_{cc} are floating supplies. The point is placed in the center of a cylinder in order to improve charge uniformity. From [72].

5.2 VARIABLE GRID VOLTAGE MODE

The grid voltage is controlled by means of a feedback circuit [71] so that the potential difference between the grid and the sample surface is kept constant. Experimentally, the charging current is kept constant by using a constant current supply V_g. As Figure 9 shows, the charging current is fed into the feedback input of the current supply and its value can be monitored with the floating electrometer [72]. Then, measuring the voltage V_g of the current supply necessary to keep $I(t) = I_0$ we can determine the sample potential through the relation

$$V(t) = V_g(t) - V_s \tag{3}$$

provided that V_s, the potential difference across the air gap, is known [72]. Since the amount of space charge in

the gap is dependent on the corona current I_C, this latter quantity must be also kept constant, which is performed by operating the V_c supply in the constant current mode. Therefore, this setup allows both the control of the ion flux to the sample and the determination of the sample surface potential by measuring $V_g(t)$, and there is no need to vibrate the sample.

There are a number of limitations associated with the operation mode 5.1 [69,70]. Although the grid voltage is supplied by a 0 to 10 kV voltage supply, it is difficult to operate it at high potentials because grid emission occurs. Also, varying V_c produces small alterations in the charging current which imposes a maximum limit of 2 nA cm2 to the charging current (for $V_c \lesssim 10$ kV). Another problem relates to the charge uniformity at the initial stages of the charging process. Uniformity was maintained only because the grid mesh was specially designed (by trial and error) to keep a uniform distribution of field lines. Problems also arise in the surface potential measurement because of noise inherent in the vibration of the sample.

These problems were obviated when operation mode 5.2 was used [73]. The major breakthrough was the realisation that the charging current could be space-charge limited for low potential differences V_s between the grid and the sample [72,73]. V_s assumes a small, constant value if the corona and the grid voltage supplies are operated in the constant current mode. Higher charging currents can be now reached since the grid will not emit and small variations in the grid voltage cause large changes in the charging current I_0. Another innovation introduced in the triodes operating with mode 5.2 is the use of a biased metallic cylinder around the tip which acts as an electrostatic lens and makes the deposition of corona ions over the sample more uniform. It should be mentioned that a thick PVC cylinder also has been used [73] to the same effect. Since in a very short time the PVC becomes corona charged, it can also be used as an electrostatic lens.

Constant current corona triodes are now used in several laboratories around the world. The triodes in Russia [74] and China [75] use the Kelvin method for measuring the surface potential, while the others in Portugal [76,77] and Brazil [72] utilise the operation mode 5.2. A triode which can also be considered as belonging to the constant-current class has been developed in the USA [78]. This one does not use any control either over the corona or grid voltage, but makes use of the fact that, for very large grid voltages there is a region where changing V_g causes no change in the charging current, I_0. Therefore, provided that the triode is operated in this region, the charging current is constant. In this case, however, the surface potential of the sample cannot be obtained from the grid voltage, because the current is independent of the sample potential. It could, nevertheless, be measured

using a vibrating capacitor as in the operation mode 5.1, though this was not attempted.

5.3 ELECTRICAL CHARACTERISTICS OF TRIODES

The driving force for studies of the electrical characteristics of corona triodes (with bare sample holders) has been the need to establish the optimum conditions under which a triode should be operated, and also the academic interest arising from the challenging electrostatic problems that such a system poses. Several investigations have been undertaken to study a variety of issues, including the uniformity of the current density distribution over the sample holder, the electrical transparency of different grids, and effects from corona polarity, corona wind and space charge. Theoretical models [79–81] have been developed to explain the electric characteristics of corona triodes, some of which take into account the corona wind generated in the corona discharge, the effect of accumulation of space charge between the grid and the sample, and the electric transparency of the grid. These models later were extended to account for the radial dependence of the current density produced by a corona tip [73].

Figure 10.

Current-voltage characteristics of a corona triode. For low grid voltages, the charging current varies quadratically with the grid voltage, as predicted for the space charge limited current (SCLC) regime. From [81].

Figure 11.

Potential profiles of a Teflon FEP charged with the triode of [73]. Curves A and B correspond to different charging conditions (charging current and grid voltage).

With regards to the operation of corona triodes, perhaps the most important results deriving from electrical characteristics studies relate to the determination of the charging current-grid voltage curves (I *vs.* V_g). Of particular relevance was the identification of a space charge limited current (SCLC) regime for low values of the grid voltage [81] (see Figure 10). In subsequent work, Giacometti [73] demonstrated that when the corona triode is operated in the SCLC regime (mode 5.2), a much better sample surface charge uniformity can be achieved, as can be seen in Figure 11.

Uniformity of charge deposition is so important that we shall elaborate on the subject a little further. A uniform deposition is an essential requirement for the correct measurement of the sample potential because the sample surface must be an equipotential. It is well known [34]

Figure 12.

Measured potential profiles of Teflon FEP samples charged with the triode of [70] which are related to the charge distribution over the sample. An almost uniform charge distribution was obtained because a special grid was used

that the presence of a grid controls the charge deposition leading to uniform distribution at the end of the charging process when the surface potential reaches the grid voltage. However, at intermediary stages the distribution is not uniform if a common mesh grid is used [82]. This problem was first circumvented in the building of a corona triode by using a composite grid, made of two close layers looking like a lens, the convex face directed downward [83]. Almost uniform charge profiles could be obtained with such a grid even for potentials much smaller than the grid voltage V_g as can be seen in Figure 12 which illustrates the charging process of a negatively charged, 25 μm FEP sample. The fluctuations which appear in the profiles are believed to be of minor importance because the sample potential is taken as the average value. Other alternatives have been suggested for improving sample charge profile. For instance, an aperture inserted into the grid-to-sample gap was shown to improve the uniformity to a considerable degree [84] at the end of the charging process. In all corona triodes, it is assumed that the charging current always has the polarity of the corona. However, it has recently been shown [65] that an important exception exists when the point-to-plate distance is small and the grid is biased with inverted polarity relative to the corona tip. This inverted current has a host of implications in the surface potential decay measurements of polymer films, particularly with regards to polymer surface treatment, as pointed out in Section 4.

6. RESULTS WITH CONSTANT CURRENT CORONA TRIODES

In this Section we discuss a number of experimental results and their interpretation obtained with constant-current corona triodes. It already has been mentioned that one of the main advantages of this type of triode lies in the possibility of integrating differential equations governing charge transport, in particular because one important parameter, the charging current, is kept constant. We shall therefore present the general relations usually employed in the theoretical models, which will then be followed by the discussion of experimental results.

6.1 GENERAL RELATIONS

The total current density through the sample J_o is given by

$$J_o = J_c(x,t) + \frac{\partial D(x,t)}{\partial t} \qquad (4)$$

where $J_c(x,t)$ is the conduction current density, $D(x,t)$ the electric displacement given by $D(x,t) = \epsilon E(x,t) + P(x,t)$, and $P(x,t)$ being the electric polarisation. The conduction current is dependent on the kind of process that occurs in the sample. For instance, it is equal to $gE(x,t)$ for a pure intrinsic conductivity, and $\mu\rho_F(x,t)E(x,t)$ for the transport of space charge. Here g is the conductivity, $\rho_F(x,t)$ the free space charge density and μ is the mobility of the free carriers.

Because the charging current is constant, it is possible to integrate Equation (4) over the sample area A and thickness L to give

$$I_0 = C\frac{dV(t)}{dt} + I_c(t) + A\frac{dP(t)}{dt} \tag{5}$$

where C is the sample capacitance, and $I_c(t)$ and $P(t)$ are the mean conduction current and the mean value of the polarisation, respectively. $I_c(t)$ and $P(t)$ are defined as

$$I_c(t) = \frac{A}{L}\int_0^L J_c(x,t)dx \tag{6}$$

$$P(t) = \frac{1}{L}\int_0^L P(x,t)dx \tag{7}$$

Two important pieces of information can be readily gained from the surface potential buildup of a polymer sample: the sample capacitance C which is given by

$$\frac{I_0}{C} = lim_{t\to 0}\frac{V(t)}{t} \tag{8}$$

while for samples exhibiting negligible conductivity and polarisation, as is the case for Teflon when the surface potential increases less than proportionally with time, it indicates carrier injection into the sample. From Equation (5) it is readily seen that I_0/C is the maximum rate at which the surface potential can rise.

Two materials were used in the work with constant current corona triodes: Teflon and PVDF (and its copolymers with trifluorethylene), which are non-polar and polar materials, respectively.

Figure 13.

Surface potential buildup of a negatively charged FEP sample. The surface potential increases linearly in the beginning of the charging process, and then increases sublinearly until reaching a steady-state value. No decay is observed when the corona is switched off. From [86].

6.2 RESULTS WITH TEFLON

Because Teflon has neither intrinsic conductivity nor polarisation, Equation (5) is greatly simplified, as will be shown below. It is known that this material possesses surface as well as bulk traps, and upon corona charging under constant current (either positive or negative) the sample potential initially rises linearly as shown in Figure 13, as the carriers are trapped at the surface. Sample capacitances can then be obtained and they are usually found to agree with the capacitance measured in a capacitance bridge within 3% [72,85,86]. An interesting result in this regard was presented by Ferreira and Oliveira [87] in which the capacitance obtained from positively charged samples was slightly larger than either the capacitance measured in a bridge or the one calculated for negatively charged samples. The reason behind such a difference was probably that the surface traps for positive charges were located a little beneath the geometric surface of the sample, confirming earlier measurements by von Seggern [54] who used the heat pulse technique. After the initial linear rise in surface potential, a sublinear behavior is observed, either due to the complete filling of surface traps, or to detrapping of carriers from the shallow surface traps which brings about a non-zero conduction current. That charge injection took place was confirmed by measurements of the centroid of the charge distribution $\rho(x,t)$ using the heat pulse or Collins technique [36], where the centroid is given by

$$r(t) = \frac{\int_0^L x\rho(x,t)dx}{\int_0^L \rho(x,t)dx} \tag{9}$$

which for the constant-charging current case, is

$$\frac{r(t)}{L} = 1 - \frac{CV(t)}{I_0 t} \tag{10}$$

provided that the electric charges had not arrived at the back electrode of the sample. Figure 14 illustrates the surface potential build up of a positively charged FEP sample together with the calculated centroid using Equation (10). As can be seen, the centroid is initially zero, and increases as injection proceeds [69].

Figure 14

Surface potential and charge centroid versus charging time. A 25 μm Teflon FEP was positively charged and the centroid measured. The centroid lies on the surface in the beginning of the charging process, but shifts towards the bulk of the sample as the charging proceeds. Charging current was 1 nA. From [69].

When injection occurs, the mean conduction current

$J_c(t)$ is dependent upon the trapping-detrapping dynamics, usually described by

$$\frac{\partial \rho_T(x,t)}{\partial t} = \frac{\rho_F(x,t)}{\tau}\left[1 - \frac{\rho_T(x,t)}{\rho_{Tm}}\right] + \frac{\rho_T(x,t)}{\tau_d} \quad (11)$$

where $\rho_F(x,t)$, $\rho_T(x,t)$ and ρ_{Tm} are the free charge density, the trapped charge density and the maximum charge density in the bulk traps, respectively. τ and τ_D are respectively the trapping and detrapping times for the carriers.

Theoretical models [50, 70, 86, 87] have been used to explain surface potential *vs.* time curves for Teflon FEP. Since there is no intrinsic conductivity nor polarization, the total current equation in Equation (4) may be written as

$$J_0 = \mu \rho_F(x,t) E(x,t) + \epsilon \frac{\partial E(x,t)}{\partial t} \quad (12)$$

where μ is the mobility of the carriers. For the transport of free carriers only (in the complete absence of traps) the constant current condition allows the derivation of analytical solutions for $V(t)$ [50, 70], with surface charge accumulation or not. These solutions are not of great practical value, though, as charge transport in Teflon is dominated by trapping.

When trapping is important, the Poisson equation which relates the electric displacement to the total charge density, is used together with Equation (11) and (12), normally with $\rho_i \ll \rho_{tm}$

$$\frac{\partial D(x,t)}{\partial x} = \rho_f(x,t) + \rho_T(x,t) \quad (13)$$

and a very large τ_D, to yield the following system of partial differential equations in $E(x,t)$ and $\rho_i(x,t)$

$$J_0 - \mu E(x,t)\left[\epsilon \frac{\partial E(x,t)}{\partial x}\right] - \rho_T(x,t) + \epsilon \frac{\partial E(x,t)}{\partial t} \quad (14)$$

and

$$\frac{\partial \rho_i(x,t)}{\partial t} + \frac{\epsilon}{\mu \tau E(x,t)} \frac{\partial E(x,t)}{\partial t} - \frac{J_0}{\mu \tau E(x,t)} = 0 \quad (15)$$

This system is normally solved using numerical methods [88] which allows the sample surface potential to be determined from the calculated electric field through Equation (1). The potential decay after t_d, which is the time when the corona is switched off, is easily obtained by setting $J_0 = 0$.

Studies aimed at explaining the surface potential build up of Teflon film have shown that, although ions are the charge carriers that impinge onto the sample, charge transport is dominated by electrons and holes for the negatively and positively charged samples, respectively [86, 87]. Important parameters obtained in these studies are

Figure 15.

Surface potential buildups of Teflon FEP. The curves show that the surface potential for the positive corona is lower (curve II), under the same conditions of charging, than for the negative corona (curve I). Charging current was 1 nA. From [90].

the product mobility times trapping time, the detrapping time, and the trap density both at the surface and in the bulk.

Discrepancies exist between the experimental results obtained under approximately the same conditions by different authors and even between results obtained with different batches of samples of the same polymer by a given author. Of course, such discrepancies could be attributed to differences in sample processing between manufacturers, but it seems that even the thickness of the sample may affect the experimental results [87]. There are, nevertheless, points which have been well established upon confirmation from independent studies using different experimental techniques. For instance, traps exist at the polymer surface as well as in its bulk [53], charges are initially trapped at the surface and then injected into the bulk, and the charge transport is dependent on the product carrier mobility times trapping time (and not specifically on these quantities) [86, 87, 89]. Another finding that appears to be established beyond doubt is that negatively charged samples display a better stability [90], and this is also reflected on the surface potential buildup (see Figure 15).

On the other hand, considerable uncertainty remains about the value of the carrier mobility, trap density and the process of trap-filling. There are some cases in which saturation of all surface and bulk traps occurs [86, 91, 92], but this is not general. Also, for Teflon FEP the schubweg (*i.e.* the mean free path for a carrier before it is trapped) has been reported to be field independent [92], but in other work it has been found to depend on the electric field [86, 87]. The charge stability is another controversial point. Though there is reason to believe that most polymer electrets are very stable at room temperature, in most cases some charge decay is observed at lesser or greater extent. However, for a particular batch of Teflon FEP samples, the traps were reported to be so deep that no charge release occurred, and consequently there was no charge decay (see Figure 13) [86].

The latter result illustrates the case in which there is an apparent 100% violation of the so-called conduction current conservation relation (CCCR) that represents the charge conservation in the sample when the corona is turned off at time t_d [93]. This relation is derived by assuming the continuity of the mean conduction current

at t_d. i.e. $I_c(t_d^-) = I_c(t_d^+)$, and using Equation (5) and (8)

$$\frac{I_0}{C} = lim_{t\to 0}\frac{V(t)}{t} = \frac{dV(t_d^-)}{dt} - \frac{dV(t_d^+)}{dt} \qquad (16)$$

where t_d^- and t_d^+ are the instants immediately before and after the time t_d.

As can be seen in Figure 13, the time derivative at t_d is practically zero which would tend to indicate that charge is not conserved. The explanation for this apparent failure lies in the fact that there is direct injection of short-lived carriers into the sample which contribute to the potential a quantity that is of the order of the voltmeter resolution [93], and therefore the time derivative cannot be measured accurately. In these particular samples of Teflon FEP the electron mobility was so high that it prevented free-space charge accumulation. The limited resolution of the voltmeter is then responsible for such an apparent failure (see a fuller explanation in [93]).

So far the main advantages mentioned of using a constant-current triode have been the improvement of charge control and also that the study of charge transport is facilitated. A recent paper [75], however, suggests that constant charging at elevated temperatures improve charge stability in Teflon PFA. The charge centroid is found to be deeper into the sample when it is corona charged under constant current rather than constant voltage. This means that with constant-current charging a larger number of deep bulk traps is filled which improves stability. In work [94] by a research group in China, similar results were obtained with muscovite that was also charged in a constant-current corona triode.

Finally, it is worth mentioning the importance that moisture has on the experimental results obtained with a corona triode. When samples are placed under humid conditions, charges are less stable in the traps and charge transport is also facilitated, the overall effect being lower sample surface potentials for higher relative values of humidity. This has been observed for both positive and negatively corona charged samples [86], though the effect appears to be more pronounced for positive corona [87].

6.3 PVDF AND ITS COPOLYMERS P(VDF-TrFE)

Polar materials such as PVDF and its copolymers have been poled by corona discharge as mentioned in Section 4. One of the first attempt to obtain information during the poling process was presented by Gerhard-Multhaupt [95] who used a corona triode for poling ferroelectric PVDF samples. In his setup, a high voltage (~ 5 kV) was applied to the grid, and the charging current was measured. The sample then had its surface potential neutralized and was poled again, according to the same procedure and

using the same grid voltage and polarity. The charging currents measured in these two consecutive charging processes were integrated and the difference between them was related to the value of the remanent polarisation in the sample.

As for the use of constant current corona triodes, studies with PVDF and P(VDF-TrFE) have also concentrated on their ferroelectric properties. Of particular relevance is the fact that surface potential measurements in a corona triode can be used to obtain ferroelectric hysteresis cycles [96], as shown below.

Figure 16.

Surface potential buildup for a β-PVDF sample. Positive corona, charging density J_c = 20 nA/cm^2. The dashed line corresponds to the theoretical curve showing the three stages of the charging process

Figure 17.

Hysteresis cycle. Surface potential measurements in the constant current triode were used to generate the hysteresis cycle for a β-PVDF sample 12 μm thick. From [96].

The way by which hysteresis loops can be obtained from surface potential measurements has been illustrated [96] by examining a hypothetical case of a sample with no conductivity and that has all of its dipoles reoriented when the electric field is Ec, the coercive field. Figure 16 shows the surface potential behavior of such a sample submitted to negative and positive charging. The two regions where V increases linearly with time denote capacitive behavior, while the plateau appears because at E_c all the charges impinging onto the sample are compensated by the reorientation of the dipoles. This causes the surface potential to remain at a fixed value, equal to E_cL where L is the sample thickness. For obtaining the hysteresis cycles, the axis of time is transformed into the electrical displacement $D(t) = I_0t/A$ where A is the area of the sample, and the electric field is calculated as V/L. The remanent polarization is equated to $J_0t_r/2$ where t_r is the period of time during which the plateau is observed, and the factor 2 appears because in the initial condition the sample was polarized with opposite polarity.

In the actual measurements with PVDF, probably there is not a unique value for the coercive field and some conductivity is also likely to exist. Nevertheless, hysteresis cycles can still be obtained from surface potential measurements which are remarkably close to hysteresis cycles measured using the conventional techniques such as the Sawyer-Tower circuit [97]. A cycle obtained with the corona triode measurements is shown in Figure 17.

Theoretical models to explain the surface potential build up for these polar materials must now include the way by which the polarisation changes with time and its dependence on the electric field. For a Debye-like polarisation, for instance, an expression usually employed is

$$\frac{\partial P(x,t)}{\partial t} + \frac{P(x,t)}{\tau} = \frac{\chi E(x,t)}{\tau} \qquad (17)$$

where τ is the relaxation time and χ is the electric susceptibility. For the case of a ferroelectric polarisation, the right-hand term of Equation (17) is replaced by a constant term, equal to P_o/τ. Measurements of dipole switching in PVDF and its copolymers, for instance, have been interpreted using an equation similar to Equation (17) [98]

$$\frac{\partial P(x,t)}{\partial t} = \frac{P_s - P(x,t)}{\tau} \qquad (18)$$

where P_s is the remanent polarisation and τ is given by BE^{-n} where B and n are empirical constants.

Arkhipov *et al.* [74] have recently proposed a model including multiple trapping of injected carriers and nonlinear field dependence of an irreversible polarization for PVDF films. In another paper by the same group [99], three stages were identified in the polarisation build up which correspond roughly to the three regions shown in Figure 16. Their results were explained by assuming a strong polarization that nucleates at the beginning of the second process and is similar to the propagation of domain walls in ferroelectrics.

Another work in which PVDF has been used in a constant current corona triode was published by Gross *et al.* [100] in which unstretched PVDF samples were charged at low currents to relatively low electric fields. Under these conditions, the sample potential reached a steady-state regime whose value was proportional to the charging current. When the corona was switched off, the sample potential decreased to zero due to bulk conductivity. That the conductivity arose from intrinsic carriers was demonstrated by essentially identical results obtained for both polarities and for samples with one or two electrodes. It was found also that the conductivity increases with the relative humidity of the gas for the corona discharge. Humidity effects have also been observed in PVDF samples that displayed ferroelectric behavior [76, 77].

Figure 18.

Surface potential buildup for a P(VDF-TrFE) sample 6 μm thick. Same as in Figure 16 but with a P(VDF-TrFE) sample. From [102].

The results for the P(VDF-TrFE) of various contents are similar to the experimental results obtained with

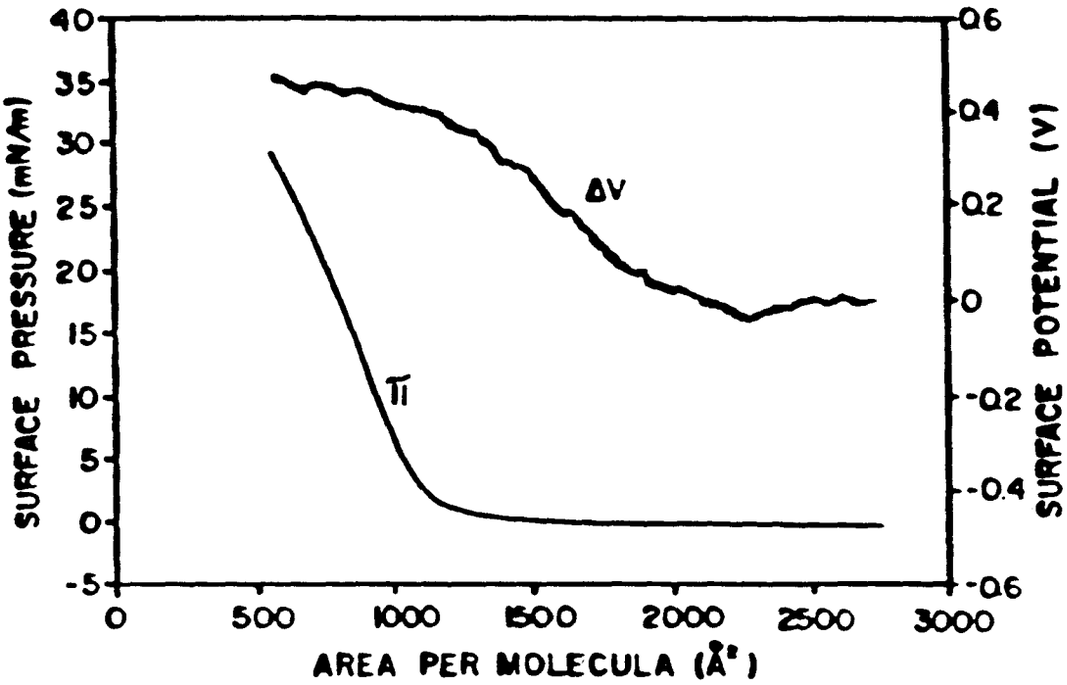
SURFACE PRESSURE (mN/m)
SURFACE POTENTIAL (V)
AREA PER MOLECULA (Å²)
ΔV
π
40
35
30
25
20
15
10
5
0
-5
0.6
0.4
0.2
0
-0.2
-0.4
-0.6
0
500
1000
1500
2000
2500
3000

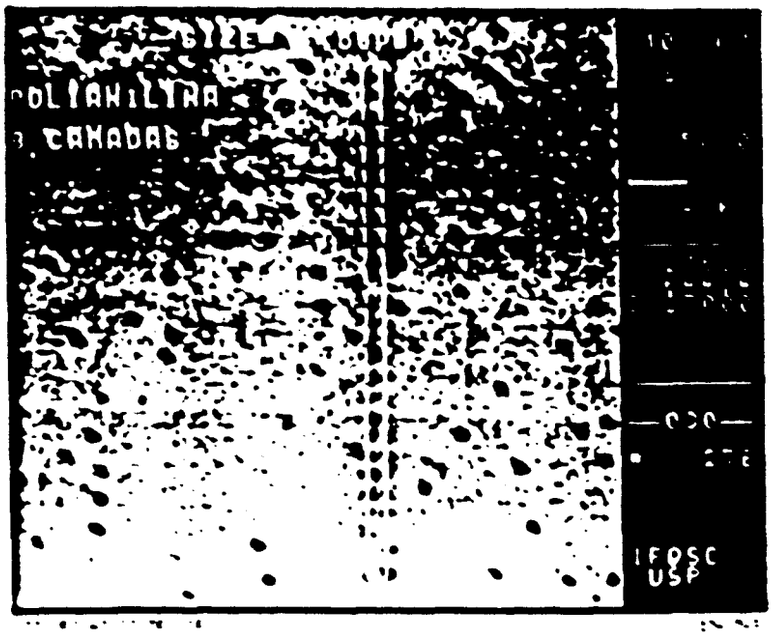
IFOSC
USP

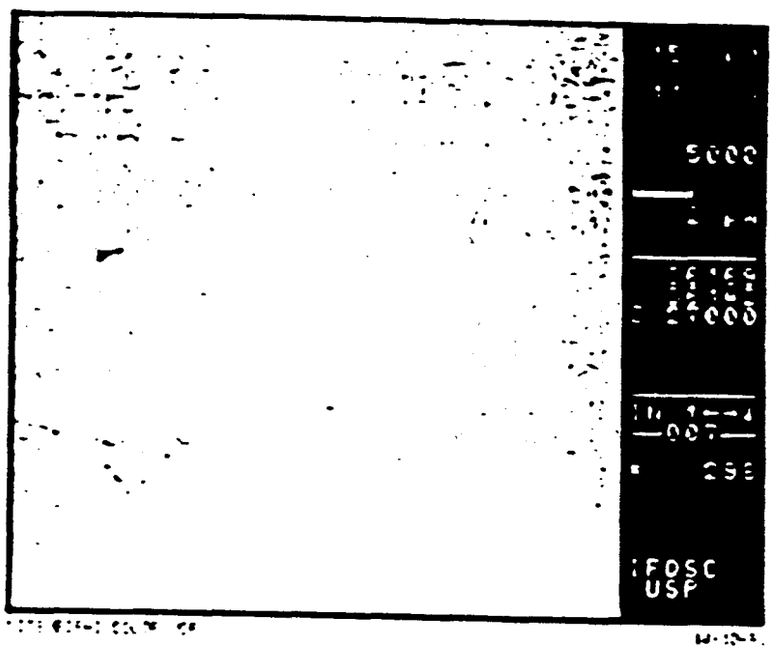
IFOSC
USP

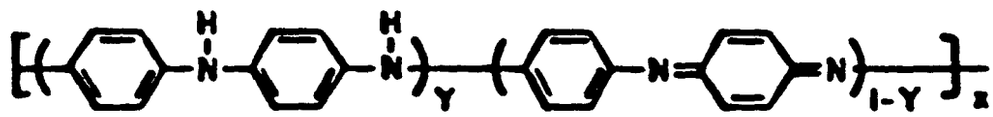

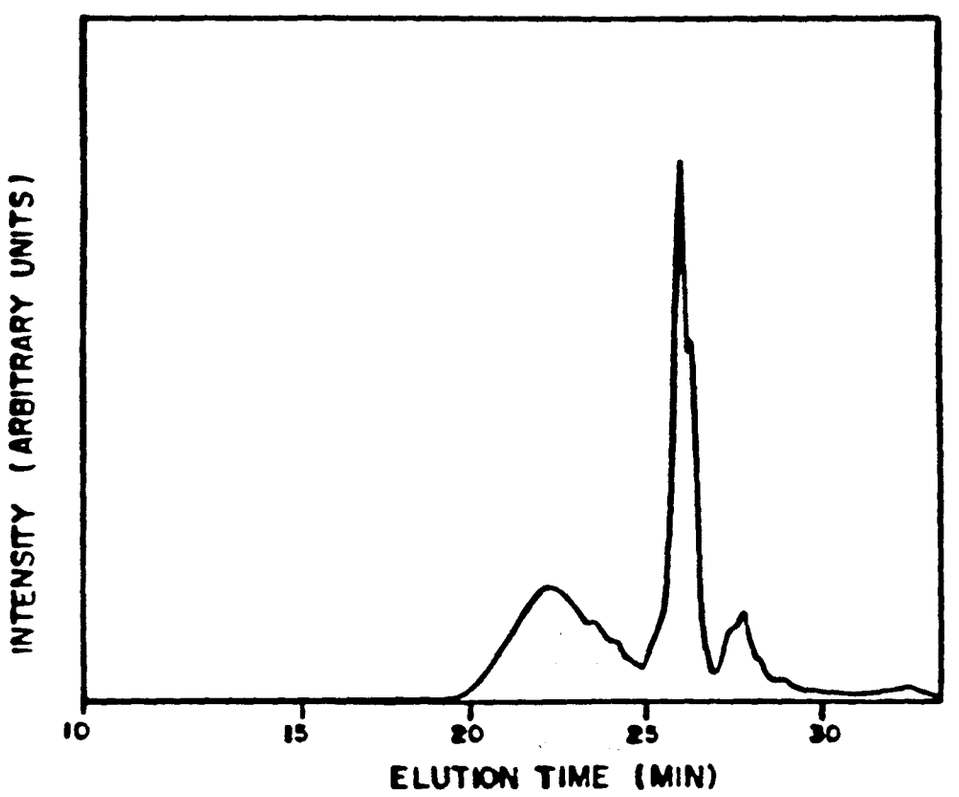
INTENSITY (ARBITRARY UNITS)
10
15
20
25
30
ELUTION TIME (MIN)

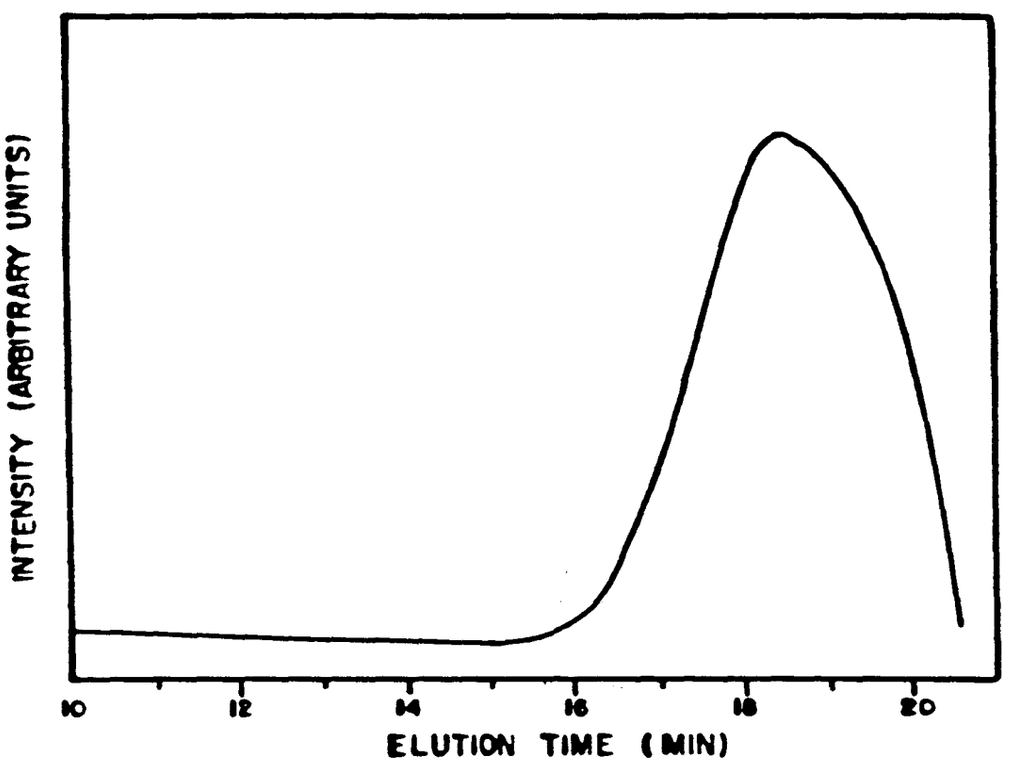
INTENSITY (ARBITRARY UNITS)
10
12
14
16
18
20
ELUTION TIME (MIN)

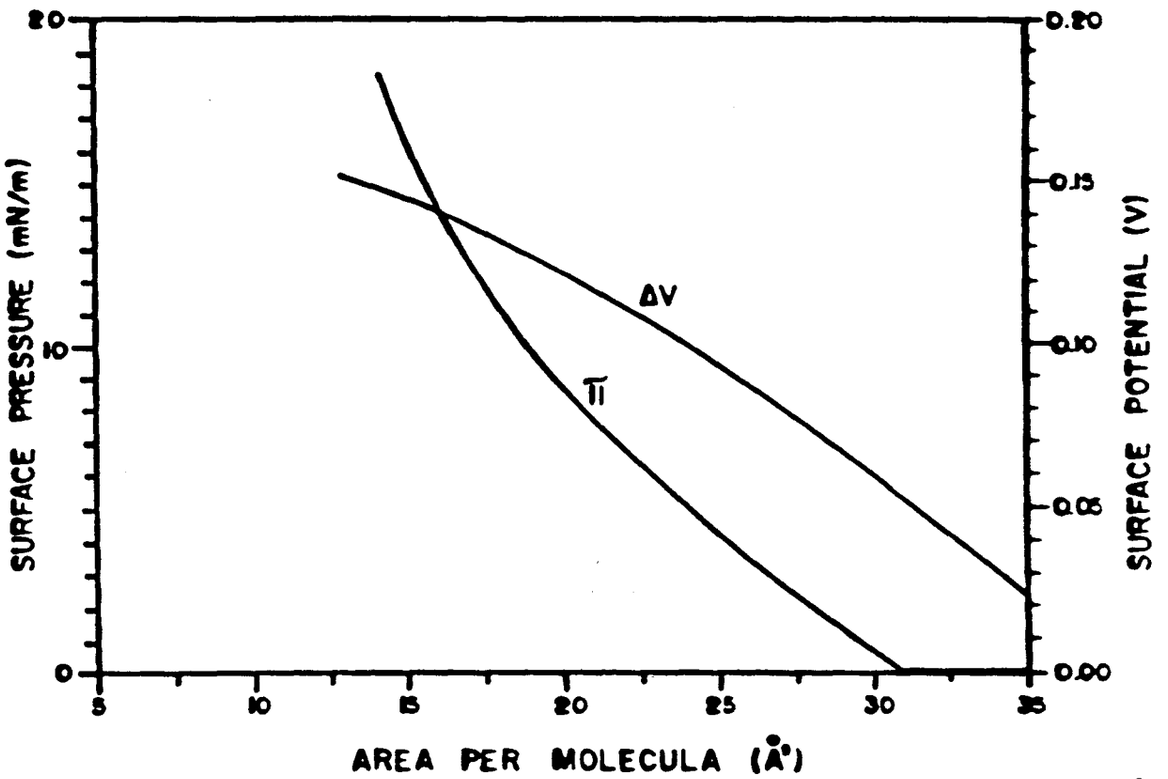
20
10
0
0.20
0.15
0.10
0.05
0.00
5
10
15
20
25
30
35
SURFACE PRESSURE (mN/m)
SURFACE POTENTIAL (V)
AREA PER MOLECULA (Å²)
ΔV
π

PVDF [101]. The main difference lies in the better defined plateau that is observed for the copolymer. Figure 18 shows the surface potential buildup of a 70 30 copolymer (70% VDF, 30% TrFE) sample which was submitted to a negative charging current of 10 nA [102]. This type of curve can be interpreted by assuming a ferroelectric polarisation which is proportional to the degree of crystallinity of the sample and a Debye-like polarisation that probably arises from the relaxation of dipoles in the amorphous parts of the polymer [102]. These models are similar to the nucleation-growth models which have been employed for other ferroelectric materials [103].

Finally, the constant-current corona triode also has been used in the poling of non-polar α-PVDF samples which undergo a phase transition to the polar α_p form. The phase transition is facilitated when the corona polarity is positive under dry air [104], and the ferroelectric behavior can be identified in the surface potential buildup by a plateau analogous to the one shown here in Figure 16

7. CONCLUDING REMARKS

An overview of the corona charging of polymers has been given which has focused on the use of corona triodes. The constant-current versions of the corona triode, now available in several countries, are quite promising because they serve not only as a means for charging polymer samples, but also as a method for investigating charge transport and ferroelectric properties. A number of polymer characteristics such as the occurrence of trap filling in Teflon FEP have been established unequivocally from studies using constant current corona triodes. The power of the method has also been illustrated by the generation of ferroelectric hysteresis cycles from surface potential measurements, which show that charging samples with a constant corona triode may suffice for identifying the ferroelectric activity in polymer samples. The trend now is for the building of increasingly sophisticated triodes that allow temperature and atmosphere control, and investigations using these triodes may make it possible to monitor the humidity and temperature effects on the polymer properties. The possibility of poling and characterizing polymer samples doped with nonlinear optics dyes is also exciting because it opens up a number of new possible applications.

REFERENCES

[1] G. W. Trichel. "The mechanism of the negative point to plane corona near onset", Phys. Review, Vol. 54, pp. 1078–1084, 1938.

[2] J. E. Jones, M. Davies, A. Goldman, and M. Goldman. "A simple analytic alternative to Warburg's law", J. Phys. D: Appl. Phys. Vol. 23, pp. 542-552. 1990.

[3] M. Robinson. "Movement of Air in the electric wind of the corona discharge", Trans. Am. Inst. Elec. Eng Vol. 80, pp. 143-152, 1961.

[4] M. M. Sahin. "Nature of charge carriers in negative coronas", Appl. Opt. Suppl. Electr. Photogr. Vol. 82, pp. 106-110, 1969.

[5] M. M. Sahin. "Mass-Spectrometric studies of corona discharges in air at atmospheric pressures", J. Chem. Phys. Vol. 43, pp. 2600-2605, 1966.

[6] D. K. Brandvold, F. Martinez, and D. Droguel. "Polarity dependence of N_2O formation from corona discharge", Atm. Environment, Vol. 23, pp. 1881-1883, 1989.

[7] B. Gravendeel, *Negative Corona Discharges. A fundamental Study*, Ph D. Thesis Technische Universiteit, Eindhoven 1987.

[8] A. Goldman and J. Amoroux, *Electrical Breakdown and Discharges in Gases: Macroscopic Processes and Breakdown*, Part B, pp. 293-346, ed. E. E. Kunhardt and L. H. Luessen, Plenun Press 1981.

[9] R. S. Sigmond, *Electrical Breakdown in Gases*, ed. J. M. Meek and J. D. Craggs, chapter 4, John Wiley and Sons 1978.

[10] M. Goldman and A. Goldman, *Gaseous Electronics*, Vol. 1, ed. M. N. Hirsh and H. J. Oskam, chapter 4, Academic Press 1978.

[11] R. S. Sigmond and M. Goldman, *Electrical Breakdown and Discharges in Gases: Macroscopic Processes and Breakdown*, pp. 1-64, Part B, ed. E. E. Kunhardt and L. H. Luessen, Plenun Press 1981.

[12] E. Badareu and I. Popescu, *Gaz Ionisés. Décharges Électriques dans les Gaz*, chapter 1, Editions Dunod 1968.

[13] L. B. Loeb, *Electrical Coronas*, University of California, Berkeley, 1965.

[14] E. Nasser, *Fundamentals of Gaseous Ionization and Plasma Electronics*, John Wiley, New York 1971.

[15] R. J. Van Brunt, "Stochastic Properties of Partial Discharge Phenomena: A Review", IEEE Trans. Elec. Insul. - Digest of Literature on Dielectrics, pp. 902-948, 1991.

[16] C. F. Carlson, "Electrophotography", U. S. Patent 2.297.691, 1942.

[17] J. H. Dessauer and H. E. Clark,*Xerography and Related Process*, Focal Press, London, 1965.

[18] R. M. Schaffert,*Electrophotography*, The Focal Press, 1975.

[19] M. Hohlfeld, "Das Niederschlagen des Rauches durch Elektricität", Archiv. für dir gesammte Naturlehre, Vol. 2, pp. 205, 1824.

[20] H. J. White, *Industrial Electrostatic Precipitation*, Addison- Wesley Co, 1963.

[21] A. D. Moore, *Electrostatics and Its Application*, John Wiley & Sons, 1973.

[22] B. Hilcser and J. Malecki, *Electrets*, Elsevier, 1986.

[23] G. M. Sessler and J. E. West, *Electrets*, edited by G. M. Sessler, chapter 7, Springer-Verlag 1980.

[24] S. Mascarenhas. "Electret radiation dosimetry: a review", in Proc. of 5th International Symposium on Electrets, Germany 1985.

[25] G. M. Sessler, *Electrets*, chapter 2, ed. G. M. Sessler, Springer Verlag 1980.

[26] P. W. Chuldleigh, R. E. Collins, and G. D Hancock. "Stability of liquid charged electrets", Appl. Phys. Lett. Vol. 23, pp. 211–212, 1973.

[27] P. W. Chudleigh, "Mechanism of charge transfer to a polymer surface by a conducting liquid contact", J. Appl. Phys. Vol. 47, pp. 4474–4483. 1976.

[28] G. M. Sessler and J. E. West, "Production of high quasipermanent charge densities on polymer foils by applications of breakdown fields", J. Appl. Phys. Vol. 43, pp. 922–926, 1972.

[29] R. A. C. Altafim, J. A. Giacometti and J. M. Janiszewski, "A novel method for electret production using impulse voltages" to be published in the IEEE - Trans. Elec. Insul.

[30] W. Stark. "Electret formation by electrical discharge in air", J. of Electrostatics, Vol. 22, pp. 329–339, 1989.

[31] B. Gross, R. Gerhard-Multhaupt, A. Berraissoul, and G. M. Sessler, "Electron-beam poling of piezoelectric polymer electrets", J. Appl. Phys. Vol. 62, pp. 1429–1432, 1987.

[32] W. D. Greason and B. H. Beyer, "Corona charging method for controlled production of film electrets", in 1982 Annual IAS-IEEE Meeting pp. 1148–1152.

[33] T. T. Wang, J. M. Hebert, and A. M. Glass ed. *The Applications of Ferroelectric Polymers*, Blackie 1987.

[34] P. M. Galletti, D. E. De Rossi, and A. S. DeReggi ed. *Medical Applications of Piesoelectric Polymers*, Gordon and Breach Science Publishers, NY 1988.

[35] C. F. Liaw and I. C. Chen, "Poling of multiple PVDF films by moving corona discharge", Ferroelectrics, Vol. 99, pp. 127–132, 1989.

[36] S. J. Bethke, S. G. Grubb, H. L Hampsch, and J. M. Torkelson, "Atmospheric effects on corona poling of nonlinear optical doped polymer films", Proceedings of the SPIE - The International Society for Optical Engineering, Vol. 1216, pp. 260-71, 1990.

[37] R. H. Page, M. C. Jurich, B Reck, A. Sen, R. J. Twieg, J. D. Swalen, G. C. Bjorklund, and C. G. Wilson, "Electrochromic and optical waveguide studies of corona-poled electron-optic polymer films", J. Opt. Soc. Am. B, Vol. 7, pp. 1239-1250, 1990.

[38] M. A. Mortazavi, A. Knoesen, S. T. Kowel, B. G. Higgins, and A. Dienes, "Second harmonic generation and absorption studies of polymer-dye films oriented by corona-onset poling at elevated temperatures", J. Opt. Soc. Am. B., Vol. 6, pp. 733-741, 1989.

[39] M. Eich, A. Sen, H. Looser, G. C. Bjorklund, J. D. Swalen, R. Twieg, and D. Y. Yoon, "Corona poling and real-time second-harmonic generation study of a novel covalently functionalised amorphous nonlinear optical polymer", J. Appl. Phys., Vol. 66, pp. 2559-2567, 1989.

[40] R. A. Moreno and B. Gross "Measurement of potential buildup and decay, surface charge density, ad charging currents of coronacharged polymer foil electrets", J. Appl. Phys., Vol. 47, pp. 3397-3402, 1976.

[41] J. van Turnhout. Thermally Stimulated Discharge of Polymer Electrets, Elsevier. 1975. R. E. Collins. "Distribution of charge in electrets", Appl. Phys. Lett., Vol. 26, pp. 675-677, 1975.

[42] R. E. Collins. "Distribution of charge in electrets", Appl. Phys. Lett., Vol. 26, pp 675-677, 1975.

[43] A. S. DeReggi, C. M. Guttman, F. I. Mopsik, G. T. Davis, and M. G. Broadhurst, "Determination of charge or polarization distribution across polymer electrets by the thermal pulse method and Fourier analysis", Phys. Rev. Lett., Vol. 40, pp. 413-416, 1978.

[44] G. M. Sessler and G. Gerhard "A review of methods for chargeor field-distribution studies on radiation-charged dielectric films", Radiat. Phys. Chem., Vol. 23, pp. 363-370, 1984.

[45] C. Alquie, G. Dreyfus, and J. Lewiner, "Stress-Wave probing of electric field distributions in dielectrics", Phys. Rev. Lett., Vol. 47, pp. 1483-1487, 1981.

[46] A. G. Rozno and V. V. Gromov, Soviet Technical Letters, Vol. 5, pp. 266-267, 1979.

[47] W. Eisenmenger and M. Haardt, "Observation of charge compensated polarization in PVDF films by piezoelectric acoustic step-wave response", Sol. Stat. Com., Vol. 41, pp. 917-920, 1982.

[48] S. B. Lang and D. K. DasGupta, "Laser-intensity-modulation method: a technique for determination of spatial distributions of polarisation and space charge in polymer electrets", J. Appl. Phys. Vol. 59, pp. 2151-2160, 1986.

[49] K. K. Kanasawa, I. P. Batra, and H. J. Wintle, "Decay of Surface Potential in Insulators", J. Appl. Phys., Vol. 43, pp. 719-720, 1972.

[50] I. P. Batra, K. K. Kanasawa, B. H, Schechtman, and H. Seki, "Charge-Carrier Dynamics Following Pulsed Injection", J. Appl. Phys. Vol. 42, pp. 1124-1130, 1971.

[51] H. Seki and I. P. Batra, "Photocurrents Due to Pulse Illumination in the Presence of Trapping. II", J. Appl. Phys., Vol. 42, pp. 2407-2420, 1971.

[52] I. P. Batra, K. K. Kanasawa, and H. Seki, "Discharge Characteristics of Photoconducting Insulators", J. Appl. Phys., Vol. 41, pp. 3416-3422, 1970.

[53] C. C. Kao and I. Chen, "Xerographic Discharge Characteristics of Photoreceptors with Bulk Generation", J. Appl. Phys., Vol. 44, pp. 2708-2717, 1973.

[54] I. Chen, "Effects of Bimolecular Recombination on Photoconduction and Photoinduced discharge", J. Appl. Phys., Vol. 49, pp. 1162-1172, 1978.

[55] D. C. Hoesterey, "Effect of Dielectric Breakdown on the Charging of ZnO Xerographic Layer", J. Appl. Phys., Vol. 33, pp. 992-995, 1962.

[56] A. I. Rudenko, "Passage of a Space-Charge-Limited Current Pulse Through a Solid in the Presence of Traps", Soviet Physics -Solid State, Vol. 14, pp. 2706-2709. 1973.

[57] A. Reiser, M. W. Lock, and J. Knight, "Migration and Trapping of Extrinsic Charge Carriers", Trans. Faraday Soc., Vol. 65, pp. 2168-2185, 1969.

[58] H. J. Wintle. "Surface Charge Decay in Insulators with non Constant Mobility and with Deep Trapping", J. Appl. Phys. Vol. 43, pp. 2927-2930, 1972.

[59] T. J. Sonnonstine and M. M. Perlman, "Transient Injection Currents in Insulators with Pre-Existing Trapped Space Charge", Physical Review B, Vol. 12, pp. 4434-4442, 1975.

[60] E. A. Baum, T. J. Lewis, and R. Toomer, "The Decay of Surface Charge on n-octadecane Crystals", J. Phys. D: Appl. Phys., Vol. 11, pp. 703-716, 1978.

[61] M. Campos and J. A. Giacometti, "Surface-Potential Decay in Insulators with Deep Traps", J. Appl. Phys., Vol. 52, 4546-4552, 1981.

[62] M. Campos, J. A. Giacometti, and M. Silver, "Deep Exponential Distribution of Traps in Naphthalene", Appl. Phys. Lett., Vol. 34, pp. 226-228, 1979.

[63] M. Campos and J. A. Giacometti, "Surface-Potential Decay in Naphthalene", Appl. Phys. Lett., Vol. 32, pp. 794-796. Year?

[64] M. H Woods and R. Willians, "Injection and Removal of Ionic Charge at Room Temperature Through the Interface of Air with SiO_2", J. Appl. Phys., Vol. 44, pp. 5506-5510, 1973.

[65] S. W. Ing Jr and J. H. Neyhart, "Dark Discharges in Amorphous As2 Se3 Films", J. Appl. Phys., Vol. 43, pp. 2670-2680, 1972

[66] H. J. Wintle, "Decay of Static Electrification by Conduction Processes in Polyethylene", J. Appl. Phys., Vol. 41, pp. 4004-4007, 1970.

[67] T. Mizutani, T. Oomura, and M. Ieda, "Surface Potential Decay in Polyethylene", Japan. J. Appl. Phys., Vol. 20, pp. 855-859, 1981.

[68] D. K. Das-Gupta, "Charge Decay on Polymer Surfaces", J. of Electrostatics, Vol. 23, pp. 331-340, 1989.

[69] M. M. Perlman, T. J. Sonnonstine, and J. A. St. Pierre, "Drift Mobility Determinations Using Surface Potential Decay in Insulators", J. Appl. Phys., Vol. 47, pp. 5016-5021, 1976.

[70] H. J. Wintle, "Decay of Surface Electric Charge in Insulators", Japan. J. Appl. Phys. vol. 10, pp. 659-660, 1971.

[71] R. Toomer and T. J. Lewis, "Charge Trapping in Corona-Charged Polyethylene Films", J. Phys. D: Appl. Phys., Vol. 13, pp. 1343-1355, 1980.

[72] M. Ieda, G. Sawa and U. Shinohara, "A Decay Process of Surface Electric Charges Across Polyethylene Film", Japan. J. Appl. Phys. Vol. 6, pp. 793-794, 1967.

[73] G. F. Leal Ferreira and M. T. Figueiredo, "Corona Charging of electrets. Models and Results", to be published in the IEEE -Trans. Elec. Insul.

[74] H. von Berlepsch, "Interpretation of Surface Potential Kinetics in HPDE by a Trapping Model", J. Phys. D: Appl. Phys., Vol. 18, pp. 1155-1170, 1985.

[75] R. M. Faria, A. Jorge, and O. N. Oliveira Jr., "A novel spacecharge effect in thermally stimulated current measurements on β- PVDF", J. Phys. D: Appl. Phys., Vol. 23, pp. 334-337, 1990.

[76] H. von Seggern, "Identification of TSC peaks and surface voltage stability in Teflon FEP", J. Appl. Phys., Vol. 50, pp. 2817-2821, 1979.

[77] H. von Seggern, "Isothermal and thermally stimulated current studies of positively corona charged Teflon FEP", J. Appl. Phys., Vol. 52, pp. 4081-4085, 1981.

[78] D. K. Das Gupta and K. Doughty, "Changes in X-ray diffraction patterns of PVDF due to corona charging", Appl. Phys. Lett., Vol. 31, pp. 585-587, 1977.

[79] J. A. Giacometti and A. S. DeReggi, "Thermal pulse study of the polarisation distributions produced in PVDF by constant current corona poling", submitted to J. Appl. Phys

[80] P. D. Southgate, "Room-temperature poling and morphology changes in pyroelectric PVDF", Appl. Phys, Lett., Vol. 28. pp. 250-252, 1976.

[81] N. Takahashi, J. Rault, A. Goldman and M. Goldman, "Surface modification of polyethylene films by neutral activated species of a corona discharge", Proc. 2nd IEEE Intern. Conf. Cond. Breakdown in Solid Diel.; Erlangen, pp. 179-185, 1986.

[82] M. Raposo, P. A. Ribeiro, J. A. Giacometti, M. A. Bento, and J. N. Marat-Mendes, "Effect of the corona discharge in different atmospheres on the thermally stimulated charge injection of Teflon FEP, in Proc. of 7th International Symposium on Electrets, pp. 687-692, 1991 Germany.

[83] J. Sarlaboux and C. Mayoux, "On the effect of corona treatment on polypropylene for capacitors", J. Phys. D: Appl. Phys., Vol. 12, pp. L13-17, 1979.

[84] B. Leclerq, M. Sotton, A. Baszkin, and L. Ter-Minassian-Saraga. "Surface modification of corona treated PET film: adsorption and wettability studies", Polymer, Vol. 18, pp. 675-680, 1977.

[85] J. L. Linsley Hood, "The corona discharge treatment of plastics films", 1980 Sixth Int. Conf. on Gas Discharges and their Applications, pp. 86-90, 1980.

[86] C. J. Dias, J. N. Marat-Mendes, and J. A. Giacometti, "Effects of a corona discharge on the charge stability of Teflon FEP negative electrets", J. Phys. D: Appl. Phys., Vol. 22. pp. 663-669, 1989.

[87] K. J. Kao, S. S. Bamji, and M. M. Perlman, "Thermally stimulated discharge current study of surface charge release in polyethylene by corona-generated excited molecules, and the crossover phenomenon", J. Appl. Phys., Vol. 50, pp. 8181-8185, 1979.

[88] E. A. Baum, T. J. Lewis, and R. Toomer, "Decay of Electrical Charge on Polyethylene Films". J. Phys. D: Appl. Phys., Vol. 10, pp. 487-497, 1977.

[89] E. A. Baum, T. J. Lewis, and R. Toomer, "Further Observations on the Decay of Surface Potential of Corona charged Polyethylene Films", J. Phys. D: Appl. Phys., Vol. 10. pp. 2525-2531, 1977,

[90] S. Haridoss and M. M. Perlman, "Chemical modification of near surface charge trapping in polymers", J. Appl. Phys., Vol. 55, pp. 1332-1338, 1984.

[91] D. L Chinaglia, G. F. Leal Ferreira, J. A. Giacometti, and O. N. Oliveira Jr, "Corona-triode characteristics: on effects possibly caused by the electronic component", in 7th International Symposium on Electrets, pp. 255–259, Germany 1991.

[92] D. K. Das Gupta, "Decay of electrical charges on organic synthetic polymer surfaces", IEEE Trans. Elec. Insul., Vol. 25, pp. 503–508, 1990.

[93] D. K. Das Gupta, "Charge decay on polymer surfaces", J. of Electrostatics, Vol. 23, pp. 331–340, 1989.

[94] D. K. Das Gupta, K. Doughty, and A. Goodings, "Charge motion on moist polymer surfaces", in 1986 Annual Report of CEIDP, IEEE, pp. 77, 1986.

[95] Z. A. Weinberg, D. L. Matthies, W. C. Johnson, and M. A. Lampert, "Measurement of the steady-state potential difference across a thin insulating film in a corona discharge", Rev. Sci. Instrum., Vol. 46, pp. 201–203, 1975.

[96] C. W. Reedyk and M. Perlman, "The measurement of surface charge", J. Electrochemical Soc., Vol. 115, pp. 49–51, 1968.

[97] B. Gross, J. A. Giacometti, and G. F. Leal Ferreira, "Corona method for investigation of charge storage and transport in dielectrics", Annual Report of Conf. on Elec. Insul. and Diel. Phenomena pp. 39–44, USA 1981.

[98] J. A. Giacometti, *Corona with constant current: A new method for studying charge storage and transport in insulators*, Ph. D. Thesis 1982, University of S. Paulo, Brazil (in portuguese).

[99] R. Haug, French Patent 8.414.209, 1985. Title?

[100] J. A. Giacometti and J. S. Carvalho Campos, "Constant current corona triode with grid voltage control. Application to polymer foil charging", Rev. Sci. Instrum., Vol. 61, pp. 1143–1150, 1990.

[101] J. A. Giacometti, "Radial current-density distributions and sample charge uniformity in a corona triode", J. Phys. D: Appl. Phys., Vol. 20, pp. 675–682, 1987.

[102] V. I. Arkhipov, S. N. Fedosov, D. V. Khramchenkov, and A. I. Rudenko, "Dispersive Transport in ferroelectric polymers", Journal of Electrostatics, Vol. 22, pp. 177–184, 1989.

[103] X. Zhong-fu, D. Hai, Y. Guo-mao, L. Ting-ji, and S. Xi-mim, "Constant-current corona charging of Teflon PFA", IEEE Trans. Elec. Insul., Vol. 26, pp. 35–41, 1991.

[104] P. A. Ribeiro, J. A. Giacometti, M. Raposo, and J. N. Marat- Mendes, "Effect of the air humidity on the corona polarization of β-PVDF films", in 7th International Symposium on Electrets, pp. 322–327, 1991 Germany.

[105] P. A. Ribeiro, J. A. Giacometti, M. Raposo and J. N. Marat-Mendes, "Constant current corona charging of biaxially stretched PVDF films under humidity controlled atmospheres", Submitted to IEEE Trans. Elec. Insul.

[106] J. A. Giacometti and A. S. DeReggi, "Thermal Pulse study of the polarisation distributions produced in PVDF by constant current corona poling", Submitted to J. Appl. Phys.

[107] K. J. Mclean, Z. Herceg, and R. I. Boccola, "Electrical transparency of a corona triode", Journal of Electrostatics, Vol. 9, pp. 211–222, 1981.

[108] R. Haug. J. Lebas, and Y. Teysseyre, "Numerical simulation of the ionic transparency for a grid in an ionised gas-flow", J. Phys. D: Appl. Phys., Vol. 15, pp. 1709–1720, 1982.

[109] R. Haug. J. Lebas, and Y. Teysseyre, "Ion current calculation in a system of plane grids in an ionised gas flow", J. Phys. D: Appl. Phys., Vol. 17, pp. 357–366, 1984.

[110] O. N. Oliveira Jr and G. F. Leal Ferreira, "Grid to plate current-voltage characteristics of a corona triode", Rev. Sci. Instrum., Vol. 56, pp. 1957–1961, 1985.

[111] R. Gerhard-Multhaupt and W. Petry, "High resolution probing of surface-charge distributions on electret sample", J. Phys. E: Sci. Instrum., Vol. 16, pp. 418–420, 1983.

[112] R. A. Moreno, *A method for studying charge transport in dielectric foils using a corona discharge*, Ph. D. Thesis 1977, University of São Paulo, Brazil (in portuguese).

[113] H. von Seggern, "Improved surface voltage uniformity of electrets obtained by modified corona charging method", 1983 Conf. Record, IEEE-IAS Annual Meeting pp. 1093–1097, 1983.

[114] J. A. Giacometti and J. S. C. Campos, "Constant current corona triode with bias grid voltage control", in 6th International Symposium on Electrets, pp. 404–408, England 1988.

[115] O. N. Oliveira Jr and G. F. Leal Ferreira, "Electron transport in corona charged 12 m Teflon FEP with saturable deep traps", Appl. Phys. A, Vol. 42, pp. 213–217, 1987.

[116] G. F. Leal Ferreira and O. N. Oliveira Jr, "Hole transport in corona-charged 12 μm Sheldahl FEP samples interpreted through a field-dependent schubweg model", Phys. Stat. Sol. (a), Vol. 105, pp. 531–539, 1988.

[117] G. E. Forsythe and W. R. Wasow, *Finite Difference methods for partial differential equations*, pp. 15–37, John Wiley, New York 1967.

[118] J. A. Giacometti, G. F. Leal Ferreira, and B. Gross, "Negative charge transport in FEP by constant current method", Phys. Stat. Sol. (a), Vol 88, pp. 297–307, 1985.

[119] B. Gross, J. A. Giacometti, and G. F. Leal Ferreira, "Charge storage and transport in electron-irradiated and corona-charged dielectrics", IEEE Trans. Nucl. Sci., Vol. 28, pp. 4513–4522, 1981.

[120] B. Gross, J. A. Giacometti, G. F. Leal Ferreira, and R. A. Moreno, "Trap-controlled charge transport in corona-charged Teflon", Proc. Sec. Japan-Brazil Symposium on Science and Technology 1980, pp. 166–174, 1980.

[121] B. Gross, J. A. Giacometti, and G. F. Leal Ferreira, "Constant schubweg for hole transport in corona charged Teflon FEP", Appl. Phys. A, Vol. 37, pp. 89–94, 1985.

[122] G. F. Leal Ferreira, L. N. Oliveira, O. N. Oliveira Jr, and J. A. Giacometti, "An experimentally verified current-conservation relation", IEEE Trans. Elec. Insul, Vol. 21, pp. 275–279, 1986.

[123] X. Zhongfu and J. Jian, "Electret behavior of muscovite and its charge storage", in 7th International Symposium on Electrets pp. 27–32, Germany 1991.

[124] R. Gerhard-Multhaupt, "Corona poling of polyvinylidene fluoride", in Proc. of CEIDP, pp. 545–459, USA, 1983.

[125] G. M. Sessler and R. Gerhard-Multhaupt, "Spatial and temporal buildup of polarization in PVDF ", Proc. of CEIDP, pp. 393–398, USA, 1984.

[126] N. Alves, J. A. Giacometti, and O. N. Oliveira Jr., "Measuring hysteresis loops of ferroelectric polymers using the constant charging current corona triode", Rev. Sci. Instrum., Vol. 62, pp. 1840–1843, 1991.

[127] S. Ikeda, S. Kobayashi, and Y. Wada, "Analysis of the effect of electrical conductance of ferroelectric polymers on $D-E$ hysteresis curves measured by the Sawyer-Tower method", J. Polymer Sci.: Pol. Phys. Ed., Vol. 23, pp. 1513–1521, 1985.

[128] T. Furukawa, "Ferroelectric properties of vinylidene fluoride copolymers", Phase Transitions, Vol. 18, pp. 143–211, 1989.

[129] S. Fedosov and A. Sergeeva, "Polarisation build-up during constant current corona charging of PVDF", in 7th International Symposium on Electrets pp 249-254, Germany 1991.

[130] B. Gross, J. A. Giacometti, G. F. Leal Ferreira and O. N. Oliveira Jr, "Constant current corona charging of PVF2", J. Appl. Phys., Vol. 56, pp. 1487-1491, 1984.

[131] J. A. Giacometti, J. S. C. Campos, N. Alves, and M. M. Costa, "The electric behavior of PVDF and P(VDF-TrFE) during corona poling", in the Proc of CEIDP, pp. 77–82, USA, 1990.

[132] N. Alves, *Ferroelectric properties of P(VDF-TrFE)*. Ph. D. Thesis. University of São Paulo, Brasil, 1992 (in portuguese).

[133] N. Alves, J. A. Giacometti, O. N. Oliveira Jr, and R. M. Faria, "On the equivalence of the mechanism governing switching and hysteresis phenomena", in the 7th International Symposiun on Electrets pp. 545–459, Germany 1991.

[134] J. A. Giacometti, M. M. Costa, and G. Minami. "Phase Transition in corona charged -PVDF samples in dry air", in the 7th International Symposium on Electrets pp. 432–437, Germany 1991.

MESSAGE FOR THE AUTHOR

Please proofread, mark, and return this galley as soon as possible to:
Dr. A. van Roggen, 501 Orchard Lane, Kennett Square, PA 19348-2110, USA

In case there are minor problems with the text, these are indicated in the margins or as numbered endnotes. Please pay special attention to these items and make certain that all corrections have been made. Note that the Figure and Table locations will differ in the final print, where double columns are used.

After publication of this paper, you will receive a copy of the issue in which the paper is published, and an order form for reprints. If, after the acknowledgment of the paper, the mailing labels for coauthors were filled out and returned with the copyright form, they too will receive a copy of the issue and an order form.

Manuscript was received on 30 July 1992

NOTE I just received the Figure original from DeRoggi.

CHLOROFORM-SOLUBLE POLY(O-METOXYANILINE) FOR ULTRA-THIN FILM FABRICATION

R.M.Faria[1], L.H.C.Mattoso[1], M.Ferreira[1],

D.Gonçalves[2], L.O.S.Bulhões[2] and O.N.Oliveira Jr.[1]

[1]Instituto de Física e Química de São Carlos, USP

CP 369, 13560 São Carlos, S.P. - Brazil

[2]Departamento de Química, UFSCAR

CP 676, 13560 São Carlos, S.P. - Brazil

Abstract

One of the main difficulties in spreading Langmuir monolayers from conjugated (conducting) polymers is the lack of solubility of these polymers in common organic solvents. In this work we report on a chemically synthesized polyaniline derivative, poly(o-metoxyaniline), which is soluble in chloroform and has been used to fabricate ultra-thin films in a Langmuir trough. The poly(o-metoxyaniline) synthesized comprised two fractions, one of which has a low molecular weight (in fact it is an olygomer with a few monomers) and the other has a high molecular weight of approximately 28000 g/mol. When separated, the low weight fraction yields Y-type LB films by vertical dipping whereas films could only be deposited with the high weight fraction if the horizontal lifting method was employed. When examined through the scanning electron microscope, the latter films presented less defects than the LB films obtained with the low weight fraction. This is probably because pores which may have been present in the films obtained with the vertical dipping were not present in the more rigid monolayer of the high weight fraction.

I. Introduction

Spreading Langmuir monolayers from conjugated polymers has been fraught with considerable difficulties, in particular because these polymers generally do not dissolve in organic solvents. This has prompted a number of research groups to direct efforts towards developing especially substituted conjugated polymers which would be amenable to dissolution in an organic solvent. For instance, the incorporation of electron-donor or long and flexible substituents has been reported to improve the solubility and processability of conducting polymers [1]. In this paper we present a preliminary report on poly(o-metoxyaniline) which was found to dissolve readily in chloroform permitting the formation of Langmuir monolayers, and the subsequent transfer onto glass substrates in a Langmuir trough. LB films deposited from other polyaniline derivatives have been reported in earlier works [2,3].

II. Experimental Details

The synthesis of poly(o-metoxyaniline) has been described in a previous paper [4], and so only a brief description is given here. Poly(o-metoxyaniline) (see Fig. 1) was synthesized by chemical oxidation with ammonium persulfate according to a method similar to that used for polyanilines [1]. A solution of 0.02 mol of o-metoxyaniline (from Merck) was dissolved in 200 ml of 1.0 M HCl and the solution was cooled to - 5°C using a criothermostat with an ethanol-water bath. The oxidant agent (0.03 mol) in 80 ml of 1.0 M HCl was added dropwise under vigorous stirring and

the solution changed colour from red to black as a dark green precipitate was formed. The resulting solution was left in the cold bath for 2h, after which the precipitate was collected using a Buchner funnel and washed with 1.0 M HCl until the filtrate became colourless. The polymerization yield was ca. 70%. The polymers were dried under vacuum for 48 h, and after deprotonation in 0.1 M NH_4OH (pH = 10.0) the poly(o-metoxyaniline) becomes soluble in chloroform.

Gel Permeation Chromatography (GPC) was used to determine the molecular weight of poly(o-metoxyaniline). It was found that the poly(o-metoxyaniline) could be divided into two fractions, one with a low molecular weight (LW) that is soluble in chloroform and tetrahydrofurane, and another one with a much higher molecular weight (HW) that is soluble in chloroform and a highly polar organic solvent, the N-methylpyrrolidinone (NMP). The base form of the poly(o-metoxyaniline) was studied by gel permeation chromatography (GPC), where tetrahydrofurane was the solvent for the low molecular weight fraction (LW), while NMP was the solvent used in a LiCl (0.5%) medium for the high molecular weight fraction (HW). GPC was performed on a Waters Associates GPC equipped with a Model 400 refractometer as the detector. Fig. 2 and 3 show the GPC curves for the LW and HW fractions, respectively. The LW fraction comprises oligomers made up of monomers, dimers and octomers, leading to a mean molecular weight of 500 g/mol as a monodisperse polymer. The HW fraction, on the other hand, is clearly polymeric possessing a mean molecular weight of 28000 g/mol with a polydispersivity of 2.58.

Langmuir monolayers were spread and subsequently transferred

onto solid substrates using a KSV 5000 system housed in a clean room. The LW and HW fractions of poly(o-metoxyaniline) which were previously separated by GPC were dissolved in HPLC grade chloroform (concentration between 0.2 to 0.4 mg/ml) and an aliquot of 100-300 µl was spread onto the water subphase. Ultra pure water was obtained from a Milli-RO 60 system feeding a Milli-Q Plus system. The whole system from Millipore comprises reverse osmosis, carbon and ion exchange cartridges, followed by further polishing Organex-Q and U.V. filters. A short period of time (approximately 5 - 10 min) was allowed for the chloroform to evaporate from the layer before compression. A typical π-ΔV-A isotherm was performed as follows: the monomolecular film was compressed continuously at a speed of 25 mm/min below which no difference could be detected in the shape of the isotherms. Above 25 mm/min the monolayers tend to present a smaller area per molecule, the effect increasing in magnitude as the speed of barrier compression is increased. During compression the surface pressure and surface potential were measured simultaneously while the position of the barrier gave the mean area per molecule. The surface pressure was measured with a Wilhelmy plate to an accuracy of approximately 0.1 mN/m and the surface potential was obtained with a Kelvin probe to an accuracy of approximately 10 mV, both instruments provided by KSV.

Langmuir-Blodgett films were deposited on glass slides which were prepared according to the following procedure:

- immersion during 5 min. in a concentrated solution of KOH,
- cleaned for 5 min. in concentrated chromic acid,
- rinsed with copious quantities of ultra pure water.

- dried by blowing dry nitrogen onto them.

III. Results and Discussion

Fig. 4 and 5 show the π-ΔV-A isotherms for monolayers obtained from the low (LW) and high weight (HW) fractions of poly(o-metoxyaniline), respectively. The mean area per molecule was estimated by taking molecular weights from the GPC results, i.e. 500 for the LW and 28000 for the HW. As one could expect from the complexity of the film-forming molecules the π-A curves are reasonably expanded in both cases, though no proeminent feature appears in either curves. The area per molecule for the condensed monolayers was close to 20 $Å^2$ (the same value for long chain fatty acids such as stearic acid) for the LW monolayer, which is similar to the curve obtained by Ando et al [3] for one of their alkyl polyanilines. The area per molecule in the condensed HW monolayer was approximately 1500 $Å^2$. The collapse pressure was around 30 mN/m for the LW monolayer and exceeded 40 mN/m for the HW monolayer. When left onto the water surface at a constant pressure, say 10 mN/m, both monolayers were very stable with less than 10% of area loss over a period of time of one hour.

The surface potential, which usually reflects the molecular dipole moments [5,6], can only be examined from a qualitative perspective. ΔV is zero at very large areas per molecule for both monolayers, probably because the monolayers are not sufficiently structured for the effective dielectric constant of the film-

water interface to be considerably lower than that of bulk water. As soon as the monolayer becomes structured, this dielectric constant drops and a somewhat sharp increase in ΔV is observed. Such a behaviour has also been obeerved for phospholipid and fatty acid monolayers [7-9]. The absence of any other major feature in the ΔV-A curve means that any drastic molecular rearrangement is unlikely to have taken place. These rearrangements are usually accompanied by phase transitions in π-A and especially in ΔV-A curves (see [5]).

We have tried to transfer Langmuir monolayers of both LW and HW fractions onto glass substrates using the traditional vertical dipping method. Successful deposition was achieved for the LW fraction in which Y-type multilayers were deposited with a transfer ratio close to 1. Because the film-forming molecules comprised monomer, dimers and octomers the Langmuir monolayer was not sufficiently rigid to prevent a Y-type deposition. Fig. 6 shows a Scanning Electron Micrograph (SEM) for a 7-layer LB film which shows a large number of defects (or pores). Hence, though the deposition was successful the resulting films were nevertheless non uniform.

Very poor multilayers were produced for the HW fraction when the vertical method was employed. The transfer ratio was only around 0.3 and the deposition was not uniform, and this may be explained by the rigidity of the monolayer. It is a common feature of preformed polymer Langmuir monolayers that they are too stable on the surface and cannot be transferred onto a solid substrate. It was then tried the horizontal lifting method for this HW fraction with which multilayers could be successfully

deposited.

The ultra-thin films from the HW fraction obtained by the horizontal lifting technique showed a much more compact texture, without the pores observed in the LW LB films, as can be seen in the SEM micrograph of Fig. 7 for a film with 8 layers. The most likely explanation for this experimental finding is that the HW monolayer, being much more compact than the LW one, forms pore-free films. It must be stressed that hydrophobic substrates are normally employed in the horizontal lifting method, because it is the hydrophobic part of the molecules that sticks onto the substrate. Surprisingly, the HW monolayers could be deposited on hydrophilic glass slides which probably means that hydrophilic parts protrude from the water surface allowing deposition on the substrate. This is not unlike the condensed monolayers of bipolar compounds in which a hydrophilic group is located at the monolayer-air interface thus forming Z-type multilayers [10,11].

Acknowledgements

The authors acknowledge the financial assistance of FAPESP and CNPq (Brazil). They also thank Prof. Michel Aegerter for the use of the Scanning Electron Microscope.

References

[1] M.Leclerc, J.Guay and L.H.Dao, Macromolecules, 22, 649 (1989).

[2] H.Zhou, R.Stern, C.Batich and R.S.Duran, Makromol. Chem. Rapid Commun. 11, 409 (1990).

[3] M.Ando, Y.Watanabe, T.Iyoda, K.Honda and T.Shimidzu, Thin Solid Films, 179, 225 (1989).

[4] L.H.C.Mattoso and L.O.S.Bulhões, to be published in the Synthetic Metals.

[5] O.N.Oliveira Jr., D.M.Taylor, T.J.Lewis, S.Salvagno and C.J.M.Stirling, J.Chem.Soc.Faraday Trans.,85, 1009 (1989).

[6] D.M.Taylor, O.N.Oliveira Jr. and H.Morgan, J.Coll. and Interface Sci., 13, 508 (1990).

[7] H.Morgan, D.M.Taylor and O.N.Oliveira Jr., Thin Solid Films, 178, 73 (1989).

[8] D.M.Taylor, O.N.Oliveira Jr. and H.Morgan, Chem.Phys.Lett., 161, 147 (1989).

[9] O.N.Oliveira Jr., D.M.Taylor and H.Morgan, Thin Solid Films, 210, 76 (1992).

[10] D.M.Taylor, O.N.Oliveira Jr., C.J.M.Stirling, S.Tripathi and B.Z.Guo, Thin Solid Films, 178, 27 (1989).

[11] O.N.Oliveira Jr., D.M.Taylor, C.J.M.Stirling, S.Tripathi and B.Z.Guo, to be published in Langmuir.

[12] A.G.MacDiarmid, J.C.Chiang, A.F.Richter and A.J.Epstein, Synth. Metals, 18, 285 (1987).

FIGURE CAPTIONS

Fig. 1 - General Formula of conductive polyaniline where y represents the oxidation state (From ref. [12])

Fig. 2 - Gel-Permeation Chromatogram of a THF solution of the base form of poly(o-metoxyaniline). (low molecular weight fraction)

Fig. 3 - Gel-Permeation Chromatogram of a NMP-LiCl 0.5% (w/w) solution of the base form of poly(o-metoxyaniline). (high weight fraction)

Fig. 4 - Pressure-area and surface potential-area isotherms for a Langmuir monolayer of the LW fraction of poly(o-metoxyaniline).

Fig. 5 - Pressure-area and surface potential-area isotherms for a Langmuir monolayer of the HW fraction of poly(o-metoxyaniline).

Fig. 6 - Scanning Electron micrograph of a 7-layer LB film of the low weight fraction (LW) of poly(o-metoxyaniline) deposited using the vertical dipping method.

Fig. 7 - Scanning Electron micrograph of an 8-layer film of the high weight fraction of poly(o-metoxyaniline) deposited through the horizontal lifting method.

CORONA TRIODE CURRENT-VOLTAGE CHARACTERISTICS: ON EFFECTS POSSIBLY CAUSED BY THE ELECTRONIC COMPONENT

Guilherme F Leal Ferreira, Dante L Chinaglia,

José A Giacometti and Osvaldo N Oliveira, Jr.

Instituto de Física e Química de São Carlos

C.P. 369, 13560 São Carlos, S.P. - Brasil

Short Title: "Corona triode characteristics: The electronic component"

PACS Numbers: 5280, 7755

ABSTRACT

The plate current for negative corona in a corona triode is observed to become positive and saturate at a value I_s when the grid is biased positively and the point-to-grid distance is less than 15 mm for corona currents of up to 60 μA. The saturation current, I_s, decreases exponentially with increasing point-to-grid distance and this strong dependence appears to indicate that the current is linked to those high energy (hot) electrons which survive attachment, and are capable of ionising molecules below and in their way to the grid. Simple calculations based on a theoretical model for hot electrons show that their energy is sufficient for causing such an ionisation. We show that I_s may be written approximately as the product of the corona current I_c, an exponential function expressing the mentioned decrease of the eletronic current with the point-to-grid distance and another function which is related to the ionisation efficiency. This efficiency depends strongly on the point-to-grid potential difference, on the grid transparency and, to a lesser extent, on the diameter of the grid wires. Even though I_s appears not to be related to the ionic component of the corona current, its current density distribution over the plate area is not far from a Warburg-like law which is characteristic of the ionic distribution in corona discharges. This inverted polarity current can also explain surface charge decay measurements presented in the literature for polymer samples treated in a corona triode when the grid was counter-biased with respect to the corona source.

1. Introduction

The corona triode method has been extensively applied to the poling process of highly insulating and ferroelectric polymers [1]. The triode consists basically of a corona point, a metallic grid and a metallic plate (sample holder), where the grid is used to control the charging process, being biased accordingly. The constant current versions of the triode [2], in particular, have proved useful in the study of the charge transport and storage phenomena in electrets [3,4], promptly indicating charge injection and providing a simple boundary condition for the study of the transport and polarization equations. In all arrangements, it is assumed that the charging current always has the polarity of the corona. However, it is shown here that an important exception exists for negative corona when the point-to-grid distance is small and the grid is biased positively.

Performing plate current-grid voltage measurements in the absence of a polymer sample, the possible causes for this inversion are discussed alongside with its dependence on a number of parameters of the corona triode. The motivation for this work came from the results presented by Dias *et al* [5] who studied the surface potential decay of negatively charged Teflon FEP samples. This decay could not be attributed to charge injection into the sample bulk, as it had been suggested for other polymers [6-9], but rather be accounted for if positive ions generated below the grid reached the sample. These ideas are discussed more fully in Section 4.

2. Experimental Details

The corona triode, shown schematically in Fig. 1, consists of a stainless steel corona tip, P, a nickel-chrome grid, G and an aluminum plate, PL, 6 cm in diameter. The tip is attached to a holder which makes it possible to adjust the point-to-grid distance, d, to an accuracy of 0.1 mm. The high voltage supply, V_c, is connected to the point generating a corona discharge in air, and the grid is biased positively by means of a high voltage supply, V_g. The grid-to-plate distance, L, could also be adjusted. Plate current versus grid voltage measurements were undertaken for negative corona, for point-to-grid distances between 3 and 15 mm. The optical transparency of the grid, T_r, and the grid wire diameter, ϕ, were also varied. T_r is defined as the ratio of the void to the total area of the grid. In most cases the grids were home made from wires parallely arranged but the results obtained with grids made with the same wires and with the same transparency but in a rectangular array were practically the same as those with the parallel wires. The radial distribution of the plate current density was measured by using metallic apertures (concentric with the point) of different diameters which were placed in contact, underneath the grid. The aperture prevented any current from reaching the plate, unless the carriers passed through the aperture. Then the plate current measured for different aperture diameters can yield the current distribution over the plate area. In all but one case, the tip radius, r_p, was 0.08mm.

All measurements were carried under room conditions of temperature (~ 23°C) and humidity (~ 60%).

3. Results

Fig. 2 shows the plate current vs. grid voltage curve for negative corona which was obtained under a constant corona current, I_c = - 10 μA, point-to-grid distance, d = 4 mm, grid transparency, T_r = 0.81, and grid wire diameter, ϕ = 0.05 mm. As one can see, when the grid voltage, V_g, is null, the plate current, I_p, is still non-zero due to the negative ions dragged towards the plate by the corona wind [10]. As V_g increases - remember that it has opposite polarity to the corona voltage, V_c - the negative current I_p decreases continuously, crossing the I_p = 0 line and changing its sign to positive. Above a certain value of V_g, I_p reaches a saturation value, hereafter named I_s, and remain constant. I_s is much smaller than the current for V_g = 0.

In order to investigate the behavior of this saturation current, the various parameters involved in a corona triode were varied. In particular, I_s measurements were obtained for varying corona currents, point-to-grid distances, values of the optical transparency of the grid, grid wire diameters, different grid patterns, and two different corona points. Fig. 3 to 7 give representative results where the conditions for each measurement are stated, and where only one parameter a time was varied. I_s is seen to increase with the corona current I_c (Fig. 3), and decrease sharply with the point-to-

grid distance, d, (Fig. 4) even though it was found to be independent of the grid-to-plate distance, L, (not shown here). In fact, I_s varies exponentially with d, as will be shown later. Fig. 5 shows how I_s depends on the optical transparency of the grid, T_r, while in Fig. 6 T_r was kept constant but the wire diameter was increased which caused I_s to decrease. In the results shown in Fig. 2 to 6 the tip radius was 0.08 mm; measurements were also carried out with a much thicker tip, r_p = 0.3 mm. Fig. 7 shows I_s as a function of I_c for the two tips; the voltage required for the same corona current being somewhat higher for the thicker tip and, as will be seen later, this explains the difference between the results with the tips.

The current distribution in the region of the grid was studied as described. The experimental results were found to stay not far from the Warburg distribution. Fig. 8 gives the integrated current as a function of the radius of the circle whose center is the vertical projection of the corona point, and also the integrated current corresponding to the Warburg distribution [11].

4. Discussion

We have shown that the plate current in a corona triode may have opposite polarity to the corona current. Understanding the results displayed in Fig. 2 is fundamental for an analysis of the mechanisms involved to be made. First of all, if ions were dragged only by the action of the

electric field, then at $V_g = 0$, the plate current, I_p, should be zero. However, ions are dragged towards the plate also by the corona wind and by the effect of the penetration of field lines below the grid [10], causing a non-zero current of the order of 10^{-10} A for a corona current of 10 μA, more than one order of magnitude larger than the current I_s under consideration here. As V_g is increased (with the polarity opposite to the corona voltage), these ions are prevented from reaching the plate until it attains a value V_r (as defined in [10]) for which $I_p = 0$. These effects were already known for both positive and negative polarity [10] and Fig. 2 only confirms them.

The new effect to be discussed here is the inversion of polarity in the plate current in Fig. 2, when V_g was increased beyond V_r. Since the current now is positive it must be concluded that there must exist counterions (positive ions) in the grid-to-plate gap. One possibility is that the grid itself is emitting a positive corona current. However, it can be easily verified that grid emission does not occur by turning off the point voltage and confirming that there is no plate current. Another possibility would be the ionisation of air molecules caused by collision with excited neutral molecules crossing the grid (for a discussion on excited molecules, see [12]), but this has also been discarded because air blown tangentially above the grid - which removes these excited molecules - has no effect on the saturation current.

It is believed that ionisation occurs due to the

electronic component known to contribute to the negative corona current [13-15]. For such an ionisation to occur it is necessary that the kinetic energy of these electrons be greater than the ionisation potentials of the N_2 and O_2 molecules, which are 15.6 and 12.2 eV, respectively [16]. Following the theory of hot electrons given in ref. [17], the maximum kinetic energy E_m in eV is

$$E_m \quad \frac{1}{2}\left(\frac{M}{m}\right)^{1/2}\lambda_c X \qquad (1)$$

where m and M are, respectively, the electronic mass and that of the air molecule, λ_c is the electronic mean free path and X the (constant) electric field. For λ_c we take 6.3×10^{-5} cm derived from the mean value of the cross section for O_2 and N_2 given in ref. [18]. Using also a mean value for M, we get

$$E_m\ (eV) = 7.3\times10^{-3}X\ (V/cm) \qquad (2)$$

For fields as low as 2×10^3 V/cm, Eq. (2) gives values of approximately 15 eV, confirming, therefore, that the saturation current may arise from the air ionisation caused by those hot electrons surviving attachment. Since this ionisation occurs in the vicinity of the grid, the saturation current is essentially due to cations there created and the whole process resembles that occurring in an ionisation chamber [19], but with the excitation kept close to the anode.

It is known that the electronic component in the negative corona discharge is proportional to the corona

current [14], and therefore one could expect that the saturation current, I_s, should be simply proportional to I_c for constant point-to-grid distances, d. However, this simple behaviour was not observed experimentally (see Fig. 3). This is quite understandable since the ionisation efficiency depends on the energy of the electrons, which is grossly determined by the potential difference between the point and the grid, ΔV ($/V_c/ + /V_g/$). The efficiency may also depend on ϕ and T_r and therefore these dependencies are assembled in a efficiency factor, $f(\phi, T_r, \Delta)$, from which

$$I_s = f(\phi, T_r, \Delta V)\, I_c \exp(-ad) \qquad (3)$$

where a is a constant with dimension of mm^{-1}. This exponential dependence is verified by plotting I_s vs. d in Fig. 9 and 10 for several corona currents at a fixed T_r and several T_r at a fixed I_c, respectively. The value of a, approximately 0.45 mm^{-1}, was not greatly affected by changing either I_c or T_r. This value of a may be related to the attachment coefficient, n. Data for attachment obtained in the multiplication regime in oxygen [20] leads to an n of approximately 0.7 mm^{-1} for fields of the order of 2-5 kV/cm at the atmospheric pressure which is of the same order of magnitude as the experimentally determined a.

With reference to previous work on the importance of the electronic component for the corona current, such a value for a would yield too strong a dependence on the distance, in disagreement with the results for the electronic component in

ref. [14]. In the data presented there the electronic component was surmised to account for ~ 20% of the total corona current when the point-to-plate distance was 30 mm, and would surely lead an electronic component that is larger than the corona current itself (which is obviously unreasonable) if an a = 0.45 mm^{-1} was used for a distance of 4 mm. Assuming the inferences regarding the electronic component previously made [14] to be correct, the inescapable conclusion is that the electrons that contribute to the electronic component of the corona current for the large distances used in ref. [14] are not hot electrons, for these would not be able to survive distances greater than n^{-1}.

Let us now analyse how the efficiency factor, $f(\phi, T_r, \Delta V)$, depends on the various parameters. The increase in I_s with increasing transparencies shown directly in Fig. 5 and also visible in Fig. 10 indicates that f also increases with T_r, which can be explained as follows. Higher transparencies mean that less hot electrons are directly collected by the grid, and therefore the number of ions generated in the grid-to-plate gap is larger. There is a limit value for the transparency though, as shown by the decrease in I_s when T_r reached 0.93 in Fig. 5. If it is too large (or conversely, if the point-to-grid distance is too short), the grid stops from behaving like a metallic plane. An electronic current may then exist in the grid-to-plate space since field lines from the point now reach the plate, thus decreasing the overall plate current. It should be noted that in Fig. 10 plots were done only for T_r smaller than

0.93.

On the other hand, $f(\phi,T_r,\Delta V)$ increases for decreasing values of ϕ as seen in Fig. 6 (taken from Fig. 10 for d = 4 mm). The reason for this is possibly the higher electric fields prevailing in the vicinity of thinner wires which causes the hot electrons to accelerate, increasing their ionising power.

The dependence of $f(\phi,T_r,\Delta V)$ on the potential difference between the point and the grid, ΔV, can be seen in Fig. 11 where I_s/I_c, a quantity that is proportional to $f(\phi,T_r,\Delta V)$ at a constant d, is plotted against ΔV. Fig. 11 was constructed from the same experimental points of Fig. 7 and shows that the dependence thus found on the tip radius is indeed a dependence on the potential difference ΔV. It is worth mentioning that the higher voltage required for the ticker tip for the same corona current represents a weak effect and was not detected by Lama and Gallo in their comprehensive study of the negative corona current in the point-to-plane geometry [21].

The closeness of the charge distribution of the positive current (I_s) with that of the Warburg distribution shown in Fig. 8 appears surprising since one could expect the hot electron current to be more concentrated around the center and therefore to increase more steeply. It is possible that the electrons, being much lighter than the molecules, are strongly scattered on their way to the grid.

We shall now turn to the effects of corona treating on the charge decay of polymers. The charge decay in LDPE, HDPE,

PP and PTFE was studied by Perlman and co-workers [8,9] by placing negatively charged samples in a corona triode (with a negative corona voltage) and a grounded grid which removed all ions, but allowed neutral molecules to pass through. A charge decay was observed and attributed to charge injection caused by the excited neutral molecules (see, however, a discussion in [22]), the decay being much faster in the central region of the sample than in its borders. When a stream of air was blown tangentially to the face of the sample the effect practically disappeared. Similar results were obtained for polyethylene by Baum *et al* [6,7], who suggested that excited neutral molecules would be capable of causing ejection of charge carriers from surface states which would be injected into the sample bulk.

Dias *et al* [5] also observed charge decay for negatively charged Teflon FEP when samples were corona treated (without allowing ions to reach the sample). However, by using the heat pulse technique they were able to show that the centroid of the trapped charges always lies on the sample surface, thus discarding the hypothesis of charge injection, since trapping is likely to occur. They then concluded that a possible alternative was charge compensation due to the arrival at the sample surface of positive ions. The results presented here appear to corroborate such a conclusion, for positive plate currents were measured when the corona point was negative. Also, the current distribution obeys a Warburg-like behavior so that it is higher in the center of the grid. This would cause the charge compensation in a

polymer surface to be faster in the center of the sample, as indeed has been observed experimentally [5-9]. It is worth noting that the point-to-grid distance in the experiments reported in [5,8,9] was always around 10 mm for which our results have shown that an inversion in the current exists.

An approximate estimate of the effect of the saturation current on the potential decay can be made as follows. Taking a saturation current of 5.3×10^{-11} A, corresponding to a corona current of 50 μA and point-to-grid distance of 6 mm, in 20 min. a positive charge would be deposited on the negatively charged sample surface which would lead to a 212 V decay for a 12 μm thick sample. This value agrees well with the 250 V actually measured under approximately the same conditions (from Fig. 8 in [5]). Following the same procedure, one obtains a decay of 350 V for the actually measured 450 V in Fig. 7 in ref. [5]. It is concluded, therefore, that the effect of the saturation current is indeed significant and may be responsible, partially at least, for the surface charge decay reported in the experiments mentioned above.

5. Conclusions

We have shown that the plate current in a corona triode can be made positive for negative corona, provided that the point-to-grid distance is smaller than 15 mm (for corona currents of up to 60 μA) and the grid is biased positively. The positive carriers that reach the plate are assumed to be ions which were originated from the gas ionisation caused by

hot electrons that pass through the grid. Simple calculations based on a theoretical model for hot electrons showed that their energy is sufficient to bring about such an ionisation. The dependence of the saturation current with the point-to-grid distance gave results which were consistent with data obtained in electron attachment. The inverted polarity current can also explain surface charge decay measurements presented in the literature for polymer samples which were corona treated.

Acknowledgments

We wish to thank Prof. M.D.Souza Santos for having drawn our attention to the importance of the electronic component in negative corona discharges. The authors acknowledge the financial assistance of FAPESP and CNPq (Brazil).

References

[1] N.Alves, J.A.Giacometti and O.N.Oliveira Jr., Rev. Sci. Instrum. 62 (1991) 1840

[2] J.A.Giacometti and J.S.C.Campos, Rev. Sci. Instrum. 61 (1990) 1143

[3] O.N.Oliveira Jr. and G.F.Leal Ferreira, Appl. Phys. A 42 (1987) 213

[4] J.A.Giacometti, G.F.Leal Ferreira and B.Gross, Phys. Stat. Sol. (a), 88 (1985) 297

[5] C.J.Dias, J.N.Marat-Mendes and J.A.Giacometti, J. Phys. D: Appl. Phys. 22 (1989) 663

[6] E.A.Baum, T.J.Lewis and R.Toomer, J. Phys. D: Appl. Phys. 10 (1977) 487

[7] E.A.Baum, T.J.Lewis and R.Toomer, J. Phys. D: Appl. Phys. 10 (1977) 2525

[8] K.J.Bao, S.S.Bamji and M.M.Perlman, J. Appl. Phys. 50 (1979) 8181

[9] S.Haridoss, M.M.Perlman and C.Carlone, J. Appl. Phys. 53 (1982) 6106

[10] O.N.Oliveira Jr. and G.F.Leal Ferreira, Rev. Sci. Instrum. 56 (1985) 1957.

[11] J.A.Giacometti, J. Phys. D: Appl. Phys. 20 (1987) 675

[12] R.S.Sigmond and M.Goldman, In "Electrical Breakdown and Discharges in Gases", ed. by E.E. Kunhardt and L.H.Luessen, Vol. 89b, Nato ASI series, Plenum Press (1983), pp. 1-64

[13] R.S.Sigmond, J. Appl. Phys. 52 (1982) 891.

[14] G.F.Leal Ferreira, O.N.Oliveira Jr. and J.A.Giacometti, J. Appl. Phys. 59 (1986) 3045.

[15] M.F.Fréchette and S.I.Kamel, Conference Record of the 1988 IEEE International Symposium on Electrical Insulation, Boston, MA, June 5-8, (1988), p. 73.

[16] G.Herzberg, "Molecular Spectra and Molecular Structure", D. van Nostrand Co., Inc., Princeton (1963), Vol. I, p. 459.

[17] A. Von Engel, "Ionized Gases", Clarendon Press, Oxford, 2nd. edition, (1965), p.122,123.

[18] H.S.W.Massey, E.H.S.Bishop, "Electronic and Impact Phenomena", Clarendon Press, Oxford (1969), Vol. I, p. 28.

[19] B.D.Cullity, "Elements of X-Ray Diffraction", Addison-Wesley Publishing Co., Inc., (1978), p. 204.

[20] M.A.Harrison and R.Geballe, In: Electrical Breakdown in Gases, edited by J.A.Rees, John Wiley, N.York (1973), p. 116

[21] W.L.Lama and C.F.Gallo, J. Appl. Phys. 45 (1974) 103.

[22] G.M.Sessler and H.von Seggern, 1979 Annual Report, Conf. Electr. Insul. Diel. Phenom. (1979), p. 160.

FIGURE CAPTIONS

Fig. 1 - Experimental Setup. I_c and I_p are ammeters; V_g and V_c are power supplies; PL is the measuring plate, G the metallic grid; P the corona tip; d the distance between the tip and the grid and L the distance between the grid and the plate.

Fig. 2 - Saturation Current, I_s, versus grid voltage, V_g. Experimental Conditions: I_c = - 10 μA, d = 4 mm, L = 4 mm, T_r = 0.81 and ϕ = 0.050 mm.

Fig. 3 - Saturation current, I_s, versus corona current, I_c. Experimental Conditions: V_g = + 400 V, d = 4 mm, L = 4 mm, T_r = 0.87, ϕ = 0.075 mm.

Fig. 4 - Saturation current, I_s, versus point to grid distance, d. Experimental Conditions: I_c = - 30 μA, V_g = + 400 V, L = 4 mm, T_r = 0.87, ϕ = 0.075

Fig. 5 - Saturation current, I_s, versus the optical grid transparence, T_r. Experimental Conditions: I_c = - 30 μA, d = 4 mm, L = 4 mm, ϕ = 0.075 mm.

Fig. 6 - Saturation current, I_s, versus the grid wire diameter, ϕ. Experimental Conditions: I_c = - 30μA, d = 4 mm, L = 4mm, T_r = 0.81. Data taken from Fig. 10.

Fig. 7 - Saturation current, I_s, versus corona current, I_c, for two different point radius, r_p = 0.30 and 0.08 mm.

Fig. 8 - Plate current distribution over the plate area, curve I. Also shown is the curve II that is expected for a Warburg-like distribution.

Fig. 9 - Saturation current, I_s, versus point to grid distance, d, for several different corona currents I_c. T_f = 0.87 and ϕ = 0.075 mm.

Fig. 10 - Saturation current, I_s, versus point to grid distance, d, for several different grid transparencies, T_f, and grid wire diameters, ϕ, at a fixed I_c = - 30 μA. Note that for the same T_f there are 3 values for ϕ, without any major change in behaviour.

Fig. 11 - I_s/I_c versus the potential difference between the point and the grid, $\Delta V = V_c + V_g$, for two different point radii, r_p = 0.30 and 0.08 mm, taken from the same results of Fig. 7. Note that a single dependence for the two tip radii is observed.

LIST OF SYMBOLS

I_c = corona current

I_p = plate current

I_s = saturation current

V_c = corona voltage

V_g = grid voltage

ΔV = potential difference between the point and the grid ($V_c + V_g$)

V_r = counter grid potential at which $I_p = 0$

d = point-to-grid distance

L = grid-to-plate distance

ϕ = grid wire diameter

r_p = point radius

T_r = optical transparency of the grid

$f(r_p, \phi, T_r, V_c)$ = ionisation efficiency

a = constant with dimension of mm^{-1}

P = corona point

PL = metallic plate

G = grid

Fig. 1

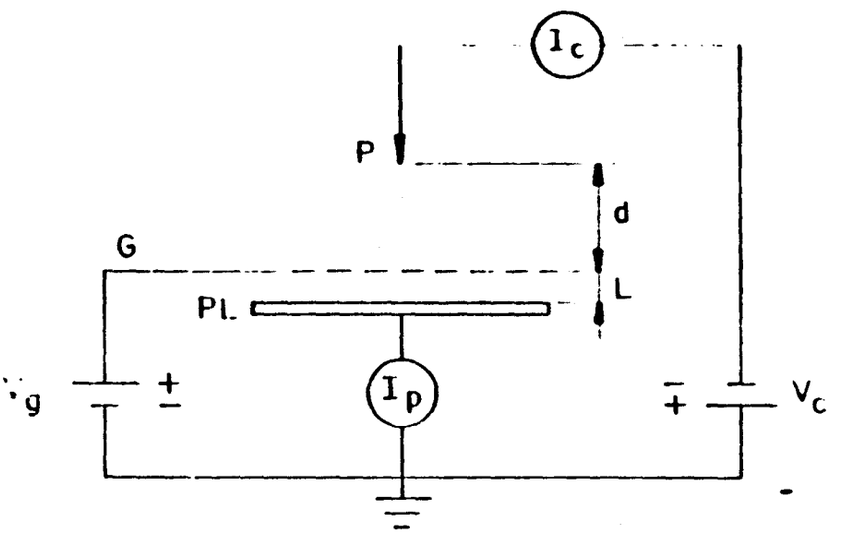
I_c
P
d
G
L
Pl.
I_p
V_g
V_c

Fig. 2

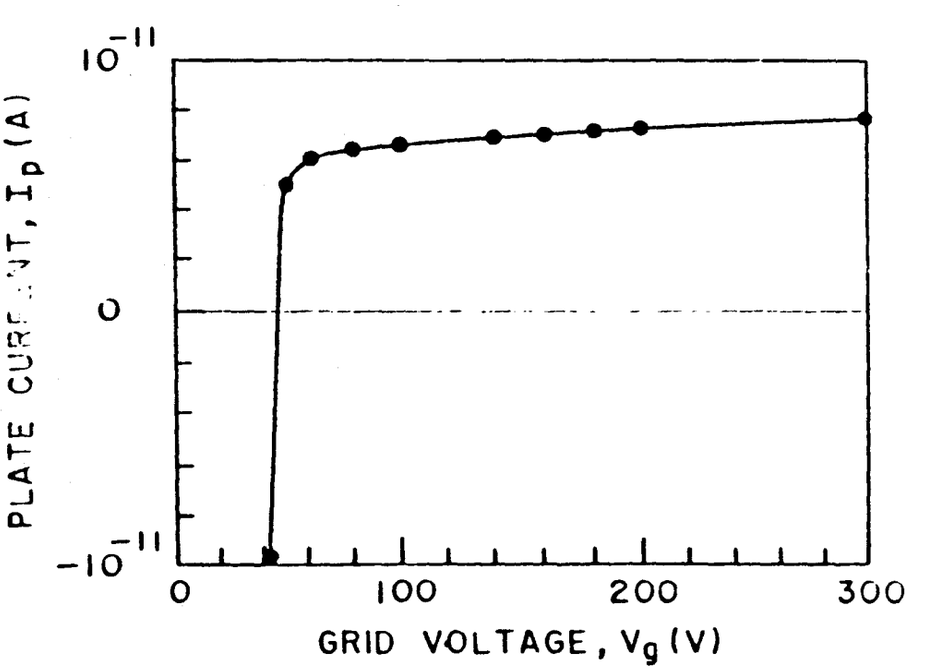
10^{-11}
0
-10^{-11}
PLATE CURRENT, I_p (A)
0
100
200
300
GRID VOLTAGE, V_g (V)

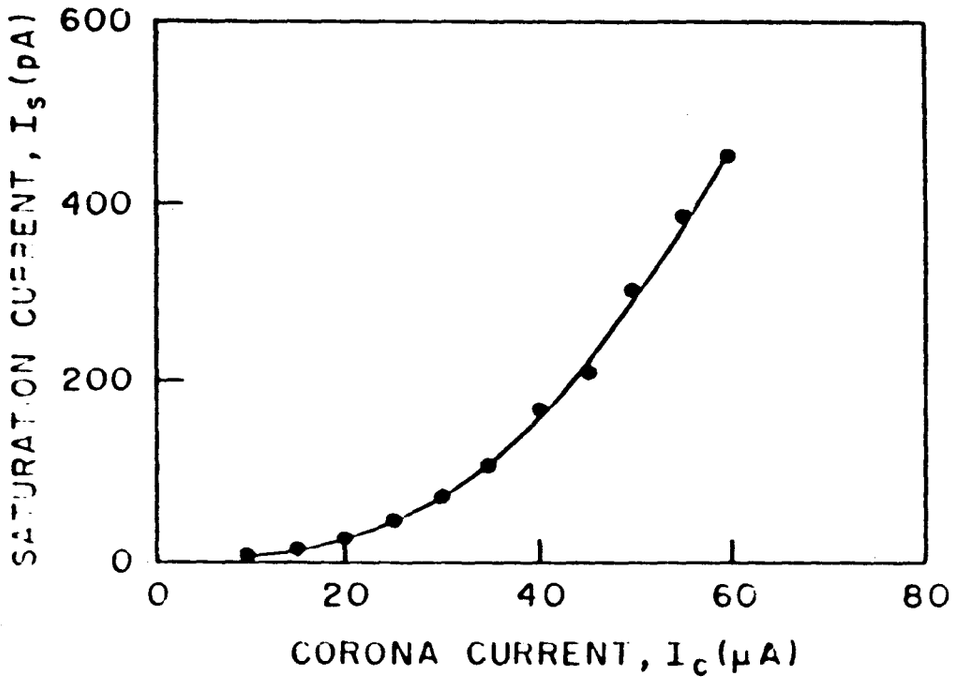
SATURATION CURRENT, I_s (pA)
600
400
200
0
0
20
40
60
80
CORONA CURRENT, I_c (μA)

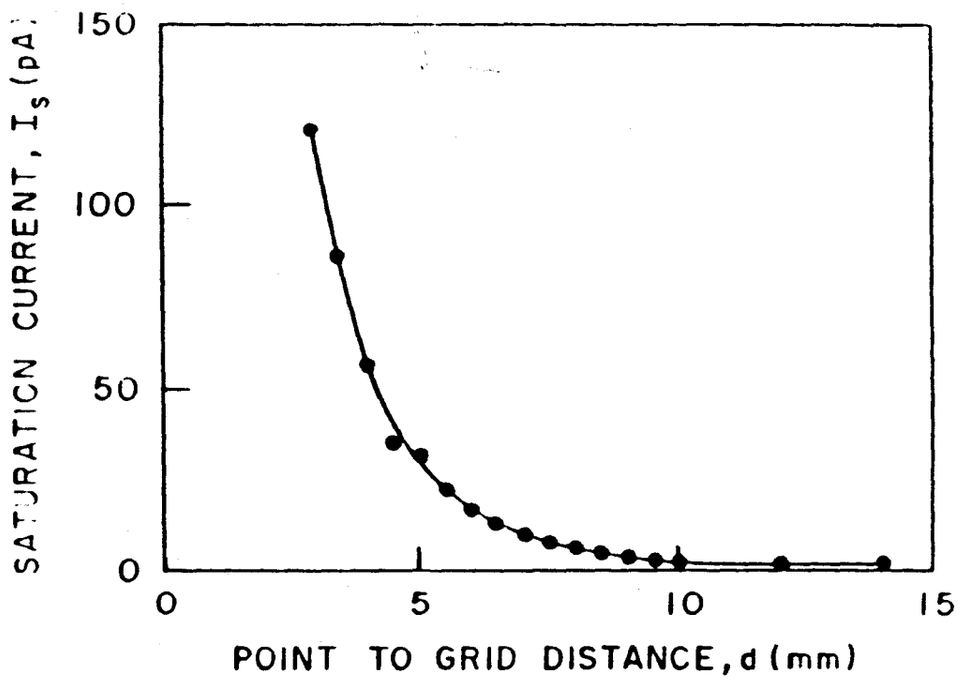
SATURATION CURRENT, I_s (pA)
150
100
50
0
0
5
10
15
POINT TO GRID DISTANCE, d (mm)

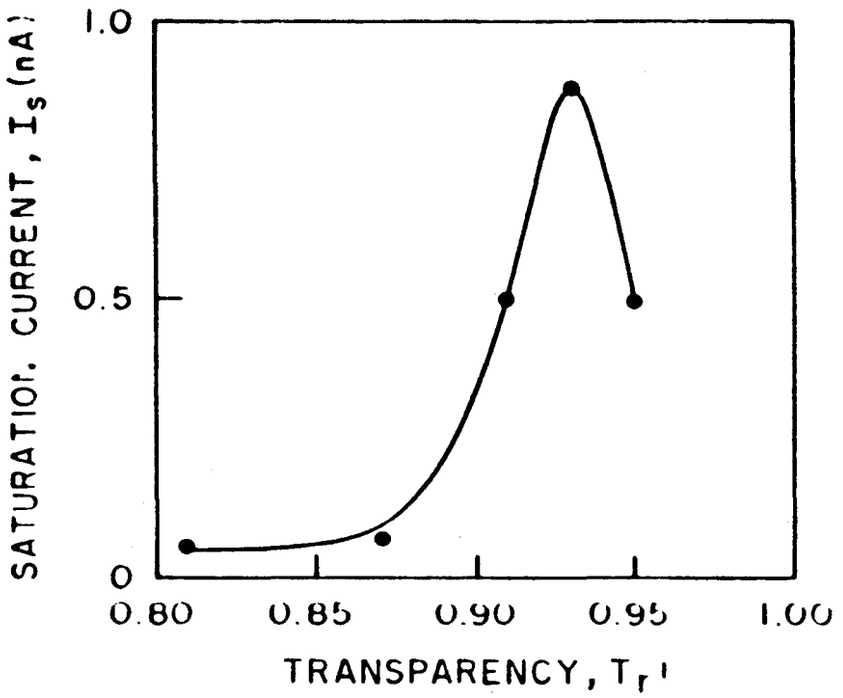
SATURATION CURRENT, I_s (nA)
1.0
0.5
0
0.80
0.85
0.90
0.95
1.00
TRANSPARENCY, T_r

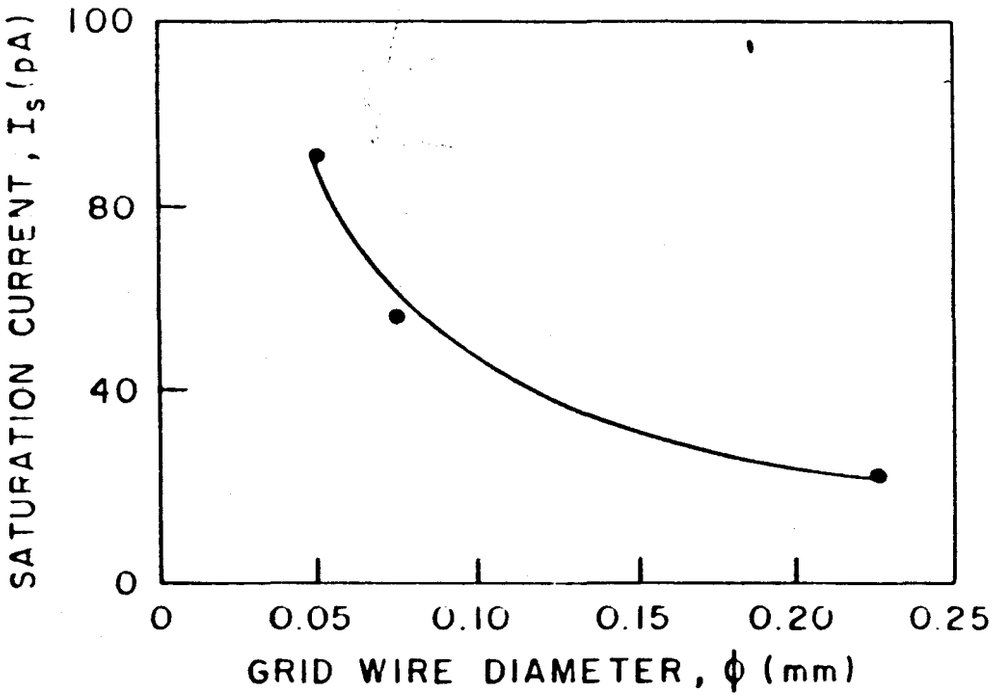
SATURATION CURRENT, I_s (pA)
100
80
40
0
0
0.05
0.10
0.15
0.20
0.25
GRID WIRE DIAMETER, ϕ (mm)

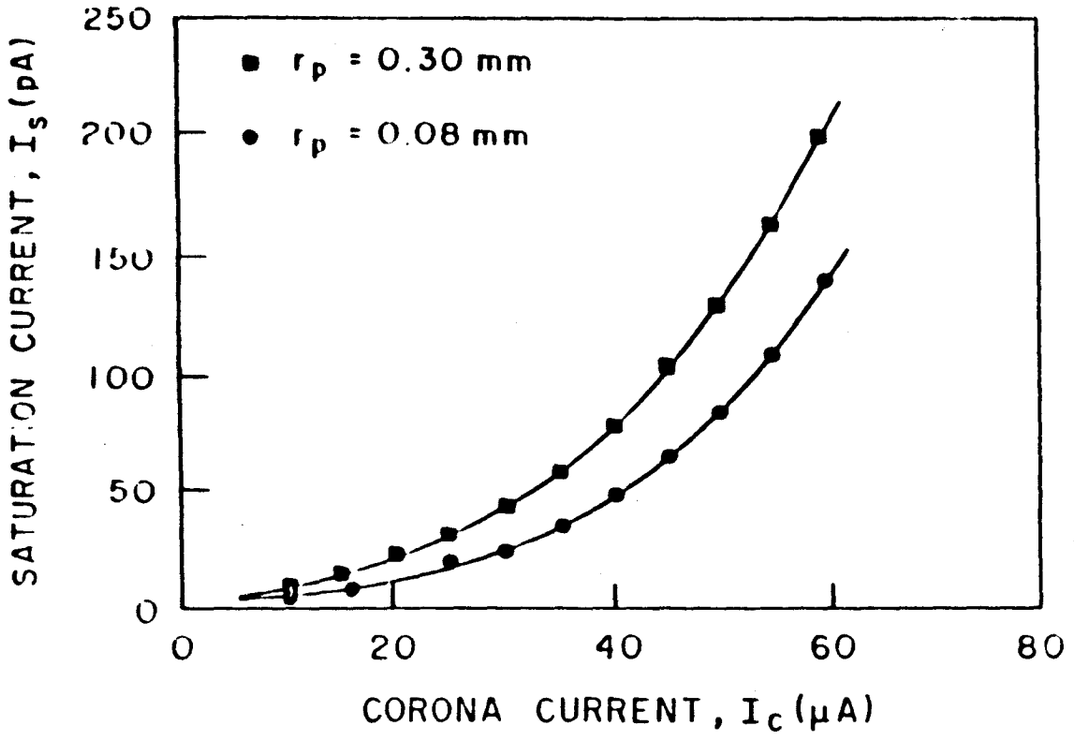
250
200
150
100
50
0
r_p = 0.30 mm
r_p = 0.08 mm
SATURATION CURRENT, I_s (pA)
0
20
40
60
80
CORONA CURRENT, I_c (μA)

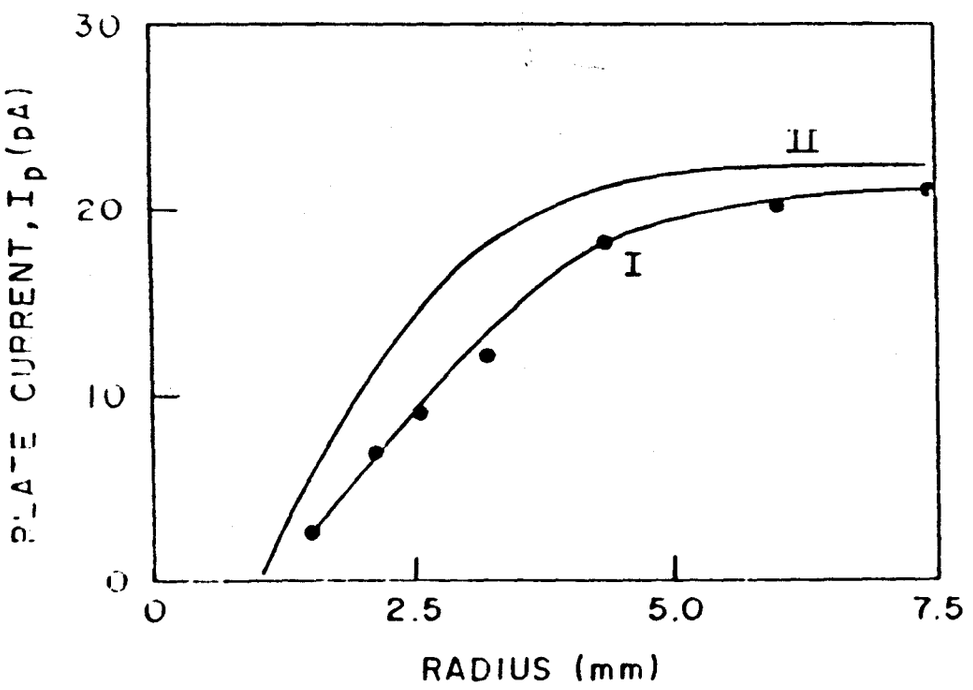
30
20
10
0
II
I
PLATE CURRENT, I_p (pA)
0
2.5
5.0
7.5
RADIUS (mm)

Fig. 3

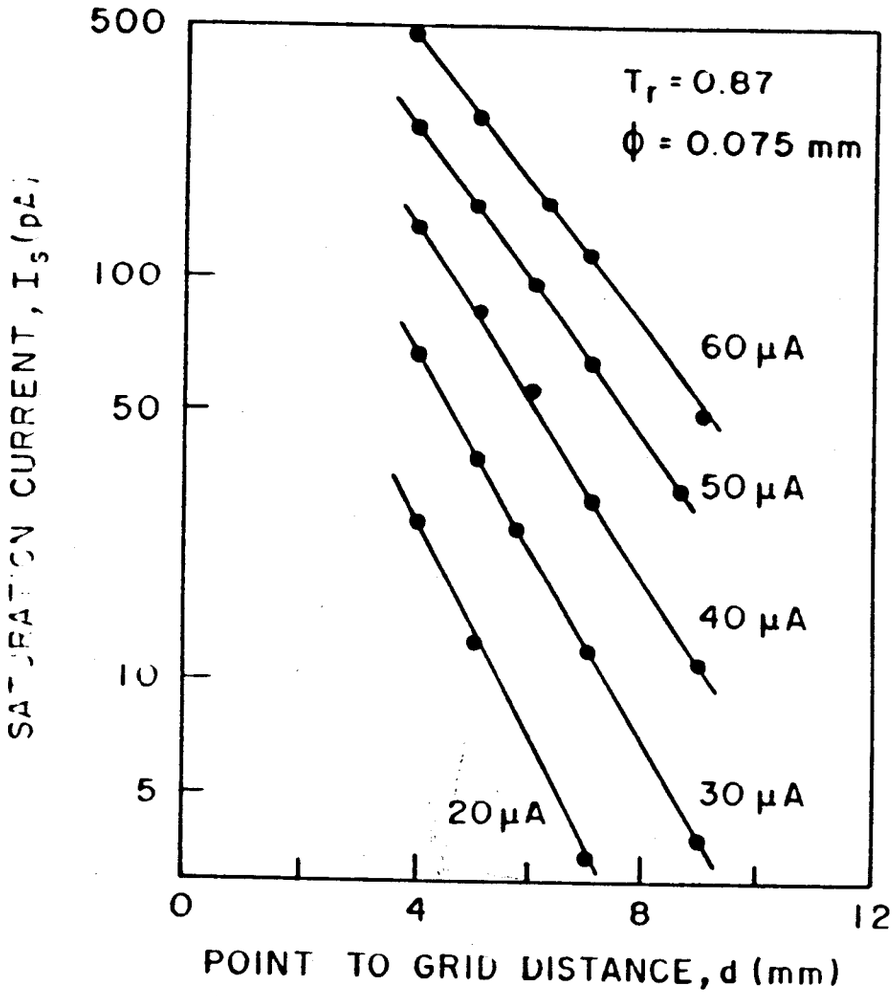
500
100
50
10
5
0
4
8
12
$T_r = 0.87$
$\phi = 0.075$ mm
60 μA
50 μA
40 μA
30 μA
20 μA
POINT TO GRID DISTANCE, d (mm)

Fig. 11

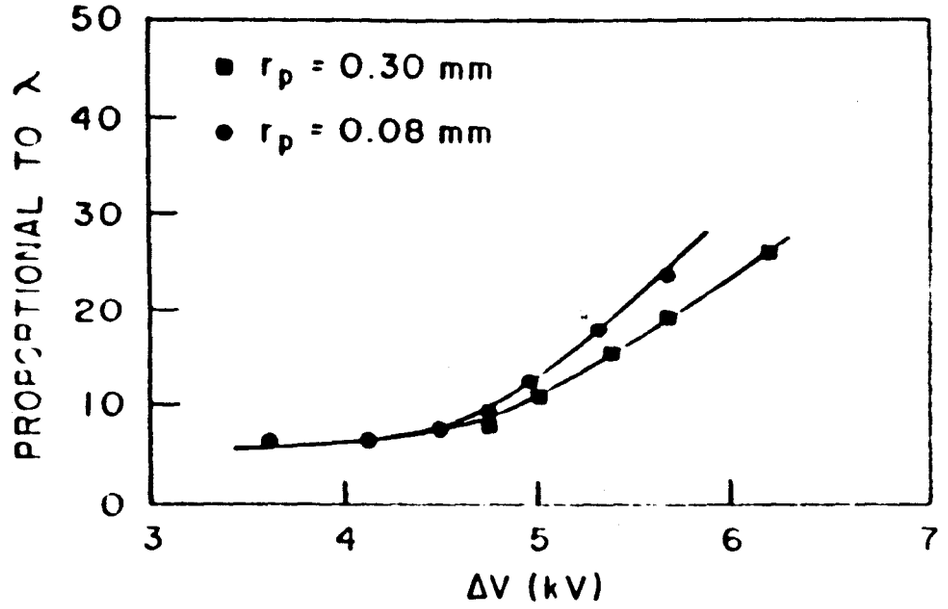
PROPORTIONAL TO λ
r_p = 0.30 mm
r_p = 0.08 mm
ΔV (kV)

Fig. 10

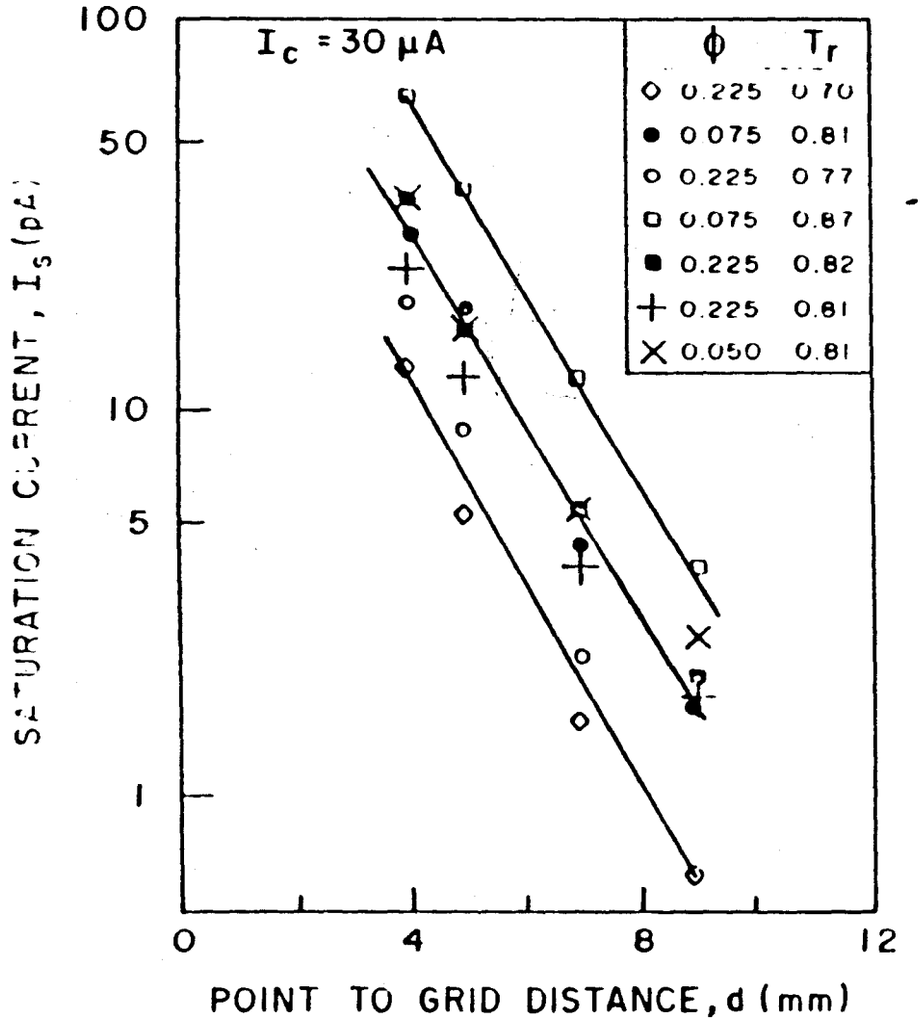
I_c = 30 μA
ϕ T_r
0.225 0.70
0.075 0.81
0.225 0.77
0.075 0.87
0.225 0.82
0.225 0.81
0.050 0.81
SATURATION CURRENT, I_s (pA)
POINT TO GRID DISTANCE, d (mm)

LANGMUIR-BLODGETT FILMS OF POLY(o-ANISIDINE)

D.GONÇALVES, R.M.FARIA, O.N.OLIVEIRA JR. and J.SWORAKOWSKI[1]
Instituto de Fisica e Quimica de São Carlos,
Universidade de São Paulo
13560 São Carlos, S.P. - Brazil

ABSTRACT

LB films have been fabricated by transferring poly(o-anisidine) (POA) monolayers from a pure water surface onto glass substrates using the conventional dipping method. The chemically synthesized poly(o-anisidine) consists of two fractions, one containing mainly octamers and another of high molecular weight (around 28000 g/mol). The low weight fraction forms condensed Langmuir monolayers which are anchored to the water surface through one single group, probably the metoxy-aniline, yielding an area per molecule of ca. 20 $Å^2$. The molecular configuration in the high-weight fraction monolayers appears to be such that one in each four or five segments of the polymer chain makes contact with the water. UV-visible spectra were obtained for the HW fraction LB films which were identical to those of POA in solution, changing from dark blue to green when the film is exposed to HCl vapour. Preliminary conductivity measurements were carried out on these LB films showing that the conductivity increases by three orders of magnitude upon exposure to HCl vapour.

KEYWORDS: Langmuir-Blodgett films, poly(o-anisidine)

INTRODUCTION

Polyaniline derivatives are among the most investigated conjugated polymers for LB film fabrication owing to their interesting electroactive and electrochromic properties (see e.g. [1,2]), and especially because substituted anilines are amenable to generate polymers that are soluble in common organic solvents. These derivatives are usually alkyl-anilines which require the incorporation of long aliphatic chains into the aniline monomer [3,4]. In our work LB films are being deposited from poly(o-anisidine) (poly(o-metoxyaniline),

---

[1]Permanent address: Institute of Organic and Physical Chemistry, Technical University of Wroclaw, 50-370 Wroclaw, Poland

hereafter abbreviated POA) which does not possess a long alkyl tail. So far we have been mainly concerned with establishing the conditions for obtaining high quality LB films. Some preliminary results have already been reported in [5], which are further extended here.

EXPERIMENTAL DETAILS

POA was synthesized by the oxidation of o-anisidine with $(NH_4)_2S_2O_8$, following the procedure described in detail in [6,7]. The solid, dark-blue product was dried during 48 hours in vacuum, washed with abundance of 0.1 M aqueous solution of ammonia, dried again and washed with tetrahydrofurane (THF) until the filtrate became colourless. As was described earlier [5], the product obtained in such a way consists of a high molecular weight (HW) fraction of mean molecular weight equal to ca. 28000 g/mol. The THF solution was found to contain mainly octamers, its mean molecular weight amounting to ca. 550 g/mol. Hereafter, it will be referred to as the low molecular weight (LW) fraction. Both fractions were also found soluble in dichloromethane, chloroform and N-methyl-pyrrolidinone. It should be noted that the molecular weights determined by the GPC method are averaged and, to some extent, uncertain. The average areas per molecule obtained from the π-A curves can, therefore, be taken only as approximate values.

The studies on Langmuir monolayers and deposition of Langmuir-Blodgett (LB) films were carried out employing a KSV5000 trough housed in a class 10000 clean room. The ultra-pure water used in the experiments reported in this paper was obtained from a Millipore system described in more detail in [5]. It has been recognized that trace impurities in the subphase can cause large variations in monolayer isotherms [8]. In our case, independent measurements of pressure-area (π-A) and surface potential (ΔV-A) isotherms of fatty acid monolayers yielded results in good agreement with those published in the literature [8] thus demonstrating a very good water quality.

The monolayers of both LW and HW fractions were obtained by spreading solutions in appropriate solvents (dichloromethane or chloroform) over the water surface and allowing for the evaporation of the solvent. The LB films of POA were deposited onto glass substrates cleaned using a procedure described in [5] and where the conventional vertical deposition method was employed, the dipping speed being 3 mm/min. During deposition, the surface pressure was kept at 10 mN/m for the LW fraction. The same pressure was maintained during most experiments with the HW polymer; however in some experiments higher pressures (up to 20 mN/m) were used.

The electrical measurements were carried out using a simple two-electrode surface configuration, with evaporated Au strips as electrodes. The currents were measured with a Keithley 610C electrometer.

RESULTS AND DISCUSSION

Pressure-area isotherms are shown in Fig. 1 for Langmuir monolayers obtained from dichloromethane solutions of both LW and HW fractions. These curves are essentially the same as those reported in [5] for chloroform solutions. The reason why we decided to use dichloromethane is that chloroform solutions were found to be unstable when stored for a certain period of time. Though freshly made solutions in both solvents exhibit identical properties, we have observed

changes of colour of the chloroform solutions (even stored in the refrigerator) occurring within a few days. No such effect was observed in dichloromethane solutions.

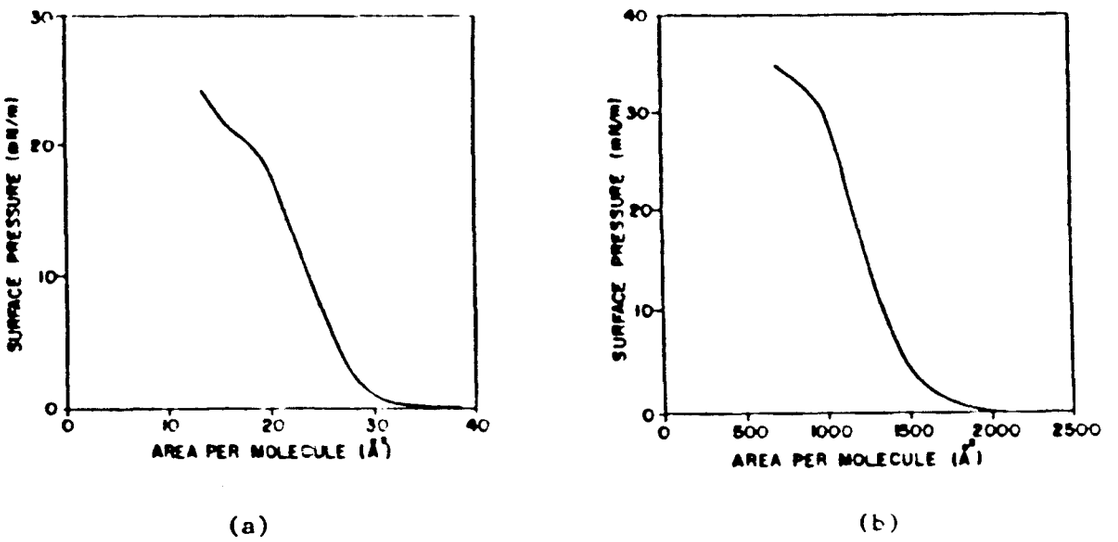

(a) (b)

Fig. 1. Pressure-area (π-A) isotherms for (a) LW Langmuir monolayer, (b) HW Langmuir monolayer.

The (π-A) isotherms shown in Fig. 1 were measured at the compression speed of 3mm/min, much lower than that used previously [5]. In our previous communication [5] we reported that the isotherms were undistinguishable for the compression speeds lower than 25 mm/min. This is indeed true sufficiently far from the collapse region. We found, however, that close to the collapse pressure the stability of the monolayers critically depends on the compression kinetics. Moreover, the films compressed at a low compression speed to the pressure just below the collapse were found to exhibit a tendence of remaining organized after the external pressure had been removed.

The mean molecular area of the LW fraction determined from the π-A isotherm was found to amount to ca. 20 Å^2, reasonably coincinding with the cross section of a polyaniline molecule determined from X-ray measurements (22-28 Å^2 [9]). Thus our results seem to indicate that the oligomers are organized in such a way that only a terminal group (probably the metoxyaniline one) is anchored to the water surface. The data obtained for the HW demonstrate that the mean area is of the order of 1000 Å^2 for the polymer chain. Speculating that the contact area is again ca. 20 Å^2, this means that, on average, one in each four or five segments of the polymer chain makes contact with the subphase surface, the chain assuming a worm-like conformation of approximately 10-15 Å thickness.

The well-known difficulty in depositing LB films from conjugated polymers using the traditional vertical method has been attributed to the excessive

rigidity of the monolayer which prevented it from being transfered onto a solid substrate. In our earlier experiments, for instance, we did not succeed in depositing LB films from the HW fraction using the vertical dipping; the transfer ratio was always 0.3 or even lower (see [5]). Having reduced the barrier compression and dipping speeds to ca. 3 mm/min, we were able to transfer some monolayers with a transfer ratio close to 1. These LB films were obtained by starting the first deposition with the substrate already immersed into the subphase. However, in these cases the transfer ratios during downstrokes were negative or at the best equal to zero. It should not be left unmentioned that in some experiments, performed under apparently similar conditions, the transfer ratios of the upstrokes were significantly less than one (0.5-0.7), while the transfer ratios of the downstrokes were no longer zero, increasing to ca. 0.3-0.5. It seems that when deposition was successful, Z-type films were obtained in which deposition occurred only in the upstrokes, probably because the substrate remained hydrophilic throughout the whole process (hydrophilic groups would protrude from the water surface).

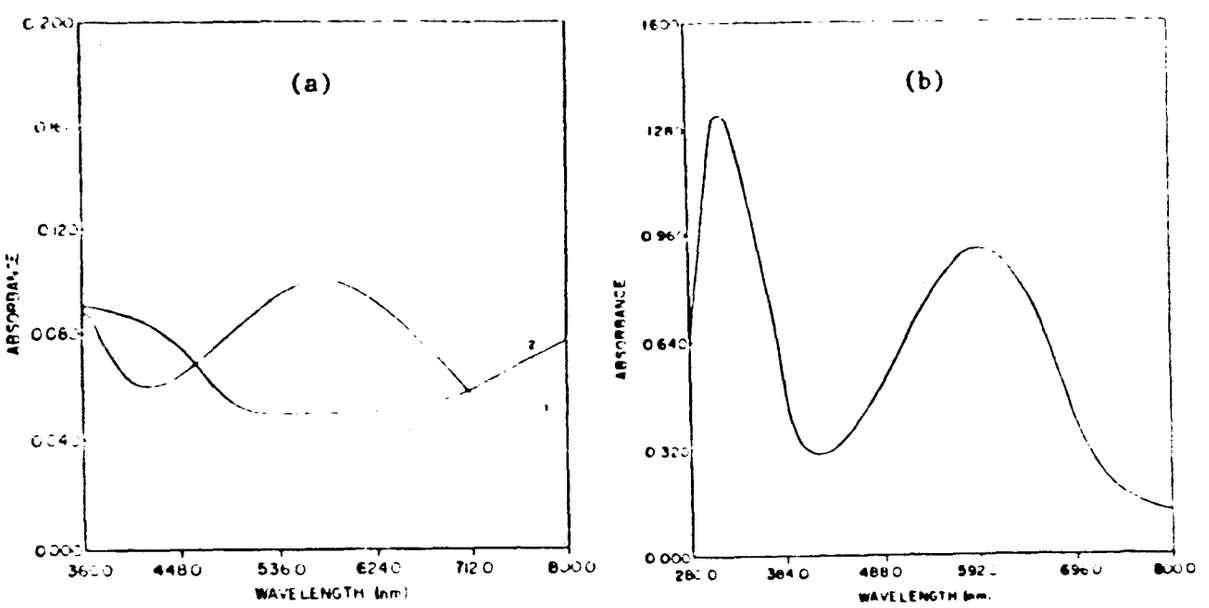

Fig. 2. Absorption spectra of (a) poly(o-anisidine) in a dichloromethane solution, (b) 16-layer LB film of the HW fraction. Curve 1 corresponds to the film as deposited, and Curve 2 corresponds to the film exposed to HCl vapour.

The UV-visible spectrum for a 16-layer LB film of the HW fraction, deposited using the vertical dipping method, is shown in Fig. 2a. Upon doping the film with HCl vapour for ca. 10 min at room temperature, the spectrum changes considerably; the absorption clearly shifts from blue to green. This occurs owing to oxidation, a process that has been shown to be reversible [10]. The spectrum for the as-deposited film is identical to the spectrum of poly(o-anisidine) in solution (see Fig. 2b). We also carried out preliminary measurements of the electric conductivity of the POA layers and their changes during exposition to HCl and NH_3 vapours. The specific conductivity of as-deposited layers (calculated using the

monolayer thickness estimated from the folded structure of POA chains put forward above) was found to amount to ca. 10^{-7} $\Omega^{-1}cm^{-1}$, in a reasonable agreement with data obtained for the emeraldine form of polyaniline [11]. Exposure to gaseous HCl resulted in an increase of the conductivity by three orders of magnitude. This effect could be partially reversed by a subsequent exposure to NH_3 vapour; the following decrease of conductivity was, however, much smaller (ca. 1 order of magnitude), and the reversibility of the process could be attained only after several repetitive exposures to HCl and NH_3.

FINAL REMARKS

We have obtained Langmuir-Blodgett films of poly(o-anisidine). A folded-chain structure of the films was propoeed. Both UV-visible spectra and electric conductivity of POA films reasonably agree with the results obtained for polyaniline.

ACKNOWLEDGEMENTS

The authors acknowledge the financial support from FAPESP and CNPq (Brazil). The stay of one of the authors (JS) in Brazil was supported by the RHAE-CNPq programme.

REFERENCES

1 S.Cattarin, L.Doubova, G.Mengoli and G.Zotti, Electrochimica Acta, 33 (1988) 1077.

2 A.G.MacDiarmid and A.J.Epstein, Faraday Discuss. Chem. Soc., 88 (1989) 317.

3 M.Ando, Y.Watanabe, T.Iyoda, K.Honda and T.Shimidzu, Thin Solid Films, 179 (1989) 225.

4 H.Zhou, R.Stern, C.Batich and R.S.Duran, Makromol. Chem. Rapid Commun., 11 (1990) 409.

5 R.M.Faria, L.H.C.Mattoso, M.Ferreira, D.Gonçalves, L.O.S.Bulhões and O.N.Oliveira Jr., Thin Solid Films, to be published.

6 M.Leclerc, J.Guay and L.H.Dao, Macromolecules, 22 (1989) 649.

7 L.H.C.Mattoso and L.O.S.Bulhões, Synthetic Metals, to be published.

8 D.M.Taylor, O.N.Oliveira Jr. and H.Morgan, Thin Solid Films, 173 (1989) L141.

9 J.P.Pouget, M.E.Jozefowicz, A.J.Epstein, X.Tang, and A.G.MacDiarmid, Macromolecules, 24 (1991) 779.

10 P.M.McManus, S.C.Yang and R.J.Cushman, J.Chem.Soc.,Chem.Commun., 760 (1985) 1556.

11 M.Angelopoulos, G.E.Asturias, S.P.Ermer, A.Ray, E.M.Scherr, A.G.MacDiarmid, M.Akhtar, Z.Kiss and A.J.Epstein, Mol.Cryst.Liq.Cryst., 160 (1988) 151.

THERMAL STUDIES ON VDF/TrFE COPOLYMERS

R.M. Faria, J.M. Guimarães Neto[1] and O.N. Oliveira Jr.

Instituto de Física e Química de São Carlos, USP

CP 369, 13560 São Carlos, Brazil

FAX: 55 (162) 713616

e-mail: faria@ifqsc.ansp.br

Abstract

Poly(vinylidene fluoride/trifluoroethylene) copolymers of different molar ratios in the range between 60:40 and 80:20 have been studied by thermally stimulated processes, viz. thermally stimulated depolarization current (TSDC), thermally stimulated current (TSC), differential scanning calorimetry (DSC), and by dielectric constant measurements. The results obtained show unequivocally that a ferroelectric-to-ferroelectric phase transition exists for 70:30 and 75:25 copolymers, in addition to the well-known ferroelectric-to-paraelectric transition which was already observed in all copolymers.

1. Introduction

The copolymers poly(vinylidene fluoride/trifluoroethylene) P(VDF/TrFE) are today the best examples of ferroelectric polymeric materials. In addition to exhibiting ferroelectric hysteresis

---

[1]Present Address: Departamento de Física, Universidade Federal do Piauí, Teresina, PI - Brazil

phenomena [1] and the switching effect [2], in the same way as the β-polyvinylidene fluoride homopolymer, they usually also display a ferro-to-paraelectric phase transition [3,4]. Based on X-ray diffraction data, Tashiro and Kobayashi [5] and Tanaka et al [6] have suggested that two ferroelectric phases coexist below the Curie temperature, and therefore in this case two phase transitions must be observed when the copolymer is heated. In this work we show unequivocally the existence of two phase transitions indicated by the appearance of two peaks in thermally stimulated depolarization conductivity (TSDC), thermally stimulated current (TSC), differential scanning calorymetry (DSC), and dielectric constant measurements for the copolymers 70:30 and 75:25, while only one phase transition appears for the copolymers 60:40 and 80:20.

2. Experimental

P(VDF-TrFE) samples were produced by pressing pellets of copolymers of 4 different VDF molar ratios at 200°C and quenching them to room temperature. The pellets of the copolymers 60:40, 70:30, 75:25 and 80:20 (i.e. 60, 70, 75 and 80% of VDF) were purchased from Atochem (France) and used as received. The samples were approximately 50 μm thick and 5 cm in diameter and were cleaned with methyl alcohol. For electrical measurements rectangular electrodes (1.0 x 2.0 cm^2) made from evaporated aluminium (50 to 100 nm thick) were located in the center of the sample. Before the TSDC and some DSC and dielectric constant measurements, samples were poled for 20 minutes at 75°C with an

electric field of 350 kV/cm. The temperature rate used in the TSDC measurements was 0.8°C/min, while for the heating and cooling processes in the DSC measurements the rate was 20°C/min. All measurements were conducted from room temperature up to around 140°C in order to avoid the copolymers melting point.

3. Results

3.1 TSDC and TSC measurements

Fig. 1 presents thermally stimulated depolarization current (TSDC) on samples of the 80:20, 75:25, 70:30 and 60:40 P(VDF/TrFE) copolymers. The samples had been previously poled by applying an electric field of 350 kV/cm during 20 min. at 75°C. In the 75:25 and 70:30 copolymers two peaks are observed which have been named Peak *A* (lower temperature) and Peak *B* (higher temperature). The *Peak A* is rather broad and is shifted towards lower temperatures as the contents of VDF is increased, while on the contrary, Peak *B* is much sharper and is shifted towards higher temperatures with the increase in the VDF contents. The 80:20 copolymer displayed only the Peak *A* even though another peak seemed to be appearing at around 130°C. The 60:40 copolymer, on the other hand, displayed only the Peak *B*. In all cases a noise appeared whose magnitude increased with increasing temperature up to the vicinity of Peak *B*, it then started to decrease until it completely vanished after Peak *B*. Such a noise was found to be due to electrode vibration induced by air circulation from a fan used to uniformize the temperature

distribution inside the oven; it disappeared when the fan was switched off. When the samples were subsequently cooled to room temperature no current was detected. It should be mentioned also that TSDC measurements with unpoled samples failed to show any measurable current.

Thermally stimulated current (TSC) measurements on the 70:30 and 60:40 copolymers under an applied field of 50 kV/cm are shown in Fig. 2. Because of the applied field, the total integrated charge under the peaks is at least two orders of magnitude higher than in Fig. 1. Note that no noise is observed in the curves, possibly because any noise such as that of Fig. 1 would not have been detected in the much higher scale used for measuring the TSC currents. As before, the 70:30 sample displayed two peaks (*A* and *B*) while the 60:40 displayed only one (*B*), the peaks appearing at the same temperatures as in the TSDC curves of Fig. 1. Upon cooling the samples, still under the applied electric field, the measured currents are much smaller and the peaks are shifted towards lower temperatures (as explained later), as shown in Fig. 3. They are now named Peak *A'* and *B'* for the lower and higher temperatures, respectively.

3.2 DSC measurements

Differential scanning calorimetry (DSC) thermograms during heating measurements are shown in Fig. 4 for unpoled P(VDF-TrFE) samples containing, respectively, 60, 70 and 75% of VDF. The shape of these DSC diagrams is similar to the TSDC curves presented in

Fig. 1. Both Peak *A* and Peak *B* are also present in the DSC curves for the 75:25 and 70:30 copolymers, whereas the curve for the 60:40 copolymer displays only Peak *B*. When DSC measurements for the 60:40 and 70:30 copolymers are taken during the cooling process of the samples, results that are similar to the cooling measurements of Fig. 3 are obtained (see Fig. 5).

3.3 Dielectric constant measurements

In Figs. 6 and 7 measurements are shown of the dielectric constant at 1 kHz for the 60:40 and 70:30 copolymer films, respectively. In both figures results are shown for poled and unpoled samples, from which one can see that the dielectric constant is consistently higher for the unpoled samples. Also, for the poled films the peaks were shifted towards higher temperatures. Measurements were taken both at the heating as well as the cooling process of samples. Though not as clear as in the previous figures, it can be seen that two peaks appear in the curves for the 70:30 sample whereas only one peak is present in the curves for the 60:40 sample. During the cooling process, the peaks were shifted towards lower temperatures.

4. Discussion

There are two main mechanisms which can yield thermally stimulated currents in ferroelectric polymers. The first one is related to either the orientation of the dipoles (so-called

polarization) or the depolarization process when the dipoles in the ferroelectric crystallites lose their orientation or are even destroyed. Thermally stimulated currents arising from this mechanism will be observed if a high electric field is causing a remanent polarization or if the dipoles in a pre-poled samples lose their orientation upon heating. The second mechanism is the removal of space charge from the polymer film. It is known that charges are preferably trapped around the ferroelectric crystallites, which may be detrapped under certain conditions such as when the crystalline part undergoes a phase transition in which the crystallites are destroyed. Currents due to space charge effects will be important when an applied field can drive the charge towards one of the electrodes, or in the case of the TSDC measurements if the zero-field point [7] does not coincide with the center of the sample for short-circuited samples.

The TSDC currents in the poled, short-circuited samples in Fig. 1 come mostly from depolarization, a view that is supported by the experimental finding that no current was measured while heating unpoled samples. A small contribution from space charge cannot be discarded, though, for charges could have been injected into the sample during the poling process and trapped in a non-uniform fashion [8]. For the much higher currents observed in the TSC measurements on unpoled samples (Fig. 2), on the other hand, the removal of space charge by the electric field must have given the most important contribution. The applied field (50 kV/cm) was not sufficient for poling the sample to a significant extent. No noise

could be detected in the TSC measurements because the currents arising from the vibration of the electrode were too low for the measuring scale employed. When the samples were cooled, currents were measured which were three orders of magnitude smaller than those in the heating process. These currents could not be attributed to space charge as the electric field was still applied as before, and their appearance indicates that some poling does take place even at such a low applied field.

The appearance of peaks are related to phase transitions in the copolymer samples. This is best illustrated by the peaks in the DSC thermograms which indicate changes in the molecular conformation of the material in hand. For the ferroelectric polymers, in particular, these changes on molecular conformation induce phase transitions of polymer crystalline parts. The analysis of peaks in the electrical measurements is a little more involved. In the TSDC for poled samples the depolarization process reaches a maximum at a phase transition and so does the measured current. It is also known [8] that a large number of charges are detrapped from the regions around the crystallites during a phase transition. The peaks in the TSC curves (during heating) with unpoled samples, therefore, are likely to have been caused by the existence of maximum rates in the removal of the space charge from the sample.

We now focus on the Peak *B* which appears in the TSDC, TSC, DSC and dielectric constant measurements for the 60:40, 70:30 and 75:25 copolymers. For the 60:40 copolymer, this peak is due to the well-known ferro-paraelectric phase transition [4], so it is plausible

to assume that the same is true for the other copolymers. The noise in the TSDC measurements was caused by the piezoelectric effect ferroelectric materials are known to exhibit, as the electrode was mechanically disturbed by the air flow due to the fan inside the oven. (It is worth noting that noise in TSDC measurements have already been reported in previous works [9].) Consistent with the piezoelectric effect, the magnitude of the noise increased with increasing temperature until the vicinity of Peak *B*. After Peak *B*, the noise disappeared completely which indicates that the sample is no longer ferroelectric. However, the noise remains in the results for 70:30 and 75:25 samples even after Peak A which means that after this peak the material is still ferroelectric, in spite of the well characterized structural phase transition. So, the latter peak must be associated with a ferro-ferroelectric transition rather than with a ferro-paraelectric one. This indicates that in addition to the high temperature paraelectric phase, there exist two ferroelectric phases (F_I and F_{II}) below the Curie temperature.

Of the two copolymers possessing only one peak, the 80:20 changes from F_I to F_{II} (Peak *A*) and remains in phase F_{II} until its melting point, while the 60:40 changes from F_I directly to the paraelectric phase. The 70:30 and 75:25 copolymers, however, present an intermediate ferroelectric phase, F_{II}. Fig. 8 shows schematically a phase diagram for varying contents of VDF. While Peak *A* is shifted towards higher temperatures with increasing VDF content, making it possible for a ferroelectric phase to exist even at relatively high temperatures the opposite is observed for

Peak B.

It is known that a relatively high electric field applied to a β-PVDF sample causes a more effective molecular packing, thus increasing slightly the degree of crystallinity of the sample. As a consequence, a decrease occurs in the number of available dipoles which can freely follow the sense of a small alternating field - such as the one applied in dielectric constant measurements. Therefore, one should expect higher dielectric constant for unpoled samples, and indeed this has been confirmed by the measurements shown in Fig. 6 and 7. Moreover, the closer molecular packing of the poled samples also causes the packing energy to increase, thus increasing the transition temperature and shifting the dielectric constant curves to higher temperatures (see Fig. 6 and 7).

It should be stressed that the peaks observed in all figures correspond to first-order transitions, as they were shifted towards lower temperatures in the cooling process, and this is characteristic of first order transitions.

5. Final Remarks

The existence of two distinct ferroelectric phases for the P(VDF-TrFE) copolymers at room temperature was suggested by Tanaka and Kobayashi [6]. According to them, one of the phases would be less ordered and would therefore suffer a ferro-paraelectric phase transition at a lower temperature than the more ordered ferroelectric phase. The formation of these two ferroelectric

phases would be associated with the way the material is crystallized from its molten phase, in particular with the rate of the cooling process. Even stronger evidence for the presence of two ferroelectric phases came from the results by Horiuchi et al [10] who obtained X-ray diffractograms at different temperatures. They proposed the appearance of an intermediate ferroelectric phase, between the room temperature ferroelectric phase and the paraelectric one.

In our work we also assume that an intermediate phase exists for the 75:25 and 70:30 copolymer films. Strong evidence in favour of the existence of an intermediate phase, rather the coexistence of two ferroelectric phases, comes from the appearance of two peaks in the TSC and DSC curves obtained while cooling the samples. The shift to lower temperatures, when compared with the curves for the heating process, also indicates that the peaks are due to first-order phase transitions. We also conclude that the intermediate phase is ferroelectric because noise due to the piezoelectric effect appears in the TSDC curves, even after the phase transition to the intermediate phase has occurred.

Acknowledgements

The authors acknowledge the financial assistance of FAPESP and CNPq (Brazil).

References

1. T. FURUKAWA T, A.J. LOVINGER, G.T. DAVIS AND M.G. BROADHURST, Macromolecules 16 (1983) 1885.
2. T. FURUKAWA, H. MATSUZAKI, M. SHIINA AND Y. TAJITSU, Jpn. J. Appl. Phys. 26 (1987) 554.
3. T.YAMADA, T.UEDA AND T.KITAYAMA, J.Appl.Phys. 52 (1981) 948.
4. R.M.FARIA AND M.LATOUR, J.Phys. France 9 (1988) 2089.
5. K.TASHIRO AND M.KOBAYASHI, Jpn. J.App. Phys. 24 (1985) 873.
6. H.TANAKA, H.YUKAWA AND T.NISHI, Macromolecules 21 (1988) 2469.
7. J.LINDMAYER, J.Appl.Phys. 36 (1965) 196.
8. M.WOMES, E.BIHLER AND W.EISENMENGER, IEEE Trans. on Elect. Insul. 24 (1989) 461.
9. R.M.FARIA AND M.LATOUR, J.Polym.Sci.: Part B: Polymer Physics 27 (1989) 913.
10. T.HORIUCHI, K.MATSUSHIGE AND T.TAKEMURA, Jpn.J.Appl.Phys. 25 (1986) L465.

Figure Captions

Fig. 1 - Thermally stimulated depolarization current (TSDC) measurements for short-circuited, copolymer samples of different molar ratios, 60:40, 70:30, 75:25 and 80:20. The samples were heated at a 0.8°C/min rate. Prior to the measurements the samples were poled for 20 min with an electric field of 300 kV/cm at 75°C. The noise that appears in the curves is caused by mechanical vibration of the sample owing to the air circulation inside the oven.

Fig. 2 - Thermally stimulated current (TSC) measurements for 60:40 and 70:30 samples under an applied electric field of 50 kV/cm. The samples were not poled prior to the measurements. The heating rate was 0.8°C/min. Note that the currents are much higher than those in Fig. 1.

Fig. 3 - The same as in Fig. 2 but during the cooling process. The applied field was also 50 kV/cm, but the currents are now much smaller than in Fig. 2.

Fig. 4 - Differential scanning calorimetry (DSC) measurements for 60:40, 70:30 and 75:25 samples obtained at a heating rate of 20°C/min. The samples were not heated beyond approximately 140°C in order to avoid their melting

point.

Fig. 5 - The same as in Fig. 4 for the 60:40 and 70:30 samples but during the cooling process.

Fig. 6 - Dielectric constant versus Temperature measurements for 60:40 copolymer samples, illustrating both the heating and the cooling processes (as indicated by the arrows). The full curves correspond to a poled sample (for 20 min. at 75°C under an electric field of 300 kV/cm), whereas the broken curves correspond to an unpoled sample.

Fig. 7 - Dielectric constant versus Temperature measurements for 70:30 copolymer samples. The full and broken curves correspond to a poled and an unpoled sample, respectively. The dotted part in the full curve corresponds to a range of temperature within which we were unable to measure the dielectric constant.

Fig. 8 - Schematic phase diagram showing the appearance of an intermediate ferroelectric phase for the copolymers P(VDF-TrFe). The melting point is above 150°C.

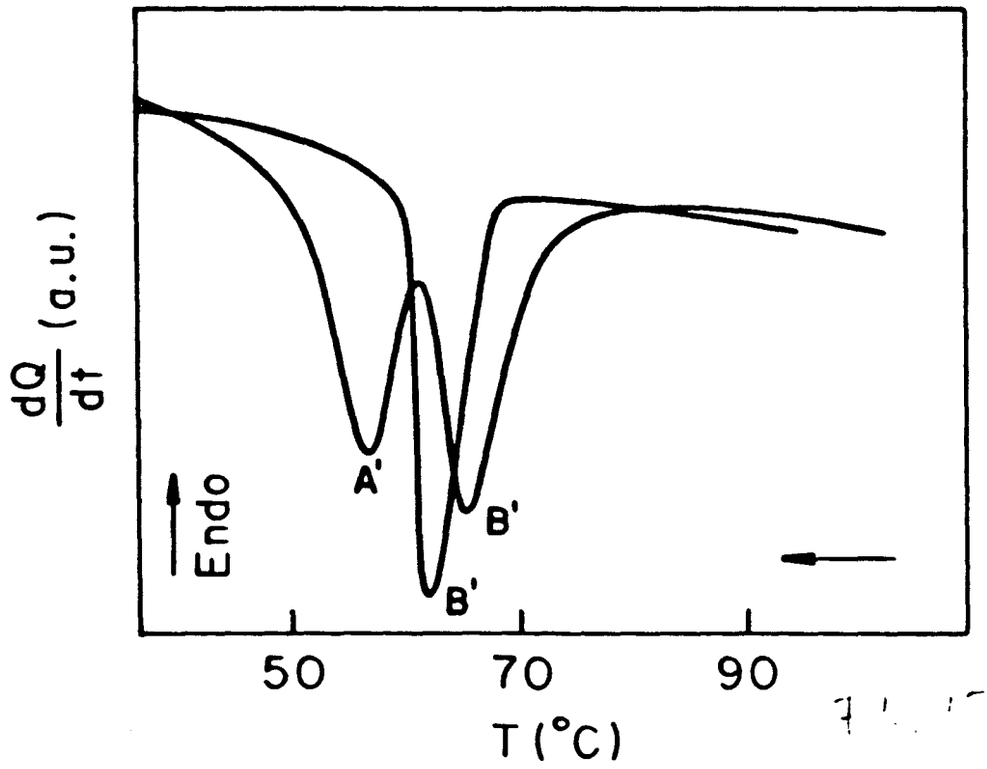

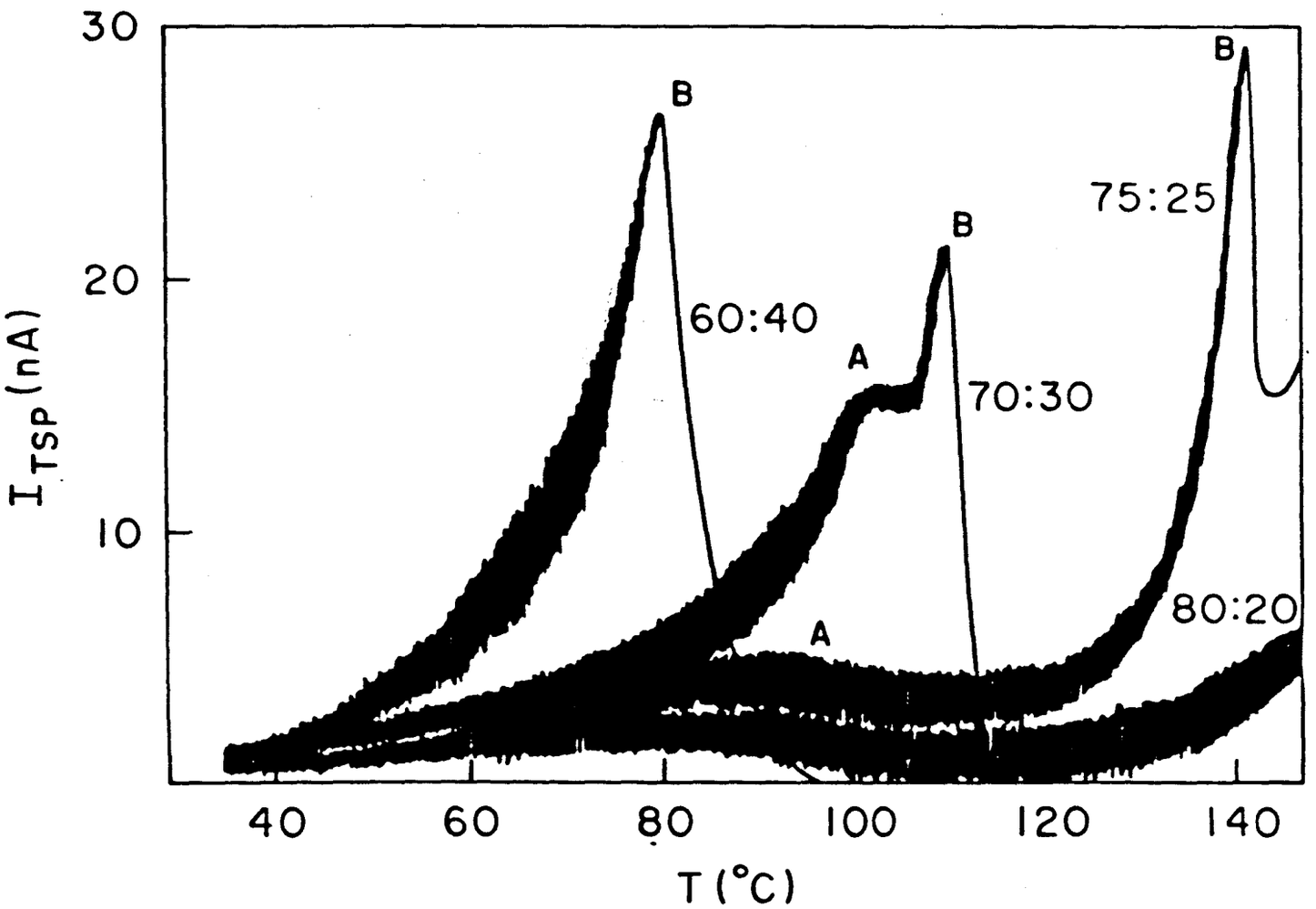

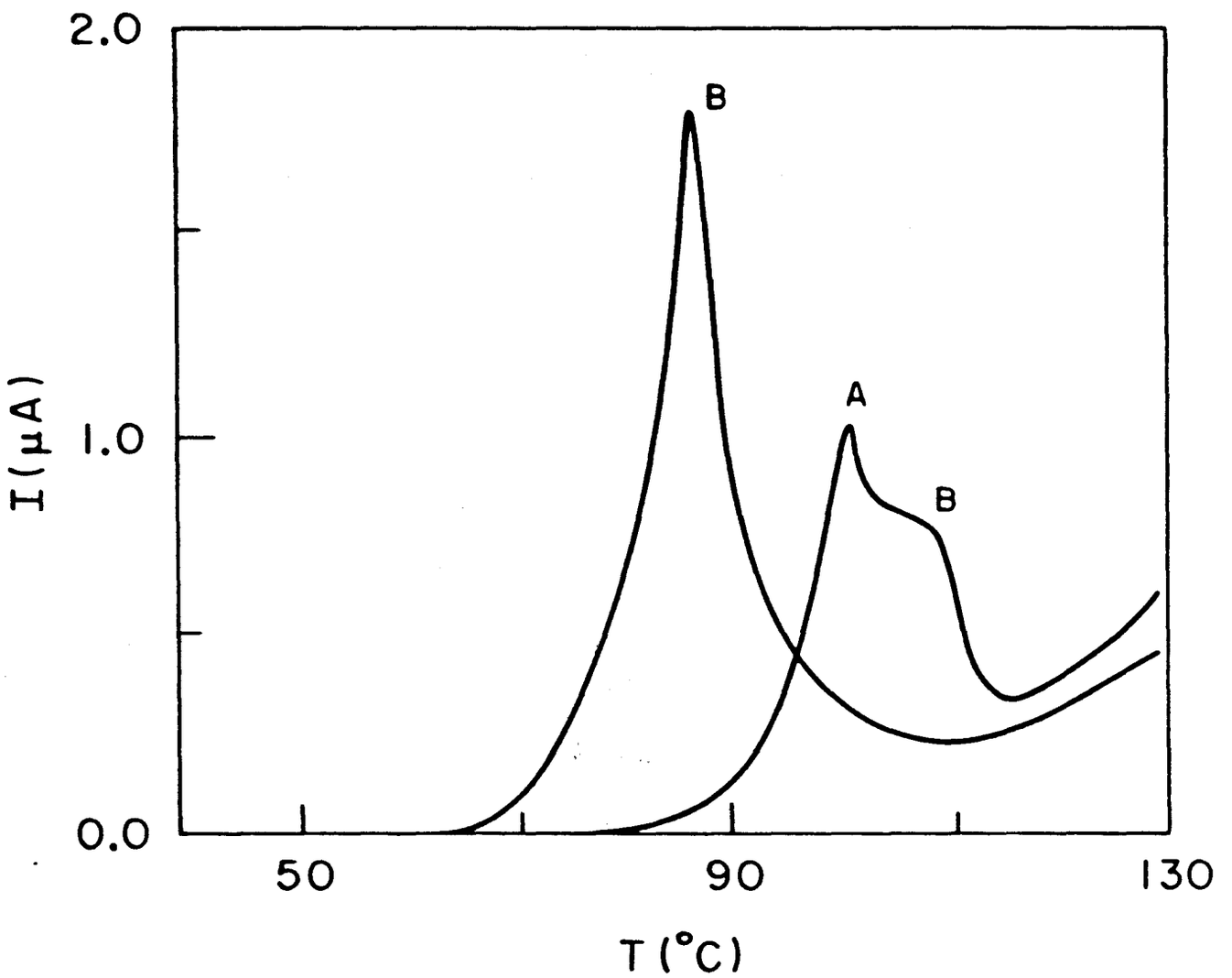
2.0
1.0
0.0
I(μA)
B
A
B
50
90
130
T (°C)

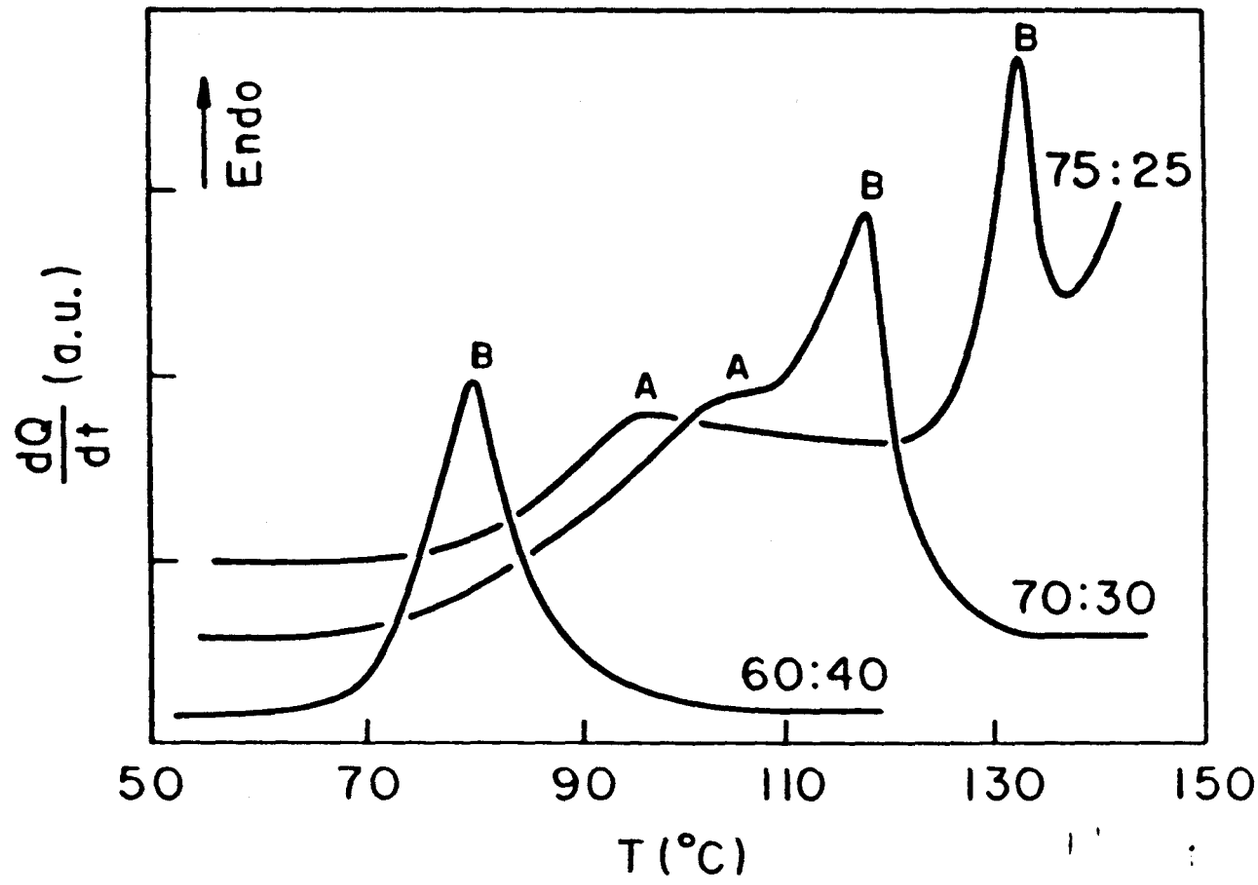
Endo
dQ/dt (a.u.)
B
B
B
A
A
75:25
70:30
60:40
50
70
90
110
130
150
T (°C)

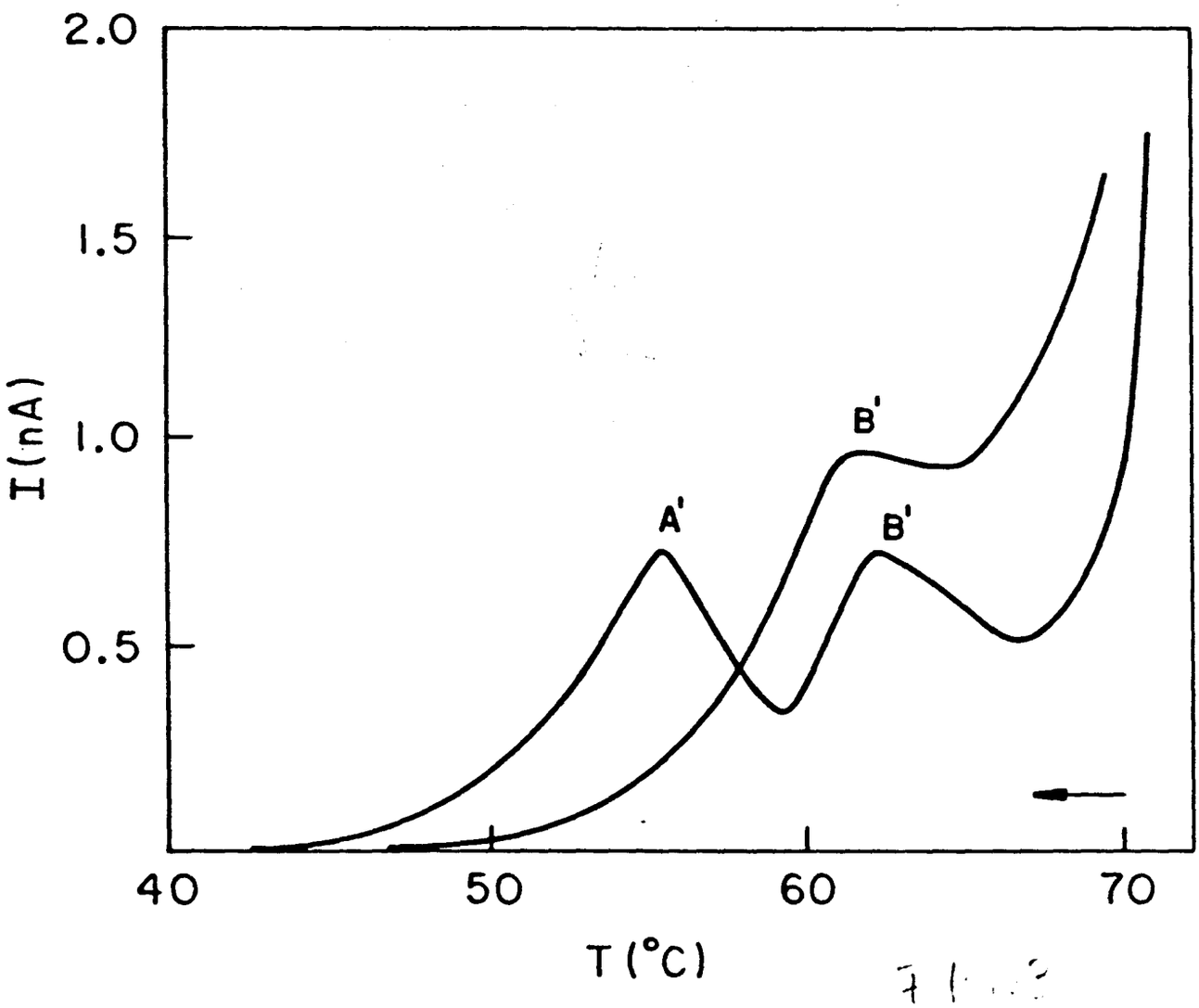
2.0
1.5
1.0
0.5
I(nA)
A'
B'
B'
40
50
60
70
T (°C)

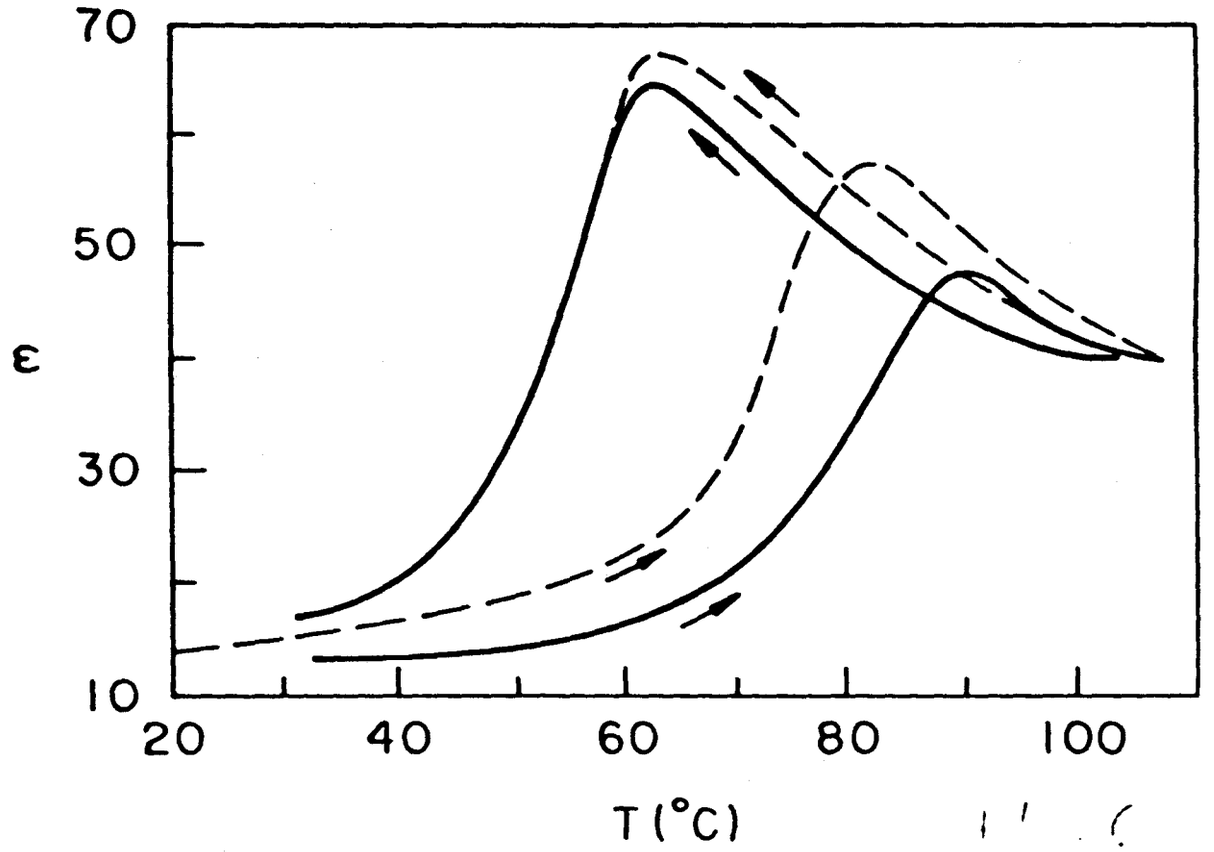

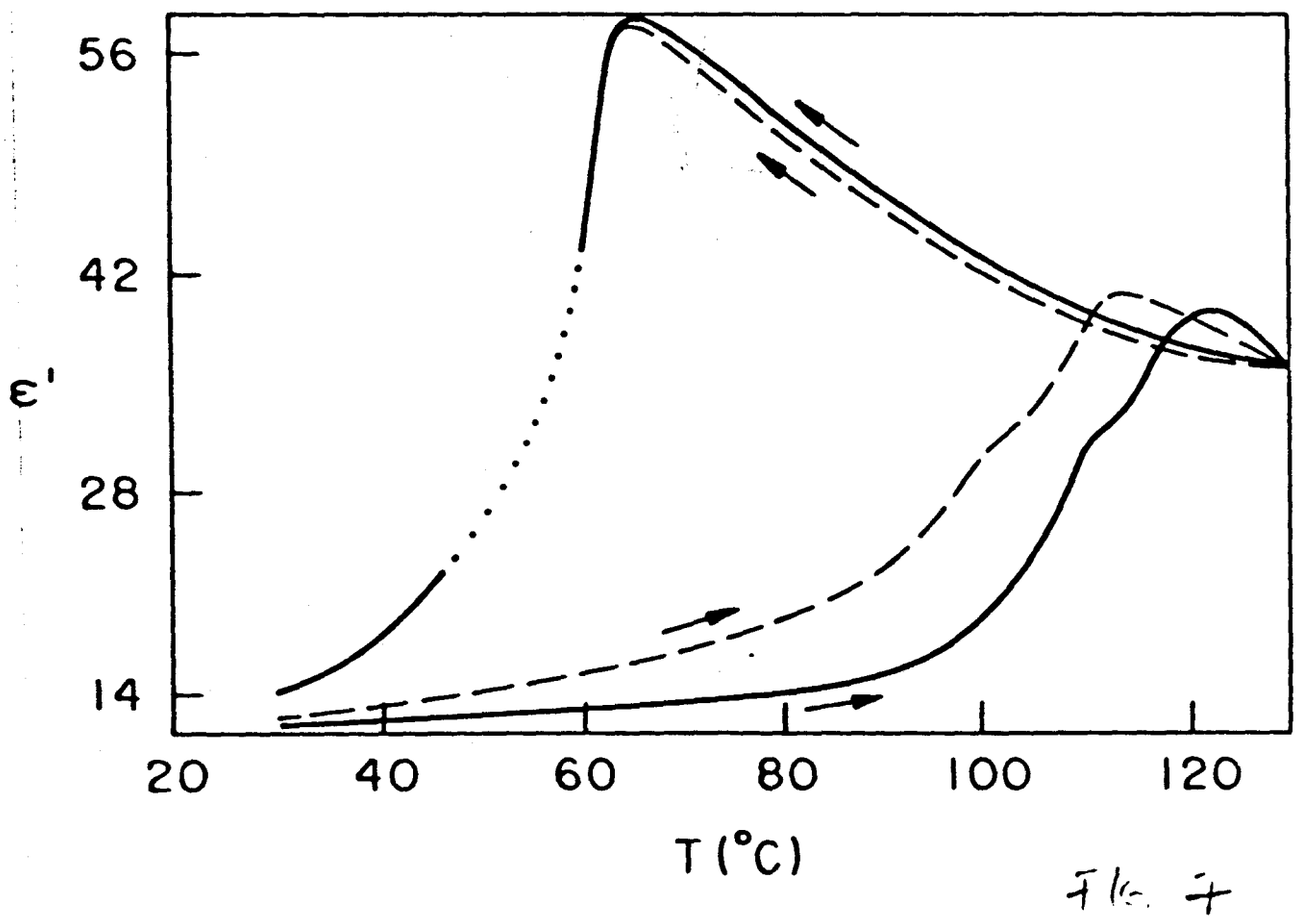

Fig. 4

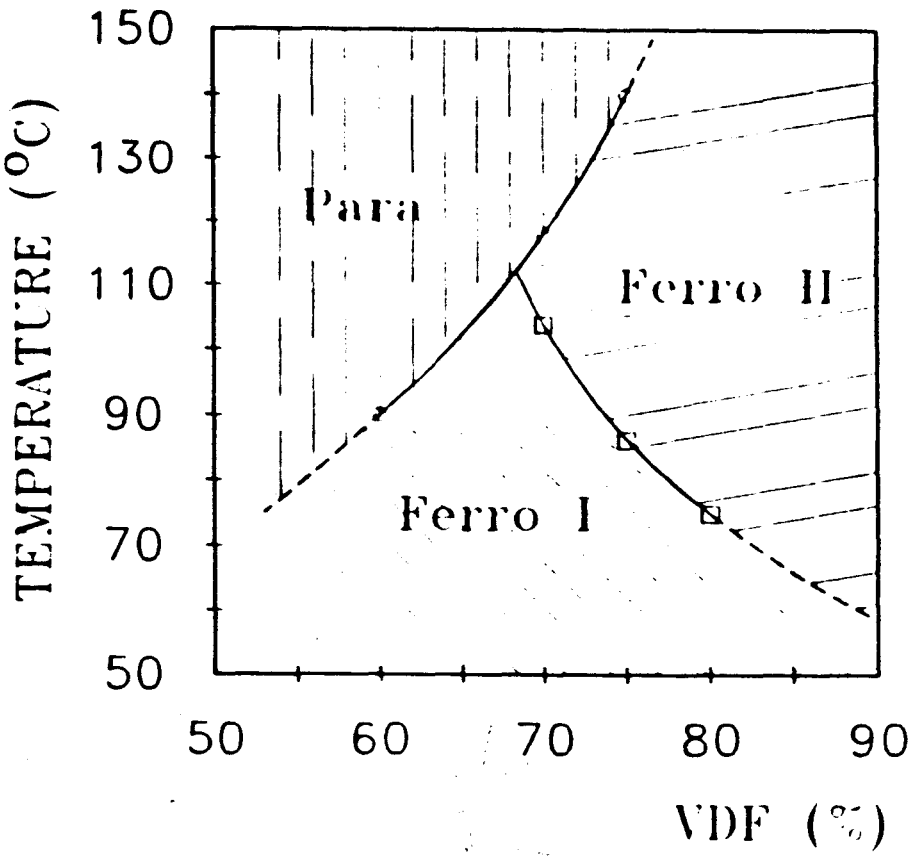
150
130
110
90
70
50
TEMPERATURE (°C)
Para
Ferro II
Ferro I
50
60
70
80
90
VDF (%)

Fig 8

Is it sound to carry on using abstract entities?

G.F.Leal Ferreira and O.N.Oliveira Jr.

Instituto de Física e Química de São Carlos

Universidade de São Paulo

CP 369, 13560 São Carlos, S.P., Brazil

FAX: 55 (162) 713616

e-mail: chu@ifqsc.ansp.br

Abstract

A critique is made of the use of abstract entities - such as the fields - in electromagnetism, in particular the need to resort to imaginary closed circuits when applying Faraday's law. It is suggested that the direct action-at-a-distance scheme, as proposed by Ritz and more recently reviewed by O'Rahily, is a plausible alternative which is based on firm physical grounds. As an application we show how this direct action scheme can be used, without resorting to non-existing entities, to calculate the potential difference between the two extremities of a metallic bar moving in a uniform magnetic field and where the reference frame is fixed at the bar.

I. Introduction

All of us have got accostumed to the concept of field defined as follows: we imagine a charge at a given place, find the force -- electric or magnetic (this is a little more complicated) - that would be produced on it, divide this force by the charge to find the field and say that there is that field at the given place. From then on we speak freely of field, field lines and flux, both electrical and magnetic, though we know that these fields become concrete entities only when acting on a real charge. In the case of the Faraday's law in circuits with changing currents, one usually states that changing the magnetic flux comprehended by the circuit generates an electric field on it. We even go as far as imagining closed circuits in order to apply the "law" of changing flux in cases in which no such a closed circuit is present. This is the case (see [1]) when the potential difference between the two extremities of a metallic bar moving in a uniform magnetic field is calculated with the reference frame fixed at the bar. We believe the use of such an imaginary circuit to be physically unacceptable, and it is in fact a reflection of the problems in the definition of the electromagnetic field as an abstract quantity. We strongly feel that better solutions should be sought.

For those who do not feel entirely comfortable with dealing with abstract quantities only, there is an alternative scheme in which the induced electromagnetic force (e.m.f.) of the Faraday law is proved to result from an extra interaction between the charges derived from the fact that they are being accelerated. This has

been shown by W. Ritz [2] and more recently by O'Rahily [3], by including retarded effects - within a certain approximation - arising from the velocity and acceleration of the charges in motion. Using this procedure the induced e.m.f. is correctly derived from the accepted Maxwell's equations, but within the perspective that Weber had previously used to explain the Faraday's law based on a modified Coulomb's law. We firmly believe this latter explanation should be given preference when compared with the one using flux variations, in particular because it is based on (presumed) physical entities. This does not mean that we are advocating that fields should never be used, as they are mathematical tools that can be extremely useful in a number of problems.

In this article we show how the direct action-at-a-distance scheme, which modifies the Coulomb interaction to take account of velocity and acceleration terms, can explain the appearance of forces in that above mentioned situation requiring the use of imaginary closed circuits. The problem is presented in Section II and in Section III we undertake the task of solving it by the direct action method. A brief comment is also made on a recent statement by Sharma [4] who claims that, in order to solve the Feynman's disc paradox [5], one has to use field ideas even for static situations.

II. The Problem

The teaching of Faraday's law is commonly illustrated with an exercise which consists in calculating the potential difference between the two ends of a metallic bar that moves in a constant magnetic field (see Fig. 1). Use is made of two reference frames: a) one inertial frame in which the bar moves with velocity $\bar{u}$, and another b) that moves with the bar, and so it is the magnet that moves with velocity $-\bar{u}$.

In case a) the potential difference between the two extremities of the bar is calculated by equating the Lorentz force on the charges in the bar to the electric field brought about by charge separation, yielding a potential difference $\Delta V = BLu$, where B is the magnetic field, L is the length of the bar, and u the velocity of the bar. In case b) there is no Lorentz force because the charges in the bar are not moving in relation to the reference frame. Using Faraday's law, the potential difference can only be calculated if an imaginary closed circuit (shown by the broken lines in Fig. 1) is used. It is assumed that the magnetic flux changes as part of the area of the "non-existing circuit" moves outside the region of magnetic field B going to a region where B = 0. The potential difference is then equated to the change of flux $-(d\Phi/dt)$, leading equally to $\Delta V = BLu$.

The problem we find in such an explanation is that an imaginary circuit must be invoked, and physical explanations should not be supported by imaginary entities. In the next section we

endeavor to address this problem from a realistic perspective, by using the direct action approach in which the electric field of moving charges is calculated.

III. Using the Direct Action Scheme

The potential difference between the extremities of a magnetic bar (length L) will be calculated by integrating the electric field on the bar caused by the magnetic field of a moving magnet (case b) above). In order to simplify the geometry of the problem we will replace the magnet poles by an infinite sheet carrying a neutral current whose mobile charges have a velocity $\vec{v}$. To reproduce the geometry of Fig. 1, the bar (not shown in Fig. 2) is placed parallel to the current flow lines, the sheet itself moving with a velocity $\vec{u}$ normal to the velocity $\vec{v}$, as shown in Fig. 2. The magnetic field due to the sheet, $\vec{B}$, the velocity $\vec{u}$ and the direction of the bar axis are then perpendicular to each other. The magnetic field due to the currents in the sheet is $B = \mu_0 \sigma v/2$, where σ is the charge density on the sheet.

Our starting point is the instantaneous electric field of a moving charge as calculated in [3], correct to the order of V^2/c^2 and to the first order in the acceleration [6,7]:

$$\vec{E}(\vec{r}) = \frac{q}{4\pi\epsilon_0 r^2}\left\{\hat{r}\left[1 + \frac{\vec{V}^2 - 3(\vec{V}.\hat{r})^2}{2c^2} - \frac{\vec{a}.\hat{r}}{2c^2}\right] - \frac{\vec{a}r}{2c^2}\right\} \qquad (1)$$

where ϵ_0 is the vacuum permittivity, $\bar{V}$ is the total velocity of the charge, q, $\bar{a}$ its acceleration, and $\bar{r}$ is the position vector for the point where the field is calculated. Eq. (1) derives directly from Lienard-Wiechert potentials within the mentioned approximation.

It should be made clear that although using the word field, this $\bar{E}$ has physical significance for us as it is employed to find the action of the charge q (on the sheet) on another electric charge that is at the point given by $\bar{r}$.

We now apply Eq. (1) to the charges on the sheet, and for this case the acceleration terms may be dropped. Since the current is neutral, two distinct cases must be considered. First, the charges that are not moving in the sheet which therefore have a velocity $\bar{u}$, and second the charges that cause the currents in the sheet which have the total velocity $\bar{v} + \bar{u}$. The electric field due to the charges at rest in the sheet is:

$$E_1 = \frac{\sigma}{4\pi\epsilon_0} \int_{-\infty}^{\infty} dy \int_{-\infty}^{\infty} dx \, \frac{f}{r^2} \left[\left(1 + \frac{u^2}{2c^2}\right) - \frac{3(\vec{u}.f)^2}{2c^2} \right] \qquad (2)$$

whereas the field due to the charges in motion is:

$$E_2 = \frac{\sigma}{4\pi\epsilon_0} \int_{-\infty}^{\infty} dy \int_{-\infty}^{\infty} dx \, \frac{f}{r^2} \left[\left(1 + \frac{u^2 + v^2}{2c^2}\right) - \frac{3[(\vec{u} + \vec{v}).f]^2}{2c^2} \right] \qquad (3)$$

where: σ = surface charge density in the sheet

$r = |\bar{r}|$ = distance from the line of charges to the point of interest.

$\hat{r}$ = versor in the direction of $\bar{r}$

$\bar{u}$ = velocity of the sheet of charges

$\bar{v}$ = velocity of the moving charges in the sheet

The positive charges were assumed to be at rest in relation to the sheet while the negative charges were assumed to be moving in the sheet. Integration is initially carried out over the x-axis, i.e. the electric field at a fixed distance y due to a line of current in the x-axis is calculated, by changing the coordinates to ϕ and y, as defined in Fig. 3a, which leads to the following relations:

$x = y \cot g\, \varphi$

$r = y \operatorname{cosec} \varphi$

The electric fields for this line of current for the charges at rest in the sheet is:

$$dE_1 = \frac{-\sigma dz}{4\pi e_0 y}\left(1 + \frac{u^2}{2c^2}\right)\int_0^{\pi}\sin\varphi\, d\varphi + \frac{3\sigma dz u^2}{8\pi e_0 c^2 y}\int_0^{\pi}\sin^3\varphi\, d\varphi \qquad (4)$$

and a similar expression is found for the moving charges. The sum of the two contributions leads to

$$dE = \frac{-2uv\sigma dz}{4\pi e_0 y c^2} \qquad (5)$$

which has by symmetry the direction of the y-axis.

Integration over z gives the contributions from all lines of current which are at a distance r from the point of interest as Fig. 3b shows. Hence, y in Eq. (4) must be replaced by r. Using the relations:

$r = y \operatorname{cosec} \theta$

$z = y \operatorname{cotg} \theta$,

where again y will be a fixed distance, and the electric field will be in the y-direction, the total electric field can be calculated:

$$E = \int_0^{\pi} \frac{uv\sigma}{2\pi\epsilon_0 c^2} \, d\theta \qquad (6)$$

which leads to:

$$E = \frac{uv\sigma}{2\epsilon_0 c^2} \qquad (7)$$

The potential difference, ΔV, between the two extremities of a metallic bar (length L) in this electric field will be

$$\Delta V = \frac{uv\sigma L}{2\epsilon_0 c^2} \qquad (8)$$

which is equivalent to $\Delta V = BLu$ if $B = \mu_0 \sigma v/2$ is used for the magnetic field due to an infinite sheet of moving charges, therefore agreeing with the result obtained with the Lorentz's force when the bar is moving through the field.

IV. Discussion

The simple example above shows how induced currents can be obtained without having to resort to imaginary entities. We wonder then how an explanation which invokes flux changes in non-existing closed circuits could have ever achieved such an overwhelming

acceptance. It can be argued that the mathematics involved is usually straightforward, which may be a sound justification on mathematical grounds but surely not on physical grounds. The main reason may be the widespread use of abstract field ideas: if the field itself is abstract there is no reason for not introducing yet another abstract, imaginary entity in the problem in hand.

There is another important issue in the discussion of the direct action versus field ideas, namely the necessity of using fields for the electromagnetic radiation. Even O'Rahily who favours the use of the direct action scheme recognizes the need of using fields in order to explain radiation emission [8]. But the extension of this argument, as implied in most textbooks and more recently by Sharma [4], going so far as stating that the introduction of the electromagnetic field should be preferred to the direct action scheme also in static cases, such as in the apparent Feynman's disc paradox, seems unsound. In this apparent paradox, the disappearance of a current in a coil centered in a plastic disc makes it to rotate if charged metallic balls are embedded symmetrically along its circumference. The explanation for this phenomenon is based on the angular momentum conservation law since crossed electric and magnetic fields possess angular momentum which pass into mechanical angular momentum when the current disappears [5].

While we have no option but to accept that for radiation emission as well as other highly oscillatory phenomena fields are a necessity, we strongly disagree with Sharma [4] in relation to

his statement on the Feynman's disc paradox. An inspection of Eq. (1) shows that the direct-action-at-a-distance scheme provides a much simpler explanation (without ghost circulations) for the apparent paradox. It can be seen from Eq. (1) that, when acceleration is present, the interaction ceases to being central. Therefore, the angular momentum needs not be conserved. The Feynman's disc would nevertheless rotate simply due to the tangential force acting on the charged metallic balls.

Acknowledgements

The authors acknowledge the financial assistance of FAPESP and CNPq.

References

[1] J.R.Reitz, F.J.Milford and R.W.Christy, *Foundations of Electromagnetic Theory*, Addison-Wesley Publish. Co., Reading, MA (1980) pp. 234-238

[2] W.Ritz, *Ges. Werk - Recherches Critiques sur l'E'lectrodynamique Générale*, Gauthier Villars, Paris (1911) pp. 317-425

[3] A.O'Rahilly, *Electromagnetic Theory, A Critical Examination of Fundamentals*, Dover Publish. Inc., Vol. I, N.York (1965)

[4] N.L.Sharma, Field versus action-at-a-distance in a static situation, Am. J. Phys. 56 (1988) 420-423

[5] R.P.Feynman, R.B.Leighton, and M.Sands, The Feynman Lectures on Physics, Addison-Wesley, Reading, MA (1964), Vol. II, pp. 17.5 and 27.11

[6] Ref. 2, p. 387

[7] Ref. 3, p. 220

[8] Ref. 3, pp. 287-288

Figure Captions

Fig. 1 - A metallic bar that moves with velocity $\bar{u}$ is inserted between two magnet poles that generate a uniform field $\bar{B}$. In order to calculate the potential difference between the extremities of the bar using Faraday's law, an imaginary closed circuit (broken line) must be used.

Fig. 2 - Lines of current in a sheet generate a magnetic field $\bar{B}$. The sheet moves with a velocity $\bar{u}$.

Fig. 3 - a) Definition of φ and r

b) Definition of θ and r

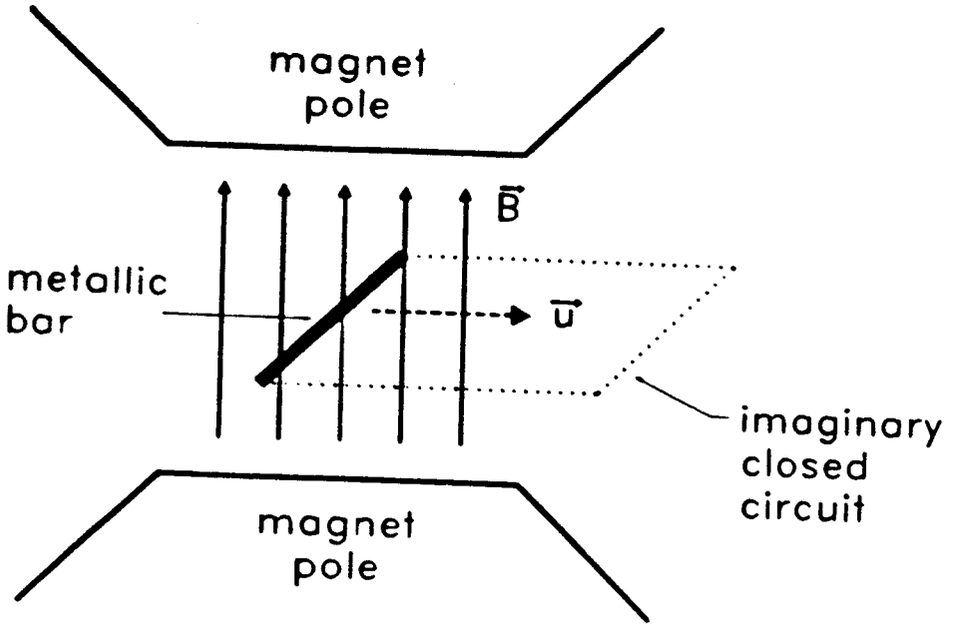
magnet
pole
$\vec{B}$
metallic
bar
$\vec{u}$
imaginary
closed
circuit
magnet
pole

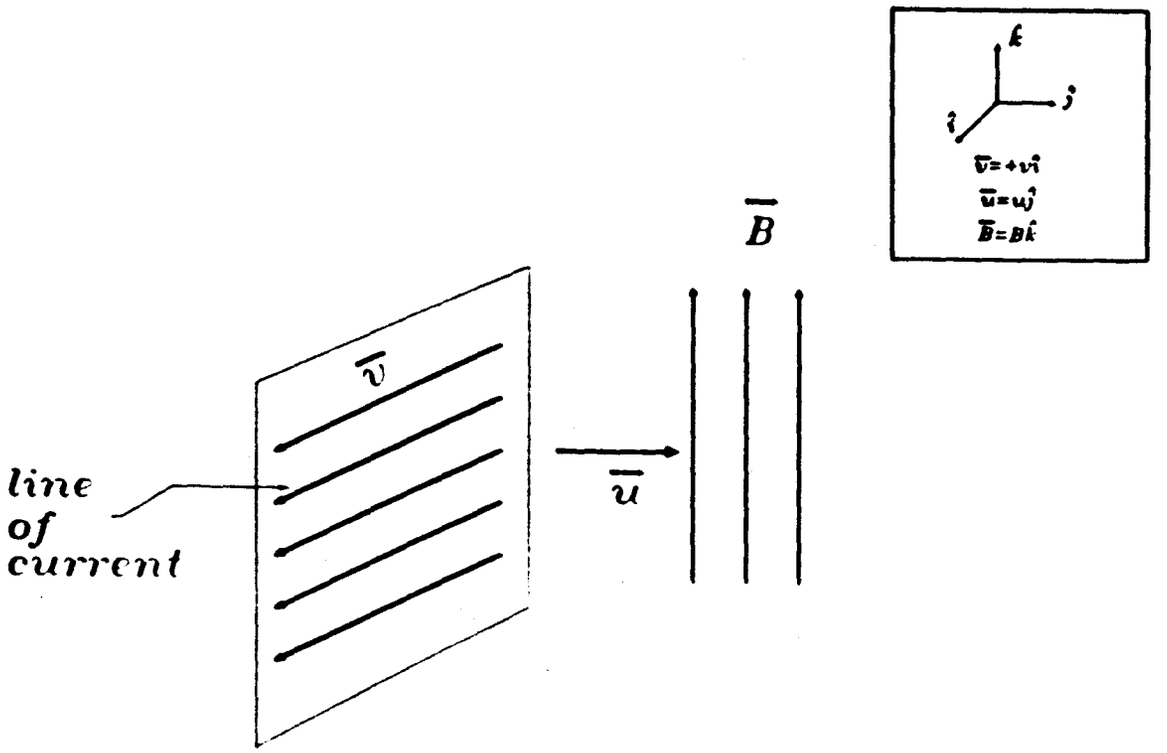
k
j
i
$\bar{v} = +v\hat{i}$
$\bar{u} = u\hat{j}$
$\bar{B} = B\hat{k}$
$\bar{B}$
$\bar{v}$
$\bar{u}$
line
of
current

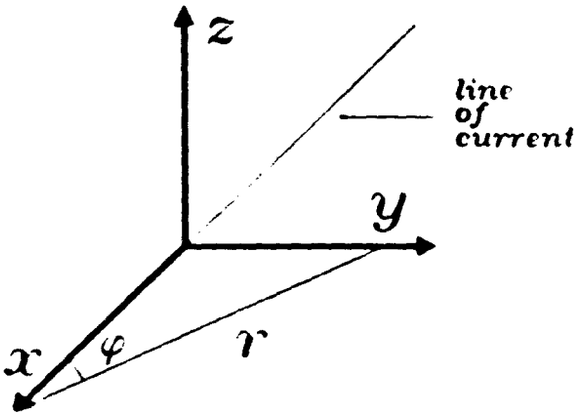

(a)

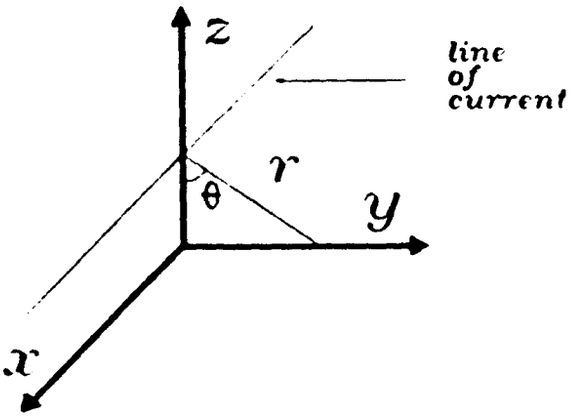

(b)

Chusaurus: A Writing Tool Resource for Non-Native Users of English

Osvaldo N. Oliveira Jr.
Instituto de Física e Química de São Carlos, USP
C.P. 369, CEP 13560 São Carlos, S.P. - Brazil
FAX: (55) 162 722218 - e-mail: chu%br.ansp.ifqsc
Sandra M. A. Caldeira
Departamento de Ciências de Computação e Estatística, ICMSC-USP
C.P. 668 - CEP 13560 São Carlos, SP - Brazil
e-mail : smacalde@brusp.bitnet

Niura Fontana
Departamento de Letras, Universidade de Caxias do Sul
Campus Universitário C.P. 1352 - CEP 95070, Caxias do Sul, R.S. - Brazil

Abstract

A novel work of reference is proposed which is to be implemented as a writing aid in the form of software tools. This reference source is named Chusaurus and is based on a compilation of well-written, useful expressions extracted from papers and books which could be used to assist in the generation of scientific text. The expressions have blank spaces (representing missing words) which should be filled in by the user to suit his/her needs. The most important feature of the Chusaurus lies in the help it provides to non-native users of English in coping very rapidly with linguistic difficulties, since it provides pieces of real language in use. For example, it assists them in producing correct phrase structuring with adequate vocabulary, which is one of the aspects of English that can be extremely different from their own native language. Two possible implementations are discussed. Firstly, the resource could be implemented as an extra function in word processors.The expressions would be accessed from menus with the compiled expressions being indexed according to their suitability for use in the different sections (and for the subjects) most likely to appear in a paper. The second implementation manner is more sophisticated and involves the development of a writing environment in which support tools would assist the user in selecting and organizing the material to be written as well as in producing a well-written text.

Key Words: Writing Tools, Text Generation, English for Non-Native Users

1 Introduction

English has undoubtedly become the international language for business, science and technology, and is currently the most commonly taught second language around the world. It is therefore of fundamental importance that scientists and businessmen alike should be able to use it, particularly in its written form, for the majority of international journals and scientific literature are written in English. For the writing of scientific work in general (formal reports, essays, theses, papers, etc.), help can be found in a number of books (1-10) which deal specifically with the question of "How to write in English" or "How to present technical information". Other writing aids such as spelling checkers, Thesaurus dictionaries and software packages (11) aimed mainly at postwriting evaluation also provide significant help.

Several studies are reported in the literature which address a variety of issues relevant to the improvement of non-native speakers' English usage (see for instance (12-15)). Nevertheless, there are still enormous difficulties facing those who need to use English on a regular basis. In order to identify these difficulties an informal study was carried out by one of us on the most frequent errors made by a group of Brazilian graduate students in the United Kingdom. One could observe that the errors are not restricted to the use of incorrect gramatical structures and inadequate vocabulary, but include the misuse or omission of cohesive elements and discourse markers usually employed by native users for specific purposes in a scientific text. All these problems encountered by non-native users clearly affect phrase structuring. This might also happen because phrase structure in English is obviously different from that of a large number of languages.

After having analysed the difficulties mentioned above we concluded that one writing strategy which could be employed to solve them was to try and write sentences based upon expressions or passages of authentic texts in an attempt to ensure that correct sentences were being produced. This strategy on the part of the foreign language learner is known as "appeal for assistance" (16), i.e. an authority (a native speaker, a teacher, books, dictionaries, etc.) is searched in order to help the learner cope with his/her problem. The strategy is likely to be quite effective, provided that adequate resources are available.

Hence, we decided to compile a list of well-written, useful expressions extracted from papers and books written by competent native speakers of English which could be useful in a writing exercise. In doing so, we realized that a relatively small number of expressions is sufficient to cover a large proportion of the words and phrases needed in our scientific work. This occurs because expressions

are employed systematically — sometimes with little variation within a canonical framework — when describing common features such as tables and figures, or even experimental procedures or when making a comparison of results. Because of its features, this is just the sort of process ideal to be automated.

We first used the mini-dictionary compiled, named Chusaurus by analogy with Thesaurus dictionaries, together with a word processor (albeit not online). We now intend to extend this use by developing a writing software environment comprising tools aimed at helping the writer not only to produce a well-written text but also to organize the material to be written. A proposal for such an environment is presented in Section 3, while in Section 2 we discuss a simpler possible application in word processors. (These two applications have not actually been implemented yet.) Section 4 discusses the advantages and disadvantages of the Chusaurus resource.

2 Implementation of the Chusaurus into a Word Processor

As a reference source, the Chusaurus can be implemented as an additional function of word processors, i.e. as an extra option on the processor Main Menu. Since the relationship that holds between linguistic items and specific sections of the scientific text is quite obvious and relevant for writing purposes, the list of compiled sentences was indexed according to the divisions of this text type, namely Introduction, Problems, Method, Discussion and Conclusion (17). Although this division can vary a little in the Teaching of English to Students of Other Languages (TESOL) or English for Specific Purposes (ESP), there seems to be a general agreement in that it covers the basic macro-structures of the scientific text. In addition to the five divisions above some subdivisions were included to make it easier for the user to identify more precisely the subject(s) and the function(s) of each section.

The implementation can be performed so that the compiled expressions would be accessed as follows. Once the option Chusaurus is selected, the user would be presented with a menu containing the names of the different sections, as illustrated in Fig.1. The user would then be requested to choose one of the sections and a sub-menu containing the subdivisions would appear on the screen. Examples of such subdivisions are given in Fig. 2a and 2b for the Introduction and Results Sections, respectively. Also shown are some examples of the compiled expressions which were indexed according to their suitability for a certain part of the written

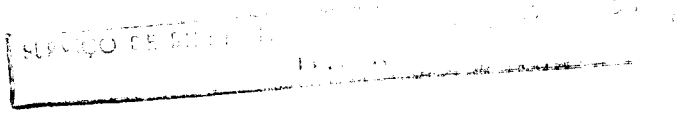

work. Obviously, some expressions will be suitable for more than one section or sub-section.

The blank spaces in the expressions should be filled in according to the user's needs. A word between brackets following the blank space is included in some cases in order to give a hint as to the sort of term which is expected to fill the gap. Facilities should also exist to allow users to select expressions to be automatically inserted into the text.

One of the main objectives of the resource is thus to provide a variety of expressions from which the user can choose when writing about certain aspects of his/her work. Let us take, for instance, the item "showing and describing figures" for which a larger number of expressions were listed in Fig. 2. The various sentences will exemplify a number of ways in which the user can present his/her data, and also describe diagrams. Furthermore, the sentences would provide the appropriate adjectives for explaining the curves, graphs, etc. Though it might be straightforward for a competent native speaker to know when to use "large" or "high", for example, the same may not be true of non-native users.

Hitherto we have referred to a sort of "fill-in-the-blank use", which is in fact the more mechanical and simpler way of using the Chusaurus as a reference source. A more cognitive and creative way of approaching the resource is to use it as an aid to plan/organize the writing process. In the next section, we discuss another possible application of the Chusaurus with such characteristics, namely, the develoment of a writing environment.

3 The Chusaurus into an Environment of Software Writing Tools

A number of software writing tools have been developed recently which could be classified into three main categories: (i) postwriting assessment tools using statistical text analysis; (ii) pre-writing tools; and (iii) writing environments. Tools of type (i) are the commonest and usually analyze writing style at word and sentence level (18-20), and allow overused words and expressions to be substituted. Some of them are commercially available such as the Right Writer (20) which is based upon a rule-based knowledge system. Tools of type (ii) are aimed at helping the writer to select and organize the material to be written, an example of which is provided by Beer (21) who proposed the use of flow charts for helping electrical engineering students to organize their laboratory reports. The third kind of tool

is, in principle, the most comprehensive as tools are developed to help the writer not only to select and organize the material to be written but also to produce and polish the final version of the text. These environments consist, therefore, of tools of type (i) and (ii). As Carlson (22) has pointed out these environments are only at an embrionary stage, and, as yet, far from being flexible and comprehensive.

In spite of the many tools already presented in the literature, no tool aimed specifically at assisting non-native users of English in composing a text from the very beginning appears to have been proposed. In this context, the implementation of the Chusaurus resource suggested here may prove extremely attractive. The implementation of an extra option into word processors as described in the last section would already be of considerable help. This resource would use techniques such as the earliest employed Natural Language Processing (NLP) for producing sentences which relied on templates (23). It would present, therefore, problems of extensibility and flexibility for not allowing intra- and inter-sentential combination, hindering the possibility of producing a large number of different texts using the same database. Since this extra option in word processors would not possess such a flexibility, we have instituted a research programme aimed at developing a writing environment, a model of which is given below.

3.1 The Model for the Writing Environment

The writing environment is to include support tools which are flexible and interactive, so that the user may play a participative role in the writing process. It is to assist the writer in the selection of the material to be written as well as in generating and structuring the text. Fig. 3 shows the main modules of the environment proposed:

- The Ideas Processor will allow the user to write comments and structure them in a semantic network. It will also be linked to the Knowledge Base for text generation.
- The Linearizer will transform the information contained in the semantic network and the expressions selected from the database into continuous prose.
- The Knowledge Base will consist of the database containing expressions and phrases extracted from books and papers, and also of knowledge base rules which will drive the selection of expressions from the database.

For the implementation of the writing environment, issues belonging to the realms of software engineering and text generation must be addressed. Hypertext techniques may be used for constructing the semantic network and navegating over it (24). The indexation system illustrated in Fig. 2 would have to be replaced by another knowledge-representation formalism (such as schemas (25) or rethorical structure theory (RST) (26) which could encode diverse kinds of information. Unlike the tool discussed in Section 2 where the choice of any sentence rested entirely with the user, the system is to suggest a number of possible sentences or expressions based upon information provided by the user to the Ideas Processor (which could even be in his own language). As for the text generation itself two stages are involved: planning and realization. Our tools will be more closely related to planning as they will help the user in the collection of topic-related ideas and text structuring. There will also be text realization to some extent, however, as prose will be output from the system even though there may be blanks to be filled in by the user. It must be stressed that text generation in our context is not completely equivalent to text generation in the NLP jargon. In NLP, the aim is to produce a syntactically, semantically and pragmatically correct text while in our case the user will ultimately be responsible for the final quality of the text.

4 Discussion

The two versions of the Chusaurus were conceived with a clear objective in mind, namely to help students/writers solve — as quickly as possible – global problems caused by lack of appropriate lexical, structural, pragmatic and discourse knowledge in academic text production. This is not an easy task, which has just reached the first attempts of partial implementation. So far, we have concentrated our efforts on the study of the techniques for text generation and for computer-aided writing, and on the linguistic aspects of writing strategies. While the development of the writing environment proposed in Section 3 is our long-term goal, the implementation of the Chusaurus resource (a mini-dictionary has already been compiled) into word processors will hopefully be forthcoming in the near future.

In the actual implementations process some drawbacks are expected to occur, mainly on the technical, linguistic and pedagogical levels. Nevertheless, the Chusaurus is expected to offer help in a more effective way than dictionaries and grammar books, because the compiled sentences which comprise the database of the resource present real language in large stretches within the context required for use.

An pedagogical implication deriving from the use of the resource is that after the user has become familiar with the expressions listed in it he/she will use some of the phrase constructions naturally which had previously seemed very unusual. This is in line with what Hovstad (12) has shown in his so-called gap tests. In these experiments, a fraction of a given text was removed and the students were asked to reproduce the text by guessing the missing words.

It is clear that while it can help with specific difficulties, the Chusaurus on its own cannot be successfully employed by users without a minimum background knowledge of English. One cannot (or should not) expect an author to write a paper without a certain proficiency in the language. Furthermore, we wish to mention that, although it has been targeted primarily at non-native users of English, the Chusaurus resource might also be useful for native speakers who have little experience in writing scientific works in assisting them to structure their documents or to produce a more formal phraseology.

Caution must be advised in using the Chusaurus, however, in spite of its strengths. Three main problems can arise from its inappropriate use: i) the production of wordy sentences, one of the most common undesirable features of many written products (16,20); ii) overuse of the author's favorite expressions; iii) misuse of expressions or their misapplication in the wrong context. We believe, however, that the help this resource can provide to non-native users of English as well as to inexperienced native writers outweigh these possible disadvantages by far.

Acknowledgments

We are indebted to a number of colleagues at the School of Electronic Engineering Science, Bangor, U.K. for many helpful discussions. Special thanks are due to Cristina Oliveira, and David Chapman. One of the authors (O.N.O.J.) acknowledges the financial assistance of FAPESP (Brazil).

References

1. G.E.Williams, Technical Literature, George Allen Unwin Ltd., London, 1948.

2. C.Turk and J.Kirkman, Effective Writing. E. F.N.Spon, London, 1982.

3. R.Barrass, Scientists Must Write, John Wiley and Sons, New York, 1978.

4. A.D.Farr, Science Writing For Beginners, Blackwell Scientific Publications, Oxford, 1985.

5. J.Kirkman, GOOD STYLE for Scientific and Engineering Writing, Pitman Publishing Ltd., London, 1980.

6. J.W.Godfrey and G.Parr, The Technical Writer, Chapman Hall Ltd. London, 1959.

7. R.O.Kapp, The Presentation of Technical Information, Constable Company Ltd., London, 1948.

8. R.A.Day, How to Write and Publish a Scientific Paper, 2nd. ed.; ISI Press, Philadelphia, PA, 1983.

9. R.Schoenfeld, The Chemist's English, VCH Publishers Ltd., Cambridge, UK, 1986.

10. T.McArthur, The Written Word - A Course in Controlled Composition, Oxford Univ. Press, Oxford, 1984.

11. N.Williams, Computer Assisted Writing Software: RUSKIN, in Computers and Writing: Models and Tools, N.Williams and P.Holt (eds.), BSP Ltd. Oxford, England, pp.1-16, 1989.

12. P.Hultfors, Reactions to Non-Native English: Part 2: Foreign Role and Interpretation, Almqvist Wiksell Inter, 1987.

13. E.E.Evans and C.K.Alexander, Jr., Increasing Aural Skills of International Graduate Students, IEEE Trans. on Education, Vol. E-27, pp 167-170, August 1984.

14. J.T.Dennett, Writing Technical English: A Comparison of the Process Native English and Native Japanese Speakers, 1988 IEEE International Professional Commun. Conf., Seattle, Washington, October 5-7, pp 249-254, 1988.

15. U.Hovstad, Computer Assisted Essay-Writing: An Inter-Disciplinary Development Project at Eikeli Grammar School, in Computers and Writing: Models and Tools, N.Williams and P.Holt (eds.), BSP Ltd, Oxford, England, pp.148-160, 1989.

16. E. Tarone, Conscious Communication Strategies in Interlanguage: a Progress Report, Brown, Yorio Cryme (eds.), On TESOL 77, Washington, 1977.

17. A.F.Deyes, Discourse, Science and Scientific Discourse (the raw material of comprehension in ESP), Working Paper No. 6, Brazilian ESP Project, Pontificia Universidade Católica de São Paulo, São Paulo, 1982.

18. N.H.MacDonald, L.T.Frase, P.S.Gingrich and S.A.Keenan, The Writer's Workbench: Computer Aids for Text Analysis, IEEE Trans. Commun., Vol. Com-30, No.1, pp 105-110, January 1982.

19. L.Cherry, Writing Tools, IEEE Trans. Commun., Vol. COM-30, pp 100 105, January 1982.

20. J.Matzkin, Grammar Checkers Improve, But Won't Replace Your English Teacher, PC Magazine, March 13, p.46, 1990.

21. D.F.Beer, Designing the Electrical Engineering Lab. Report, 1988 IEEE International Professional Commun. Conf., Seattle, Washington, October 5-7, pp 129-133, 1988.

22. P.A.Carlson, Cognitive Tools and Computer-Aided Writing, AI Expert, pp. 48-55, October 1990.

23. E.H.Hovy, Unresolved Issues in Paragraph Planning, in Current Research in Natural Language Generation, R.Dale, C.Mellish and M.Zock (eds.), London Academic Press, pp. 17-45, 1990.

24. P.Wright and A.Lickorish, The Influence of Discourse Structure on Display and Navigation in Hypertexts, in Computers and Writing: Models and Tools, N.Williams and P.Holt (eds.), BSP Ltd, Oxford, England, pp. 90-124, 1989.

25. K.R.McKeown, Discourse Strategies for Generating Natural-Language Text, in Readings in Natural Language Processing, B.J.Grosz, K.S.Jones and B.L.Webber (eds.), Morgan Kaufmann Publishers, Inc. pp.479-499, 1986.

26. W. C. Mann & S. A. Thompson, Rhetorical Structure Theory, in L. Polanyi (ed.) The Structure of Discourse, Norwood, N.J: Ablex, 1987.

Figure Captions

Fig. 1 Chusaurus menu containing the names of the various sections likely to appear in a paper.

Fig. 2 Examples of subjects which are likely to appear in (a) Introduction and (b) Results sections of a paper. Also given are examples of the compiled expressions.

Fig. 3 Model of the Environment Proposed.

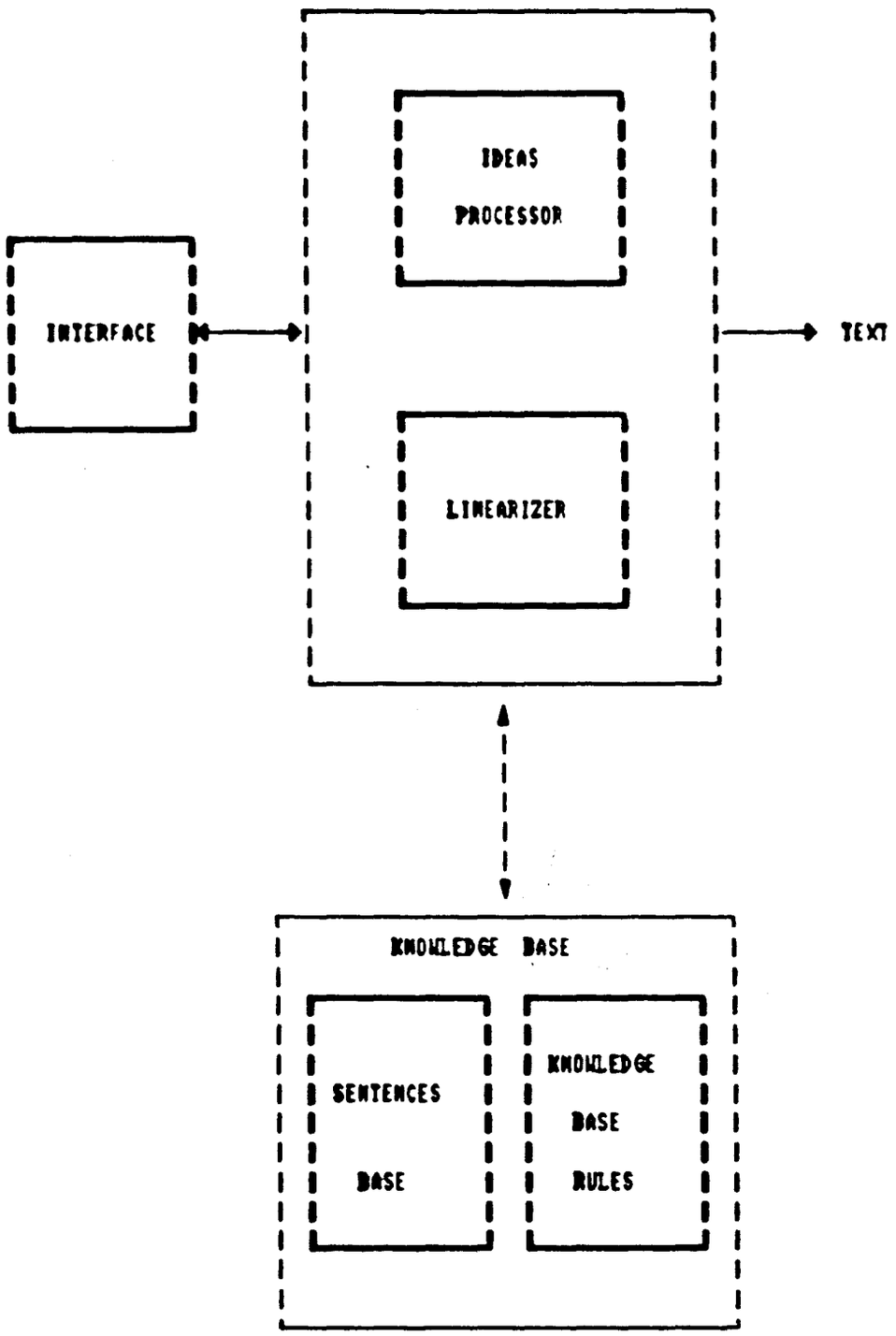
IDEAS
PROCESSOR
INTERFACE
TEXT
LINEARIZER
KNOWLEDGE BASE
SENTENCES
BASE
KNOWLEDGE
BASE
RULES

Fig. 3

WRITING TOOLS FOR NON-NATIVE USERS OF ENGLISH

S.M.A.Caldeira[1], M.C.F. De Oliveira[1], N.M.Fontana[2],

C.Y.Nacamatsu[1] and O.N.Oliveira Jr.[3]

[1]Departamento de Computação e Estatística, ICMSC, USP

CP 668, 13560 São Carlos, S.P. - Brazil

[2]Departamento de Letras, Universidade de Caxias do Sul

CP 1352, 95070 Caxias do Sul, R.S. - Brazil

[3]Instituto de Física e Química de São Carlos, USP

CP 369, 13560 São Carlos, S.P. - Brazil

Abstract

*We report on an ongoing project aimed at developing software tools to help non-native users of English in the writing of scientific papers. The environment, named **AMADEUS** (**AM**iable **A**rticle **D**evelopment **E**nvironment for **U**ser **S**upport), is based on an empirical resource which consists in providing linguistic input to the user in the form of expressions and templates stored in a sentences base, and is at an initial exploratory stage, in the sense that we are trying different user-interfaces and environments for developing the tools. One of the versions conceived for the environment is already implemented.*

Keywords: writing tools, non-native users of English, computer assisted writing

I) Introduction

The development of software writing aids requires research efforts on a number of different issues, as writers' needs may vary tremendously depending on their experience in writing, on their expertise on the subject they are writing about, and obviously on their knowledge of the language itself. Though some characteristics such as user-friendliness are always desirable, these tools must

generally be targeted at specific user-groups [1].

We have instituted a project aimed at developing software tools that may help non-native users of English in writing scientific papers. The work is essentially based on an (empirical) resource [2] which consists in providing linguistic input to the user in the form of expressions and templates stored in a sentences base. The work reported here may be considered as exploratory in the sense that we are trying different interfaces and environments for developing the tools. In this paper we address the efficacy of the resource proposed, which was analysed through the monitoring of writing exercises by Brazilian post-graduate students (Section II); and the implementation of the resource in software tools (Section III).

II) Analysis of the Resource from a Linguistic Perspective

The difficulties faced by writers when preparing texts in a foreign language seem to arise due to at least two main factors. The first one is sociolinguistic diversity, as languages differ considerably with respect to phonology, syntax and lexicon, as well as at the pragmatic level [3]. Consequently, different languages use different rhetorical patterns and elements to organize discourse [4]. The second factor which is likely to affect the learner's written outcome has to do with the relationship that holds between comprehension and production: it is now largely accepted that comprehension is beyond production. The combination of these two factors appears to be connected with a phenomenon known as <u>transfer</u> in the linguistic area, whose influence on L2 data has been investigated by several linguists. Here we follow Schachter [5] in her cognitive approach to language transfer. As transfer can often lead to transfer errors, it is our belief that

its negative effects could be prevented, to a certain extent, by providing the non-native writer with expressions from authentic texts from books and papers written by competent native speakers of English to help him/her in organizing their texts more effectively and naturally.

In order to test the efficacy of the resource proposed and also to provide feedback to the process of developing the software tools we monitored writing exercises done by post-graduate students. This was carried out as part of a course on technical writing held in the Physics Department of University of São Paulo in São Carlos. The results are extremely encouraging for using the resource minimized effects of L1 (Portuguese) transfer on L2 (English), and also enabled students to get started in their writing tasks. Indeed, getting over the writer's block has been mentioned as one of the most important problems faced by writers [1].

III) The *AMADEUS* Environment

AMADEUS will comprise composition tools to assist users in the writing of technical articles in English by offering linguistic input in the form of contextualized expressions. It is being developed within the XView (X Window-system-based Visual/Integrated Environment for Workstations)1 a user-interface toolkit to support interactive, graphics-based applications running under the X-Window system in a Sun Workstation. XView features an object-oriented style interface following the OPENLOOK Graphical User-Interface (GUI) specification. We are following a prototyping approach in the development of the environment, and the X-Windows and Emacs-based tools to be discussed shall provide starting points for further developments.

The expressions from the sentences base may be accessed by one of three ways:

1. **Taxonomy** - The expressions are indexed according to a taxonomy which is based on the main topics likely to appear in a paper, and are accessed by selecting an item in the taxonomy.

2. **Communicative Goals** - The search can be performed by selecting a communicative goal (describe, justify, compare, contrast, etc.).

3. **Keywords** - Here the search is carried out by selecting a keyword that appears frequently in texts of a given area. It can also be used for linguistic items which are usually troublesome. For instance, if the phrasal verbs *carry out* and *carry on* are chosen to be keywords, a search into the database will show the correct contextualized uses for these verbs.

Users can be classified according to two main axes, namely their background knowledge of the English language and their experience in writing papers. In order to meet different users' needs we have conceived three versions for the writing environment:

i) **Tutorial** - The whole writing process is monitored by the system; a rigid frame for the organization of the paper is offered, hints are given as to what type of material should be included, and then there is an automatic selection of expressions which guides the user throughout the writing exercise. This automatic selection is driven using expert rules. No acquisition mode for entering new expressions is made available so as to avoid inexperienced writers adding inadequate material. This version is the most demanding in terms of computational development, and has not been implemented yet.

ii) **Support** - This version is similar to the Tutorial except that it offers hints as to how better structure the paper rather than

offering a rigid frame, and allows for acquisition of new material to be entered into the sentences base (customization).

iii) **Reference** - This version requires the least computational development effort and is already implemented. The user consults the database (accessing the expressions by one of the 3 possible ways mentioned above) and selects the expressions on his/her own. The tool can be customized since it includes the Acquisition Mode by which new expressions can be entered into the sentences base.

Fig. 1 shows a screendump displaying the main features supported by the already implemented **Reference** version of the environment. Two windows are provided, one as a working area while the other displays expressions from the sentences base. Clicking the option **Main Menu** the user is returned to the menu which displays the options **Composition** and **Acquisition**. The options **Article** and **Keywords** correspond to the modes 1 and 3, respectively, for accessing the expressions. The **Communicative Goals** menu is always displayed on the screen because it is the most general mode of accessing the expressions.

An alternative way of implementing the resource is also being attempted which uses the GNU Emacs text editor, a public domain software package. Emacs was chosen because it provides hypertext facilities, it is customizable and furthermore, it is extensible which means that one can go beyond customization by writing entirely new commands, programs in the Lisp language to be run by the Lisp interpreter provided by Emacs. In our implementation use is being made of a special Emacs function called **Outline-mode**, which has built-in routines that hide and display chunks of text which can be classified hierarchically as items and sub-items of a menu or as normal text. The two windows available in Emacs are used for the text being edited and the database of expressions, and new

routines were added to the Outline-mode in order to allow the transfer of expressions from the sentences base to the text. The facilities already available are similar to the Reference Version of the tool implemented in the XView environment. Using this tool requires users to be familiar with Emacs, by no means a simple word processor to use. However, we are developing a friendlier interface which will allow users to employ the tool with a minimum background knowledge of how Emacs works.

What we had in mind when we decided to investigate an alternative implementation for the resource was to allow for customization and portability of the tool, and also investigate the possibility of introducing some degree of "intelligence" into it. Emacs seemed a natural choice for its flexibility. For instance, texts in Emacs can be generated in the Text Mode (ASCII) or in other modes so as to allow integration with wordprocessors such as TEX. Because Emacs is entirely re-programmable new functions can be added either for the introduction of expert rules or for extending the portability of a given tool. The obvious disadvantage of the Emacs alternative is its poor graphics capability (compared to XView), but at the moment it is not possible to predict whether this disadvantage will be overpowered by its other welcome features.

IV) Concluding Remarks

We should stress that the tools being developed are not aimed at generating text in the more strict sense of the so-called Natural Language Generation (NLG), for the user rather than the system will be ultimately responsible for the quality of the text. But we can, nevertheless, seek help in the techniques usually employed in NLG. In this context, systems [6,7] appeared recently

in the NLG literature which utilize essentially the same strategy discussed here. They are based on statistical analysis of large corpora in order to identify standard linguistic constructions in texts of a given field. It may well be, nevertheless, that the studies we are undertaking, related to language acquisition by a non-native user, may also be of some use to the NLG community.

References

[1] N. Williams, "Writers' Problems and Computer Solutions", CALL Volume 2: Computer Assisted Composition, Intellect, Oxford, pp. 5-25, 1990.

[2] O.N. Oliveira Jr., S.M.A. Caldeira, and N. Fontana, "Chusaurus: A Writing Tool Resource for Non-Native Users of English", in Proceedings of the XI International Conference of The Chilean Computer Science Society, pp. 59-70, 1991.

[3] N. Wolfson, "Perspectives: Sociolinguistics and TESOL" Newbury House Publishers, N.York, 1989.

[4] C. Henner-Stanchina, "From reading to writing acts", in Discourse and learning, Riley,P. (ed.), Longman, Burnt Mill, 1985

[5] J. Schachter, "A New Account of Language Tranfer", in Language Tranfer and Language Learning, Gass, S. & Selinker, L. (eds.), Newbury House Publishers, Roweley, pp. 98-111, 1983.

[6] P.L. Miller and G.D. Rennels, "Prose Generation from Expert System - An Applied Computational Linguistics Approach", AI Magazine, pp. 37-44, Fall 1988.

[7] F.A.Smadja and K.R.McKeown, Automatically Extracting and Representing Collocations for Language Generation, 28th ACL Meeting, Pittsburg, PA, 1990

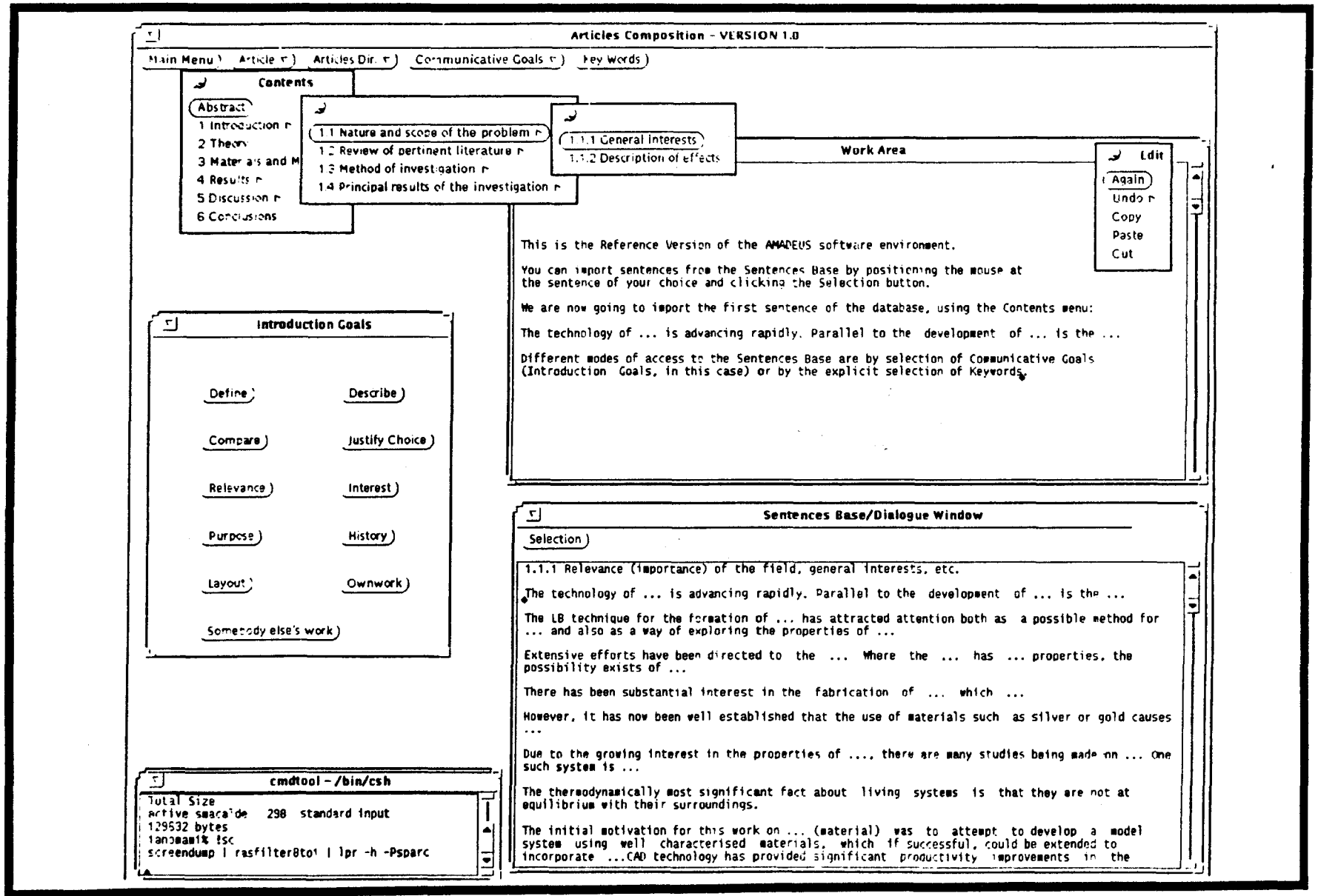

Figure 1: Screendump showing the Reference Version of the AMADEUS software environment.